LEVEL

AN ELECTRONICALLY-TUNED, PULSED COAXIAL MAGNETRON FOR KU-BAND

FINAL REPORT

D D C

JAN 10 1979

F

Prepared for:

NAVAL ELECTRONICS LABORATORY CENTER
CATALINA BOULEVARD
SAN DIEGO, CALIFORNIA

varian-beverly

79 01 09 017

REFERENCES

(1) Ishii, T. Koryu, MICROWAVE ENGINEERING, The Ronald Press Co., New York, New York, 1966, Chapter 3.

(2) Wilson, I.G., Schramm, C.W., and Kinzer, I.P., HIGH Q RESONANT CAVITIES FOR MICROWAVE TESTING, RADAR SYSTEMS AND COMPONENTS, (Bell Laboratories' Staff), D. VanNostrand Co., Inc., New York, New York, 1949.

(3) Ramo, S., and Whinnery, J.R., FIELD AND WAVES IN MODERN RADIO, John Wiley and Sons, Inc., New York, New York, 1953, Pg. 422.

(4) Ibid, Page 9.

(5) Terman, F.E., RADIO ENGINEERING, McGraw Hill Book Co., New York, New York, 1937, Chapter 3.

(6) Slater, J.C., MICROWAVE ELECTRONICS, D. VanNostrand Co., Inc. New York, New York, 1950, Pages 8083.

(7) Ginzton, E.L., MICROWAVE MEASUREMENTS, McGraw Hill Book Co., Inc., New York, New York, 1957, Chapter 10.

(8) Terman, F.E., RADIO ENGINEERS HANDBOOK, McGraw Hill Book Co., Inc., New York, New York, 1943, Page 53.

⑥ AN ELECTRONICALLY-TUNED, PULSED

COAXIAL MAGNETRON FOR KU-BAND.

⑨ FINAL REPORT, Jun 75 - Jun 76,

p1

JAN 10 1979

PREPARED FOR:

NAVAL ELECTRONICS LABORATORY CENTER

271 CATALINA BOULEVARD

SAN DIEGO, CALIFORNIA 92152

⑮

UNDER CONTRACT No. N00123-75-C-0911

PREPARED BY:

⑩ GEORGE K. FARNEY

VARIAN ASSOCIATES

EIGHT SALEM ROAD

BEVERLY, MASSACHUSETTS 01915

⑫ 242p.

⑪ 16 AUG 76

364 070

79 01 09 017

TABLE OF CONTENTS

TABLE OF CONTENTS
(CONTINUED)

TABLE OF CONTENTS
(CONCLUDED)

1.0   INTRODUCTION

This report describes the effort on a twelve month program supported by the U.S. Navy to demonstrate the feasibility of an electronically-tuned, pulsed, coaxial magnetron oscillator. The program was conducted between June 1975 and June 1976 at Varian, Beverly, Massachusetts under contract No. N00123-75-C-0911. The program was under the technical direction of the Naval Electronics Laboratory Center, San Diego, California. The emphasis on the program was the development of suitable electronic tuning techniques rather than on tube fabrication to a particular electrical and mechanical specification.

Although the primary emphasis on the program was aimed at developing appropriate tuning techniques, there were technical goals for an electronically-tuned, coaxial magnetron employing the proposed tuning techniques which were as follows:

Frequency	16.3 GHz
RF Peak Power Output	60 kW (min)
Pulse Width	0.5-2.0μsec.
Duty Cycle	0.001
Option A - Electronic Tuning Range	300 MHz
Electronic Tuning Rate	50 MHz/millisecond
Option B - Electronic Tuning Range	100 MHz
Electronic Tuning Rate	100 MHz/microsecond

-1-

It was desirable that the electronic tuning technique(s) to be developed be capable of performing both Option A and Option B. If this was not possible, then alternate solutions were to be offered which could perform either option.

The technical approach adopted by Varian utilizes PIN diodes mounted in the stabilizing cavity of a coaxial magnetron to produce tuning. The diodes and associated d.c. bias coupling leads form an LC network that is an RF circuit coupled to the RF fields of the stabilizing cavity. Discrete frequency shifts are obtained by altering the bias conditions applied to the diode. The accompanying change in RF impedance coupled to the stabilizing cavity produces the associated frequency change. This technique is a variant of a PIN diode tuning scheme that had been investigated previously at S-band on a company-sponsored program.

The efforts on the present program were directed toward several tasks. Early in the program the analysis of the coupled circuit tuning technique was extended to be applicable for use at Ku-band. This analysis will be presented in detail. It was recognized at the outset that PIN diodes with special characteristic would most likely be required for this application. The development effort for an improved diode is described in a section of this report prepared by Mr. Richard Langlais, Project Engineer in diode development. Also, it was evident that special electronic control circuitry would be required for fast switching of the diodes in a practical system application. Study efforts were conducted to assess the needs for

-2-

logic circuitry and appropriate diode driver circuits. The results
of the logic circuit study are presented in a section prepared by
Mr. James Fuller, Manager - System Engineering. Dr. James F. Reynolds,
Manager - Control Components Engineering, prepared the section des-
cribing the diode driver circuits. The coaxial magnetron develop-
ment involved both cold test experiments to verify the theory of the
tuning concept and operating tube experiments with diode tuning to
demonstrate the feasibility of the method. Both sets of experiments
will be described.

It will be seen that the feasibility of electronically-
tuning a pulsed, coaxial magnetron using PIN diode controlled,
coupled circuits has been demonstrated. There exist some problems
yet to be fully resolved and the final section of this report
will discuss further development efforts to be pursued.

2.0 BACKGROUND INFORMATION

A new electronic tuning concept evolved as the result of an in-house effort to introduce a simple tuner in an S-band, coaxial magnetron intended to produce a very small frequency excursion. The intended tuning range was sufficiently small (a center frequency adjustment for what was basically a fixed frequency tube) so that a conventional end plate tuner and drive mechanism in such a large tube was considered too complex and costly. As a result, a simple tuning plunger, whose penetration could be adjusted, was attached to the cavity wall. Such simple tuners have been used heretofore on dominant mode cavities in klystrons for tuning, but have not been employed in a higher order mode cavity such as the TE_{011} stabilizing cavity of a coaxial magnetron. It had been reasoned that such an unsymmetrical perturbation would degrade the internal Q_o of the cavity. In fact, in the design of almost all cavity and tuner configurations for coaxial magnetrons, great care is usually exercised to preserve symmetry as much as possible. Nevertheless, it was found that a small frequency shift (0.1 - 0.2%) could be obtained before excessive Q_o degradation occurred. However, it was also found that additional tuning could be obtained if a second small perturber was added located elsewhere in the cavity wall. Again, excessive degradation in Q_o occurred if the perturbation was not kept small. These results suggested that a satisfactory method of tuning a coaxial magnetron could be obtained by using a substantial number of small perturbers in a symmetrical geometry located directly within

-4-

the stabilizing cavity. This approach is advantageous since no other energy storage elements in addition to the stabilizing cavity are required.

Several possible perturbing configurations were conceived. One geometry is based upon a mode filter concept for the TE_{01} mode. It is well known that metallic conductors that are perpendicular to the RF electric field lines have a minimal affect on the TE_{01} mode. Hence, a small slotted ring or comb structure can be mounted on the wall or end plate of the TE_{011} stabilizing cavity without much degradation in cavity Q_o. See Figure 1. Tuning can be accomplished by short circuiting the slots of the comb. This can be done electronically by using PIN diodes across the open end of the slots.

PIN diodes are solid state, two terminal devices that function essentially as a switch for certain ranges of microwave frequencies. They present a very high impedance, or open circuit, when reverse biased and function as a very low impedance resistance in a forward biased state. Hence, by applying a reverse bias to the diode, the slot can be open to microwave power storage. By applying a forward bias, a near short circuit is placed across the slot and microwave power storage is inhibited. In effect, the volume of the cavity is controlled electronically. A discrete change in frequency results when the diode bias state is changed. Tuning accomplished by this method is called diode-switched tuning as opposed to continuous tuning such as can be obtained with varactor diodes.

-5-

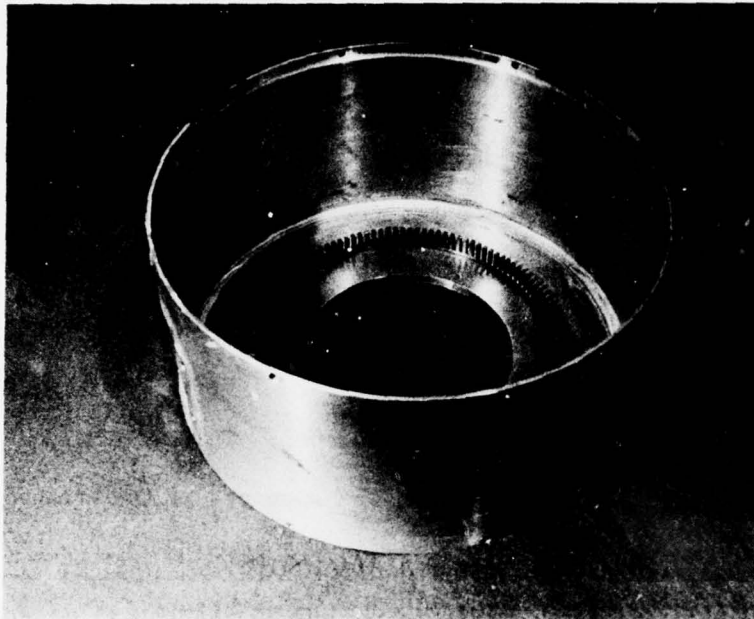## FIGURE 1

THIS PHOTOGRAPH SHOWS PART OF THE EXTERNAL COAXIAL
CAVITY USED WITH THE S-BAND SLEEVE TUBE COAXIAL MAGNETRON.
THE CIRCULAR COMB TUNER IS MOUNTED ON THE CAVITY END PLATE
AT THE APPROXIMATE MIDPOINT BETWEEN THE CAVITY OUTER WALL
AND THE ANODE SHELL. THE COMB FINGERS EXTEND INTO THE
CAVITY IN A DIRECTION PERPENDICULAR TO THE RF ELECTRIC
FIELD LINE OF THE TE_{011} CIRCULAR ELECTRIC MODE.

A second tuning approach also uses the diodes conceptually as a simple switch to control the amount of dielectric material exposed to the RF fields in the microwave cavity. This is illustrated schematically in Figure 2. The dielectric material is located along the cavity end plate or wall in the region of strong RF electric fields. The dielectric is oriented to extend in the direction of the RF electric field thereby providing dielectric loading of the cavity. The diodes can be mounted either on the surface of the dielectric or on the cavity wall. The connecting bias leads are then positioned generally in the direction of the RF electric field in a manner to surround a portion of the dielectric material. In the reverse biased condition, the dielectric material is essentially exposed to the RF electric fields in the cavity whereas in the forward biased condition, the bias leads provide a short circuit around a portion of the dielectric, thereby effectively removing it from the cavity. The diodes are envisioned as controlling electronically the amount of dielectric loading that is effective in the cavity.

In reality, PIN diodes do not function as a simple switch, but instead have other parametric features that can become very important at high frequencies. These can be taken into account by considering an equivalent circuit of the diode.

The conventional, equivalent circuit representation of the reverse biased state of a diode chip is a small value capacitor in parallel with a large value of resistance allowing only small leakage current. In addition, there are the series inductances and resistances associated with the connecting leads. The equivalent

-7-
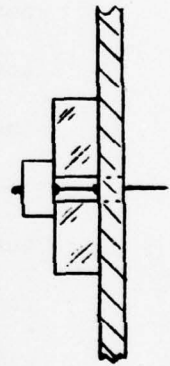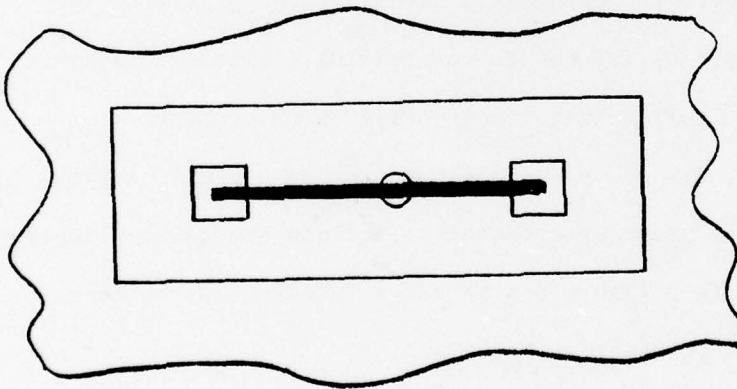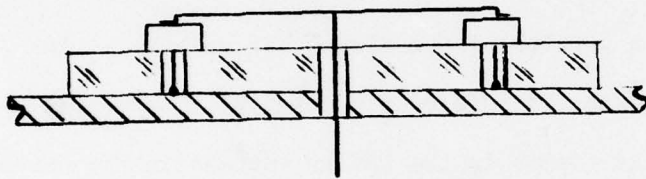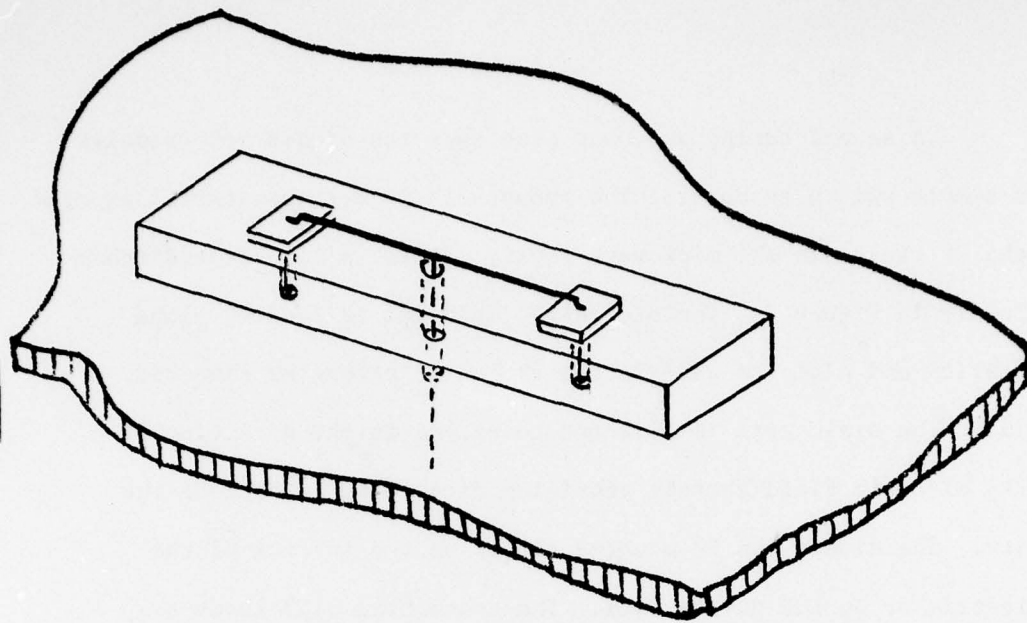
FIGURE 2

SCHEMATIC ILLUSTRATION OF PIN DIODES USED TO CONTROL
ELECTRONICALLY THE DIELECTRIC LOADING CAVITY.

circuit is more complex if additional parametric features of a packaging configuration must be taken into account. In the open circuit state, the diodes must hold off the combined RF electric voltage and d.c. reverse bias voltage without voltage breakdown or without allowing diode rectification. This restricts the RF power levels tolerable in the cavity and, therefore, the peak power levels that can be tuned effectively. In the forward biased state, as a closed switch, the diode chips have an equivalent circuit consisting of the connecting lead inductances and resistances together with a small series resistance of the order of one ohm or less. This is the RF dynamic resistance of the diode semi-conductors in the conducting state. The I^2R losses of the diode contribute to the cavity losses and lower the cavity internal Q_o. An incremental frequency shift is obtained with each diode and slot combination switched to the forward biased state. Hence, the total frequency shift obtainable is influenced by the tolerable reduction in Q_o. The ideal diodes would have very high breakdown voltage (V_{BD}) allowing tuned cavities with high peak power handling capability and would have low values for forward resistance (R_S) allowing wide tuning ranges without excessive degradation in Q_o. At sufficiently low frequencies the diode can be regarded very nearly as a simple switch without much required consideration given to details of the equivalent circuit representation.

PIN diode tuning was investigated initially under a company-sponsored program. The first tests were performed at S-band. It was decided to study the approach using a comb structure with diodes

-9-

across the open end of the comb slots. For simplicity, the first tests were made using a dominant mode, rectangular cavity. The comb structure was located on the end wall of the cavity oriented so that RF electric voltages were developed across the slot. This configuration permitted evaluation of the concept without requiring concern over possible interference from other modes that would exist in a higher order TE_{011} mode, coaxial cavity. The S-band test vehicle is shown in Figure 3.

Two diodes were used across each slot. Standard, packaged diodes were soldered together, back-to-tack, to a common bias lead. The other ends of the two diodes were then soldered into a notch in the end of the comb finger. See Figure 4. In this arangement, the diodes are in parallel for the d.c. bias voltages, but are in series for the RF voltage developed across the comb slot. This symmetrical arrangement also minimized RF-coupled power from the cavity along the bias lead. It was planned that a reverse bias voltage equal to half of the diode breakdown voltage would be applied to the combination package. An RF voltage equal to the breakdown voltage could then be applied. On each half of the RF cycle, the RF voltage would add to the bias on one diode and subtract from the other. One diode would be driven toward breakdown and the other toward rectification. The conditions alternate each half of the RF cycle.

The tuning comb for the rectangular cavity had eight slots and eight diode pairs. The obtainable tuning range varied with the comb dimensions. As expected, the tuning range increased

-10-
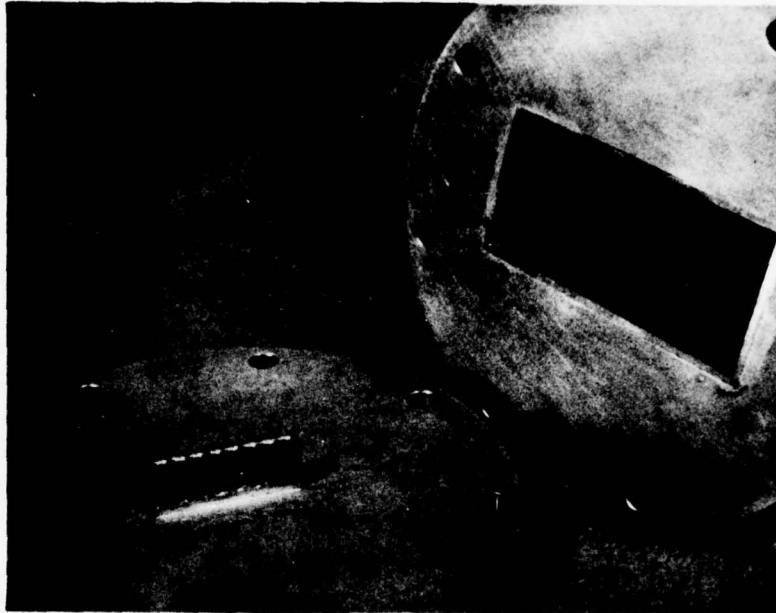
FIGURE 3

THIS PHOTOGRAPH SHOWS A COMB ASSEMBLY WITH THE BACK-
TO-BACK DIODES SOLDERED INTO THE COMB TUNER ASSEMBLY.
THIS BIAS LEADS CAN BE SEEN PASSING ALONG THE MIDPLANE
OF THE SLOTS AND OUT THROUGH A HOLE IN THE ROOT OF THE SLOT
AND HOLES IN THE END FLANGE OF THE RECTANGULAR CAVITY.

-11-

EQUIVALENT CIRCUIT

DIODE PACKAGE

TUNING COMB

BIAS LEAD
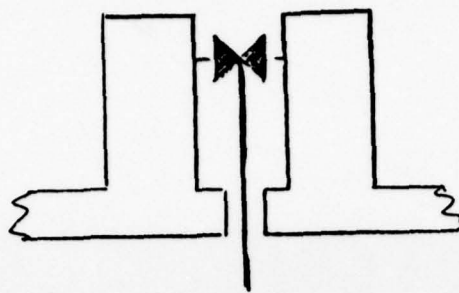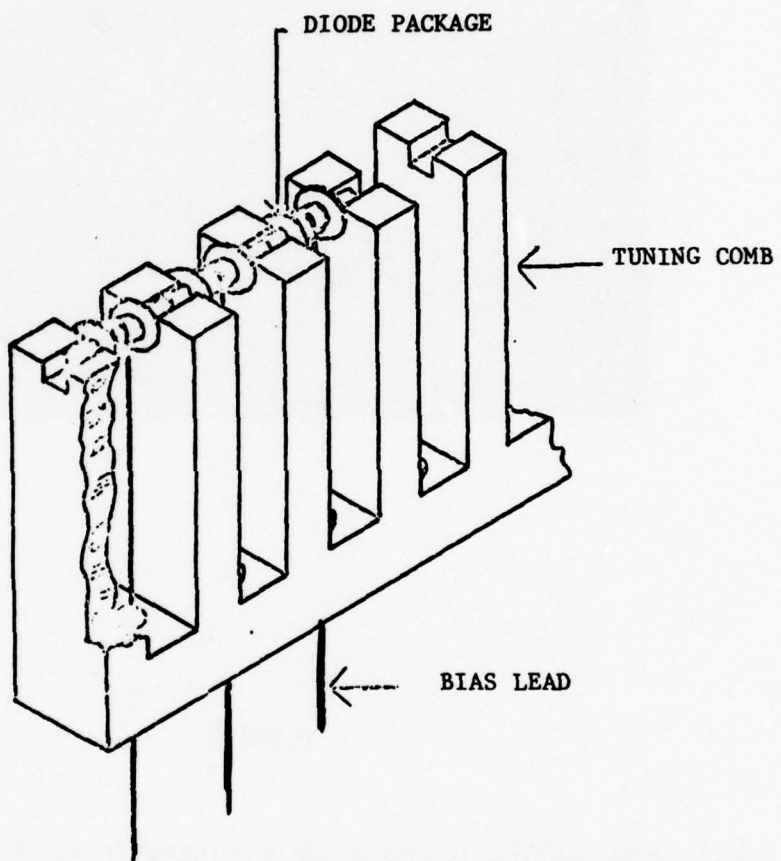
FIGURE 4

SCHEMATIC ILLUSTRATION OF PACKAGED DIODES AND TUNING
COMB STRUCTURE.

-12-

with greater penetration of the diodes into the cavity. However, this leads to exposure of the diodes to higher RF voltage and causes larger degradation of the cavity Q_o. Nevertheless, as much as three percent tuning was demonstrated with the rectangular cavity tester.

One cold test experiment was made using a TE_{011} coaxial cavity. Six diode pairs were mounted in a circular comb structure similar to that shown in Figure 1, and a total tuning excursion of 5 MHz was obtained. No hot test experiments were made at this frequency band.

The conclusion from these early experiments was that PIN diodes could certainly be used to switch the resonant frequency of a cavity in an incremental fashion. It was believed that tuning of an operating coaxial magnetron could be obtained if the diodes could be made to survive in the tube environment. Diodes with high values for breakdown voltage and low values of resistive loss would be needed. Very high values of RF voltage are developed in a magnetron cavity and any increase in resistive loss at all is undesirable. In addition, if the diodes are contained inside the vacuum envelope, they must survive through all of the fabrication and assembly processes as well as the bakeout and exhaust procedure. To meet all of these needs, it was expected that further development in diode characteristics as well as in the coaxial magnetron would be required.

3.0   <u>EXTENSION</u> <u>OF</u> <u>PIN</u> <u>DIODE</u> <u>TUNING</u> <u>TO</u> <u>KU-BAND</u>

The frequency range of interest for the U.S. Navy for an electronically-tuned, coaxial magnetron is at Ku-band. The RF properties of a PIN diode at Ku-band are quite different from what they are at S-band. Hence, it was not possible to use directly the same tuning concepts that were investigated previously. For instance, a diode with a junction capacitance of 0.1pF has a capacitve reactance of 100 ohms at Ku-band. Needless to say, this is far from being an open circuit. Furthermore, any package capacitance would only shunt this value even more. In addition, the self inductance of the connecting leads has appreciable reactance at this frequency range. For these reasons, a new tuning configuration was employed for this application.

The third tuning method does not rely conceptually upon the diode functioning solely as a switch. Instead, the junction capacitance of the diode and the series inductance of the bias leads are used as an L-C circuit which is electromagnetically coupled to the RF fields in the main cavity resonator. The diodes could be soldered directly the the cavity wall, thereby eliminating the thermal impedance of a package, and the bias leads could be arranged to intercept the RF magnetic fields of the main cavity. This mounting configuration is shown schematically in Figure 5.

Figure 6 shows an equivalent circuit of the tuning arrangement. Figure 6-A shows the equivalent circuit for the reversed biased condition where the diode is represented by a capacitance
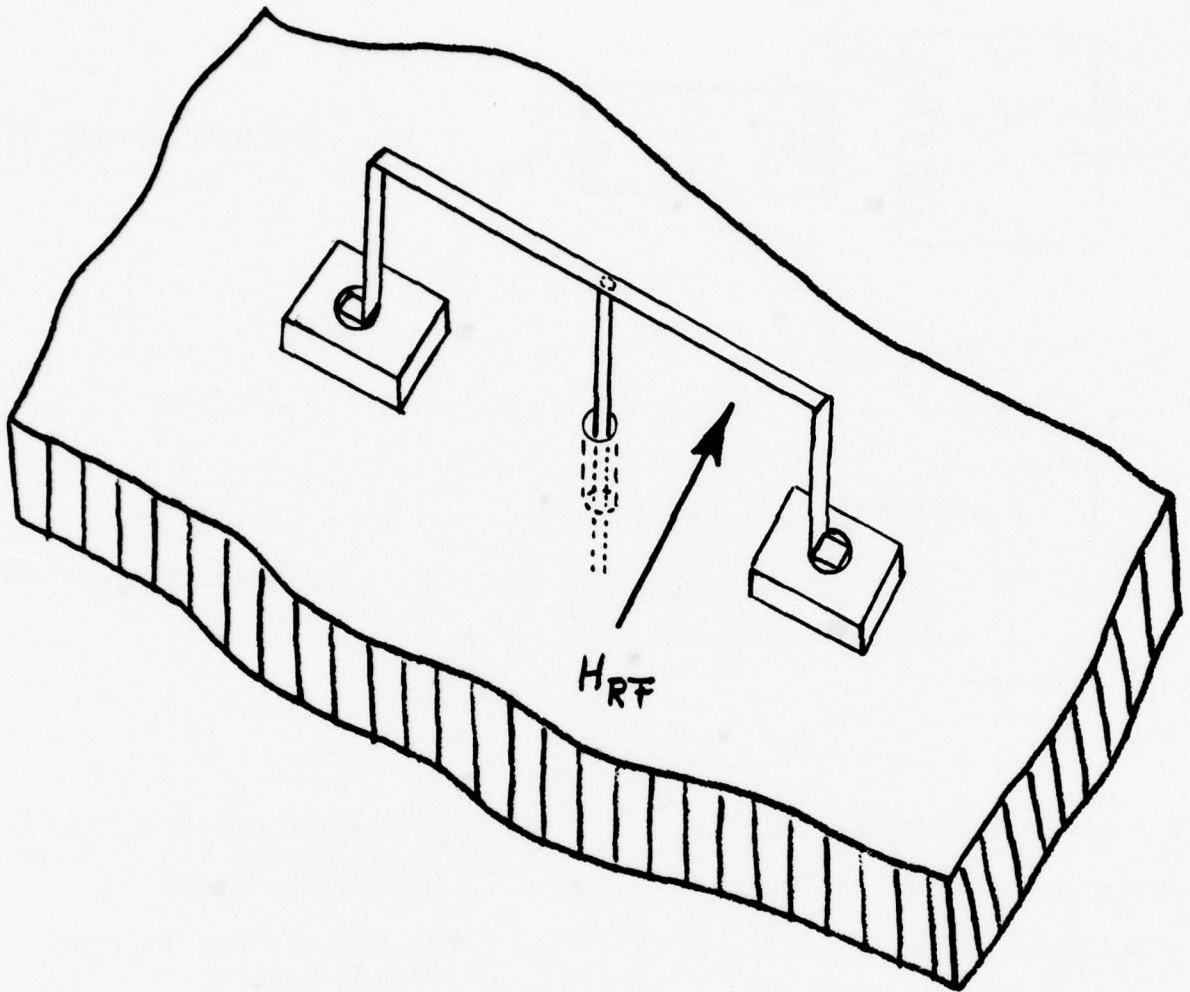
-14-

FIGURE 5

SCHEMATIC ILLUSTRATION OF A PIN DIODE CONTROLLED,
COUPLED CIRCUIT CONFIGURATION FOR ELECTRONIC TUNING

-15-

REVERSED BIASED STATE

(A)

FORWARD BIASED STATE

(B)

C_P = PRIMARY CIRCUIT CAPACITANCE

L_P = PRIMARY CIRCUIT INDUCTANCE

M_S = MUTUAL INDUCTANCE

L_S = SECONDARY CIRCUIT INDUCTANCE

C_S = DIODE JUNCTION CAPACITANCE AT REVERSED BIASED CONDITION

R_{SH} = SECONDARY CIRCUIT EQUIVALENT SHUNT RESISTANCE AT REVERSE BIASED CONDITION

R_S = SECONDARY CIRCUIT SERIES RESISTANCE AT FORWARD BIASED STATE INCLUDING DIODE SERIES RESISTANCE

FIGURE 6

EQUIVALENT CIRCUIT REPRESENTATION OF PIN DIODE CONTROLLED, COUPLED CIRCUITS FOR ELECTRONIC TUNING

FIGURE 5

SCHEMATIC ILLUSTRATION OF A PIN DIODE CONTROLLED,
COUPLED CIRCUIT CONFIGURATION FOR ELECTRONIC TUNING

-15-

REVERSED BIASED STATE

(A)

FORWARD BIASED STATE

(B)

C_P = PRIMARY CIRCUIT CAPACITANCE

L_P = PRIMARY CIRCUIT INDUCTANCE

M_S = MUTUAL INDUCTANCE

L_S = SECONDARY CIRCUIT INDUCTANCE

C_S = DIODE JUNCTION CAPACITANCE AT REVERSED BIASED CONDITION

R_{SH} = SECONDARY CIRCUIT EQUIVALENT SHUNT RESISTANCE AT REVERSE BIASED CONDITION

R_S = SECONDARY CIRCUIT SERIES RESISTANCE AT FORWARD BIASED STATE INCLUDING DIODE SERIES RESISTANCE

FIGURE 6

EQUIVALENT CIRCUIT REPRESENTATION OF PIN DIODE
CONTROLLED, COUPLED CIRCUITS FOR ELECTRONIC TUNING

(C_s) equal to the junction capacitance which is in parallel with
a large value of resistance (R_{sh}) equal to the shunt leakage
resistance across the diode. If desired, this resistance can also
be replaced conceptually with a very low value of equivalent series
resistance which introduces very little loss in the secondary circuit.
The inductance of the connecting bias leads and of the return path along
the cavity wall are represented by the series inductance (L_s). The
mutual inductance (M_s) between the two systems reflects the degree
of effective coupling between them. Figure 6-B is the equivalent
circuit for the forward biased state. The junction capacitance
has been removed together with the high value shunt resistnace
and replaced by the low value, RF dynamic forward series resistance
(R_s) of the diode. These equivalent circuits can be used for analysis
to determine the effect of circuit parameters on peak power handling
capability, obtainable tuning range, and the variation of Q_o and
power output with tuning. This equivalent circuit consideration,
taking into account the diode parameters, is very useful for analysis
of diode switched tuning technique at very high frequencies.

4.0   ## THEORY OF PIN DIODE CONTROLLED, COUPLED CIRCUIT TUNING

During the company-sponsored investigation of PIN diode
tuning at S-band, an analysis was undertaken to assess the RF vol-
tages to which the diodes would be subjected. During the early phase
of the present program, this analysis was modified to be more appli-
cable for use at Ku-band. An interim report was prepared at that
time as a working document to consolidate the ideas and viewpoints
involved. The remainder of this section is essentially a copy of
that in-house document. Some viewpoints have changed slightly
since the original preparation, but in most cases these involve
speculation about things that have not been fully resolved. For
that reason, the material has been reproduced with little change.
The speculative ideas will be noted at the appropriate location in
the rest of this report.

4.1   <u>The Lumped Element Parameters for the Equivalent Circuit</u>
          <u>of a Diode-Tuned</u>, $\underline{TE_{011}}$ <u>Coaxial Cavity Resonator</u>

          To make an analysis of the equivalent circuit, it is

necessary first to obtain the equivalent circuit parameters, C_p,

L_p, and R_p, for a primary circuit representing the coaxial cavity

and for the value for the mutual inductance, M_s. The values for

junction capacitance, C_s, and series resistance, R_s, or leakage

resistance, R_{sh}, of the diode are measured parameters. The values

for lead inductance for the diodes can be calculated.

          The circular electric mode is quite different from other

waveguide modes in that the RF electric field lines are circles that

close upon themselves. Most waveguide modes have RF electric field

lines that emanate from and terminate upon some surface area. Hence,

the concept of an equivalent lumped element capacitor is not diffi-

cult to accept intuitively. This is not so obvious for a mode

where the electric fields have no point of origin or termination.

Nevertheless, a resonant mode can be established in which stored

energy oscillates back and forth between storage as RF electric

fields and RF magnetic fields. Therefore, like many other analog

systems, a lumped element, equivalent circuit representation is

quite reasonable.

          The values for the equivalent circuit of the main cavity

are obtained from a knowledge of the cavity dimensions, the field

equations of the oscillating mode of the cavity, and the resonant

-19-

frequency, $f_o^{(1)}$. For the coaxial magnetron the oscillating mode of the stabilizing cavity is the TE_{011} coaxial mode. The field equations for this mode have been derived and are given in several references in terms of Bessel functions whose independent variable is determined by the cavity dimensions.

For a TE_{011} circular electric mode in a coaxial cavity with inner conductor radius, b, outer conductor radius, a, and cavity length, L, the form of these field equations is given by [2]:

$$E_R = o \tag{1}$$

$$E_\theta = - \sqrt{\frac{\mu}{\epsilon}} \left[J_o'(k_1\rho) - A Y_o'(k_1\rho) \right] \sin \frac{\pi z}{L} \tag{2}$$

$$E_z = 0$$

$$H_R = \frac{\lambda}{L} \left[J_o'(k_1\rho) - A Y_o'(k_1\rho) \right] \cos \frac{\pi z}{L} \tag{3}$$

$$H_\theta = 0$$

$$H_z = \frac{2r_{01}}{a} \left[J_o'(k_1\rho) - A Y_o'(k_1\rho) \right] \sin \frac{\pi z}{L} \tag{4}$$

where

$$k_1 = \frac{2r_{01}}{a} \tag{5}$$

$$r_{01} = \text{the first zero of } \left[J_o'(\eta x) Y_o'(x) - J_o'(x) Y_o'(\eta x) \right] \tag{6}$$

$$\eta = b/a \tag{7}$$

$$A = \frac{J_o'(r_{01})}{Y_o'(r_{01})} \tag{8}$$

The time dependent factor, $e^{j\omega t}$, has been omitted.

-20-

These equations could be used to calculate the equivalent circuit
parameters, but in practice the mode pattern in the magnetron
is altered by several factors. These include the presence of the
coupling slots between anode system and the stabilizing cavity, the
presence of the output coupling port, and the presence of the mode
suppressors used to inhibit unwanted interfering cavity modes.
Hence, the calculated values of the cavity field patterns based
upon an ideal coaxial cavity cannot be rigorously accurate for
the coaxial magnetron. Consequently, a simplifying assumption
is made that can still lead to considerable insight to the problem
while utilizing less tedious mathematical expressions.

The assumption is based upon noting the similarity between
the RF field patterns in the TE_{011} coaxial cavity and those in an
ordinary rectangular waveguide cavity oscillating in the TE_{101}
mode. Figure 7-A shows the sinusoidal variation of RF electric
field across the transverse section of a rectangular waveguide.
Figure 7-B shows a transition from ordinary waveguide to one with
an arcuate cross-section. Figure 7-C shows a continuation of the
transition to a full coaxial transmission line, but with a septum
between the inner and outer conductors, and Figure 7-D shows the
coaxial transmission line with the septum removed. This figure
shows conceptually how a transition between rectangular waveguide
and TE_{01} coaxial transmission line can be obtained. In fact,
broadband transitions between these two waveguide systems have
been made in just this manner.

-21-
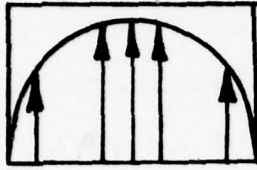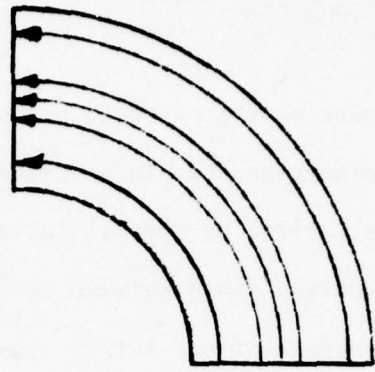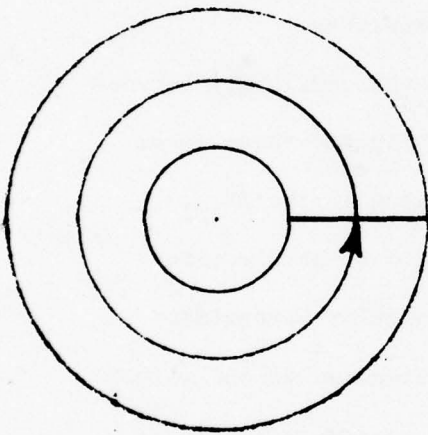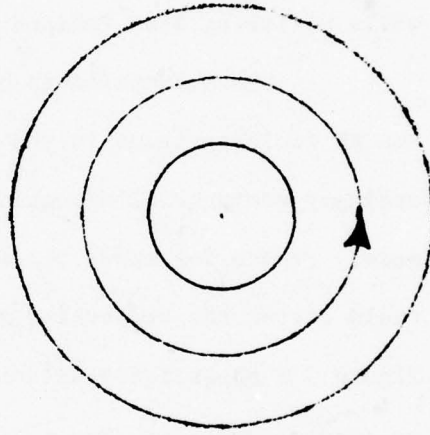
FIGURE 7

CONCEPTUAL DEVELOPMENT OF THE TE_{01} COAXIAL WAVE-
GUIDE MODE FROM THE TE_{01} RECTANGULAR WAVEGUIDE MODE

In the TE_{011} coaxial cavity mode the RF electric field
lines are closed circles with constant amplitude for any fixed
radial and axial coordinate; i.e., the magnitude is independent
of circumferential position. The field components vary sinusoid-
ally along the height of the cavity between end plates and very
nearly sinusoidally across the cavity between the inner and outer
coaxial boundaries. On the other hand, the TE_{101} rectangular
cavity mode has RF electric fields that are constant across the
height of the cavity, but which vary sinusoidally in magnitude across
the width and along the length of the cavity. In other words, any
sector of the TE_{011} coaxial cavity mode has RF electric and magnetic
field components very nearly the same as those in a rectangular
cavity of the same cross-sectional dimension, w and ℓ, as the
coaxial cavity, but of a height, h, equal to that of the coaxial
sector considered. Figure 8 shows a plot of the magnitude of the
circumferential RF electric field intensity across the coaxial
waveguide using the rigorous Bessel function solution and the
cavity dimensions of a Ku-band coaxial magnetron. For comparison
a plot is also shown of a sinusoidal variation over the cross-
section with the same peak amplitude. The difference between
the two is not great. In fact, the rigorous solution looks very
much like half a sine wave that is skewed toward the inner coaxial
cavity wall. Therefore, for the purposes considered there, the
entire coaxial cavity will be simulated as a rectangular cavity
of the same cross-section of any sector, but with a height, h,

-23-

RELATIVE RF AMPLITUDE

BESSEL FUNCTION SOLUTION

SINE FUNCTION
APPROXIMATION

FIGURE 8

COMPARISON OF THE CALCULATED RF ELECTRIC FIELD
DISTRIBUTION IN A COAXIAL CAVITY USING A RIG-
OROUS BESSEL FUNCTION SOLUTION AND A SINE
FUNCTION APPROXIMATION.

R_1

R_2

COAXIAL CAVITY RADIAL POSITION

-24-
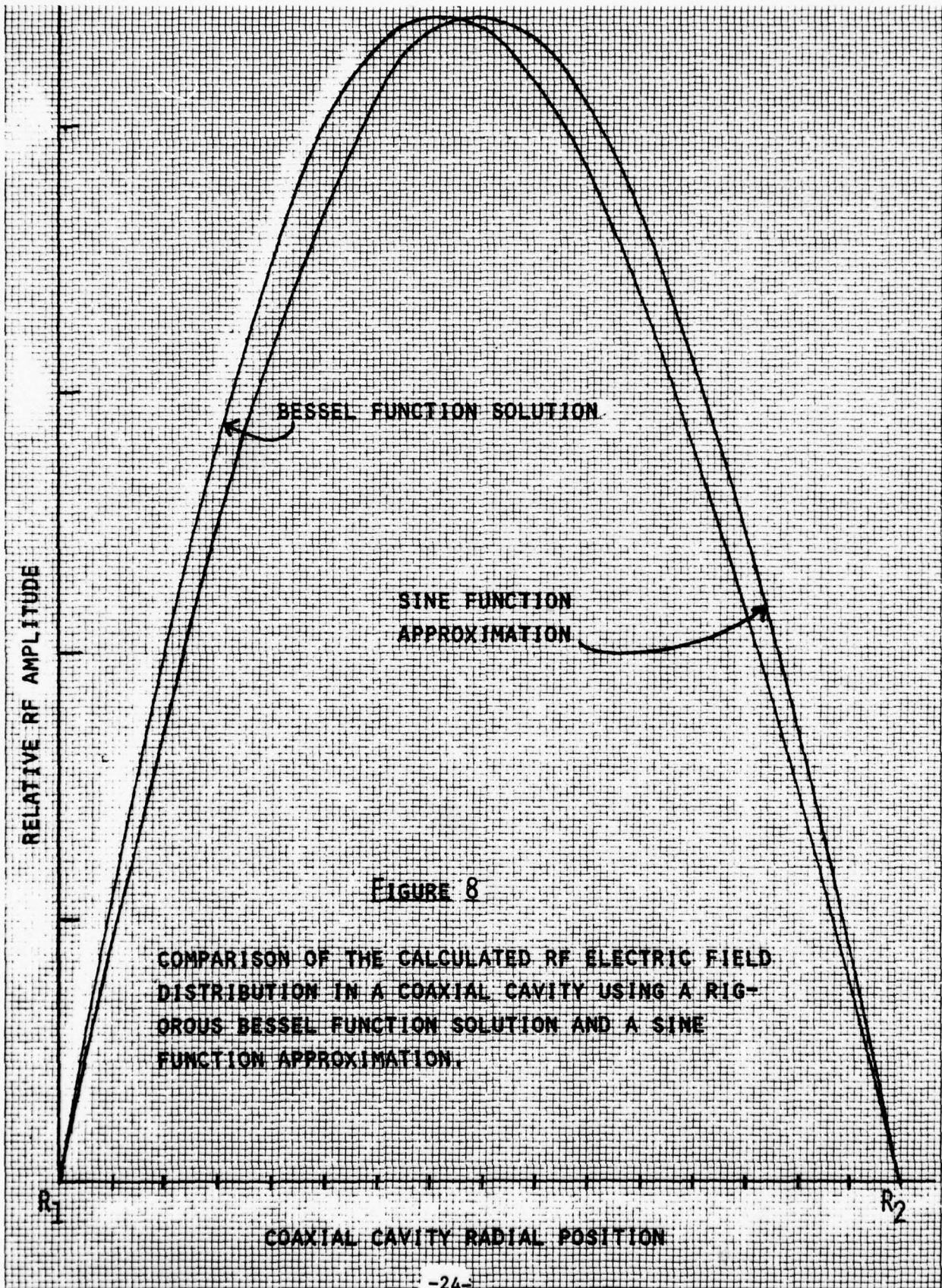
equal to the mean circumference of the coaxial cavity.

The field equations for a rectangular cavity supporting the TE_{101} mode are given below.[3] The time dependent factor, $e^{j\omega t}$, has been omitted.

$$E_y = E_o \sin \frac{\pi x}{w} \sin \frac{\pi z}{\ell} \tag{9}$$

$$H_x = -j \frac{E_o \lambda}{2\eta} \sin \frac{\pi x}{w} \cos \frac{\pi z}{\ell} \tag{10}$$

$$H_z = j \frac{E_o \lambda}{2\eta w} \cos \frac{\pi x}{w} \sin \frac{\pi z}{\ell} \tag{11}$$

The stored energy in a cavity resonator passes between the RF electric and RF magnetic fields. It can be calculated by determining the stored energy in the electric fields at the instant in time when the magnitude of the magnetic field is zero in the standing wave pattern and all energy is stored in the RF electric fields.

$$W_S = (W_E)_{max} = \frac{\varepsilon_o}{2} \int_0^w \int_0^h \int_0^\ell \left| E_Y \right|^2 dx\,dy\,dz \tag{12}$$

$$= \frac{\varepsilon_o}{2} \int_0^w \int_0^h \int_0^\ell E_o^2 \sin^2 \frac{\pi x}{w} \sin^2 \frac{\pi z}{\ell} dx\,dy\,dz \tag{13}$$

$$= \frac{\varepsilon_o \, w \, \ell \, h}{8} E_o^2 \tag{14}$$

and

$$E_o = (\frac{8W_s}{\varepsilon_o w \ell h})^{1/2} \tag{15}$$

In the equivalent lumped element, resonant circuit, the stored energy also oscillates between electric and magnetic field storage. At the instant in time when the capacitor is fully charged, the system stored energy is all in the form of electric field storage with a magnitude given by:

$$W_S = \frac{1}{2} C_p V_p^2 \tag{16}$$

In this case, V_p is the peak voltage developed across the equivalent lumped element capacitor.

The equivalent peak voltage, V_p, is defined in the cavity as the integral of the RF electric field along the maximum RF electric field contour...

$$V_p = \int_0^h E_o \, dz = E_o h \tag{17}$$

$$= (\frac{8W_s}{\varepsilon_o w h \ell})^{1/2} h \tag{18}$$

By substitution....

$$W_S = 1/2 \, C_p V_p^2 = 1/2 \, C_p \, (\frac{8W_s}{\varepsilon_o w h \ell}) \, h^2 \tag{19}$$

and

$$C_p = (\frac{\varepsilon_o w \ell}{4h}) \tag{20}$$

-26-

This calculated value has the same form as the familiar expression for the capacitance of a parallel plate capacitor without fringing electric fields. In the rectangular cavity, the RF electric fields are, indeed, straight lines between the cavity end plates and there are no fringing fields since the conductive walls of the resonator place firm boundaries on the region of stored energy. The factor (4) in the denominator of equation 20 merely reflects the fact that the RF electric field varies sinusoidally through half a cycle across the cavity end plates in two directions instead of being uniform as in a lumped element capacitor.

From the resonance equation we have...

$$\omega_o = \sqrt{\frac{1}{L_p C_p}} \tag{21}$$

and

$$L_p = \frac{1}{\omega_o^2 C_p} = \frac{4h}{\varepsilon_o \omega_o^2 \ell w} \tag{22}$$

A peak current for the equivalent circuit of the main cavity can also be defined from the condition that the current is at its maximum value and all of the stored energy is in the magnetic field of the lumped element inductance.

$$W_s = 1/2 \ L \ I^2 \tag{23}$$

Similarly, the energy dissipated in the distributed resistive wall losses (W_L) of the cavity resonator determines an equivalent series resistance of the lumped element circuit

$$W_L = 1/2 \ I_p^2 \ R_p \tag{24}$$

-27-

This calculated value has the same form as the familiar expression for the capacitance of a parallel plate capacitor without fringing electric fields. In the rectangular cavity, the RF electric fields are, indeed, straight lines between the cavity end plates and there are no fringing fields since the conductive walls of the resonator place firm boundaries on the region of stored energy. The factor (4) in the denominator of equation 20 merely reflects the fact that the RF electric field varies sinusoidally through half a cycle across the cavity end plates in two directions instead of being uniform as in a lumped element capacitor.

From the resonance equation we have...

$$\omega_o = \frac{1}{\sqrt{L_p C_p}} \tag{21}$$

and

$$L_p = \frac{1}{\omega_o^2 C_p} = \frac{4h}{\varepsilon_o \omega_o^2 \ell w} \tag{22}$$

A peak current for the equivalent circuit of the main cavity can also be defined from the condition when the current is at its maximum value and all of the stored energy is in the magnetic field of the lumped element inductance.

$$W_s = 1/2\ L_p I_p^2 \tag{23}$$

Similarly, the energy dissipated in the distributed resistive wall losses (W_L) of the cavity resonator determines an equivalent series resistance of the lumped element circuit

$$W_L = 1/2\ I_p^2 R_p \tag{24}$$

-27-

Additional information is required to obtain the correct value for the equivalent series resistance (R_p) of the main stabilizing cavity. The value for Q_o measured from the output port of a coaxial magnetron gives a composite value for the combined stabilizing cavity and the anode vane system. These two systems typically have a large disparity in their values for individual internal Q_o's. Consequently, for accuracy it would be necessary to make a separate measurement to determine the stabilizing cavity internal Q_{o-sc} with the anode system replaced by a smooth cylinder. In this case,

$$R_p = \frac{\omega_o L_p}{Q_{o-sc}} \tag{25}$$

On the other hand, experience with a large number of tubes over a wide range of frequencies has shown that the measured composite Q_o of the completed tube is of the order of one half of that for the isolated stabilizing cavity. Hence, in lieu of an actual experimental measurement and to provide some intuitive insight, we can make the approximation that:

$$R_p = \frac{\omega_o L_p}{2Q_o} \tag{26}$$

Mutual inductance between a primary circuit and a secondary electromagnetically-coupled circuit is defined in terms of the number of flux linkages in the coupled circuit per unit of current flow in the primary circuit. In addition, the self-inductance, L_p, of the primary circuit is determined in terms of the number of flux linkages in the primary circuit per unit

-28-

Additional information is required to obtain the correct value for the equivalent series resistance (R_p) of the main stabilizing cavity. The value for Q_o measured from the output port of a coaxial magnetron gives a composite value for the combined stabilizing cavity and the anode vane system. These two systems typically have a large disparity in their values for individual internal Q_o's. Consequently, for accuracy it would be necessary to make a separate measurement to determine the stabilizing cavity internal Q_{o-sc} with the anode system replaced by a smooth cylinder. In this case,

$$R_p = \frac{\omega_o L_p}{Q_{o-sc}} \tag{25}$$

On the other hand, experience with a large number of tubes over a wide range of frequencies has shown that the measured composite Q_o of the completed tube is of the order of one half of that for the isolated stabilizing cavity. Hence, in lieu of an actual experimental measurement and to provide some intuitive insight, we can make the approximation that:

$$R_p = \frac{\omega_o L_p}{2Q_o} \tag{26}$$

Mutual inductance between a primary circuit and a secondary electromagnetically-coupled circuit is defined in terms of the number of flux linkages in the coupled circuit per unit of current flow in the primary circuit. In addition, the self-inductance, L_p, of the primary circuit is determined in terms of the number of flux linkages in the primary circuit per unit

-28-

of current flow in the primary circuit or; i.e.,

$$L_p \simeq \frac{\emptyset_p}{I_p} \tag{27}$$

$$M_s \simeq \frac{\emptyset_s}{I_p} \tag{28}$$

Consequently, the mutual inductance, M_s, can be evaluated in terms of the primary self-inductance, L_p, by determining the portion of the flux linkages of the primary circuit that couple to the secondary circuit.

$$M_s = \frac{\emptyset_s}{\emptyset_p} \times L_p \tag{29}$$

The flux density, B, at any point in the cavity is given by $B = \mu H$. In particular

$$B_x = \mu H_x = -j \frac{\mu \lambda E_o}{2\eta \ell} \sin \frac{\pi x}{w} \cos \frac{\pi z}{\ell} \tag{30}$$

The value of H_x is maximum at the mid plane of the cavity at the wall. It is constant across the cavity height and decreases to zero at the center of the cavity along the same mid plane. Beyond that point, the H_x fields reverse direction since the magnetic flux lines are loops which close upon themselves. Hence, the total flux linkages in the primary cavity is proportional to the integral of B along the mid plane of the cavity from the wall to the center.

-29-

$$\phi_p \simeq \int_0^h \int_0^{\ell/2} B \, da \tag{31}$$

$$\simeq \int_0^h \int_0^{\ell/2} \mu H_x \, dy \, dz \tag{32}$$

$$\simeq \int_0^h \int_0^{\ell/2} \frac{-j\mu E_o \lambda}{2\eta\ell} \cos \frac{\pi z}{\ell} \, dy \, dz \tag{33}$$

$$\simeq \frac{-j\mu E_o \lambda}{2\eta\ell} \frac{\ell}{\pi} h = \frac{-j\mu\lambda h}{2\eta\pi} E_o \tag{34}$$

A similar calculation can be made for the flux linkages through
the secondary circuit dependent upon the cross-sectional area of
the secondary loop and its orientation and location within the
cavity. For the tuning geometries being considered, it is conven-
ient to assume that the diodes are brazed directly to the cavity
wall at the mid plane with the bias leads forming a rectangular
coupling loop as shown schematically in Figure 9. The coupling
loop extends for some distance, h', along the cavity wall and
some distance, ℓ', into the cavity toward the center. Hence..

$$\phi_s \simeq \int_0^{h'} \int_0^{\ell'} B \, da = \int_0^{h'} \int_0^{\ell'} \mu H_x \, dy \, dz \tag{35}$$
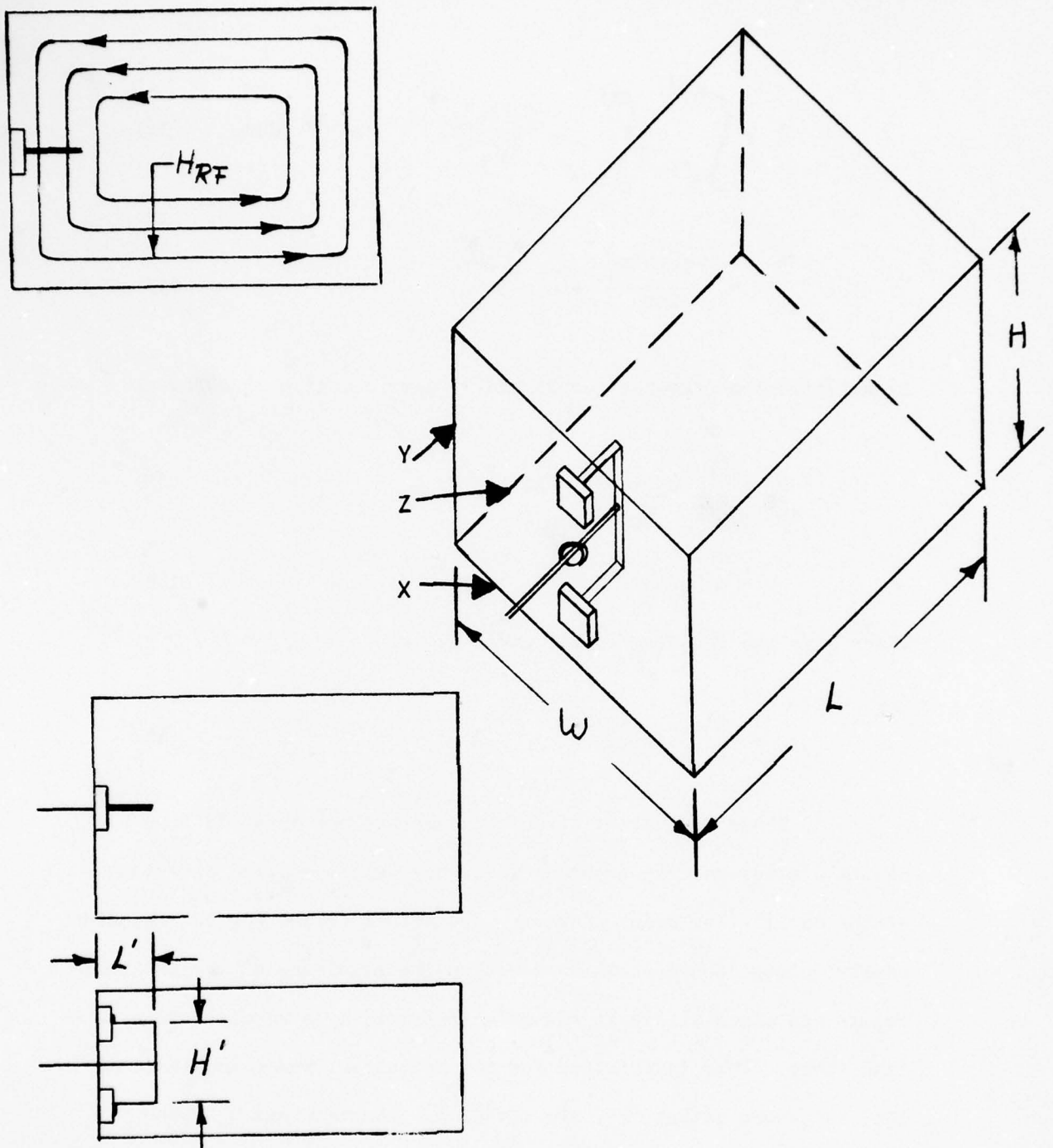
FIGURE 9

PIN DIODE CONTROLLED, COUPLED CIRCUIT LOCATED IN A
RECTANGULAR WAVEGUIDE CAVITY.

-31-

$$\phi_s \simeq \int_0^{h'} \int_0^{\ell'} \frac{-j\mu E_o \lambda}{2\eta \ell} \cos \frac{\pi z}{\ell} \, dy \, dz \qquad (36)$$

$$\simeq \frac{-j\mu\lambda h' E_o}{2\eta\pi} \sin \frac{\pi \ell'}{\ell} \qquad (37)$$

By substitution of equations 34 and 37 into equation 29 we have..

$$M_s = \frac{\phi_s}{\phi_p} L_p = \frac{h'}{h} \sin \frac{\pi \ell'}{\ell} \; L_p \qquad (38)$$

$$= a \, L_p \qquad (39)$$

where $\underline{a}$ is the coupling factor given by....

$$a = \left(\frac{h'}{h} \sin \frac{\pi \ell'}{\ell}\right) \qquad (40)$$

These equivalent circuit parameters are obtained from the cavity dimensions, the resonant frequency, and the field equations of the oscillating mode. However, the actual values for the resonant cavity voltage and current depend upon the magnitude of the RF field levels contained within it and more information is required to establish these. This is obtained for the magnetron from a knowledge of the peak power output, P_o, the loaded Q_L, the internal Q_o, the external Q_E, and the cavity resonator circuit efficiency, η_c. These parameters are determined by measurement. By definition[4]...

$$Q = 2\pi \frac{\text{energy stored in a resonant circuit}}{\text{energy lost per cycle}} \qquad (41)$$

-32-

$$= 2\pi \frac{W_S}{W_L} \tag{42}$$

Q is a dimensionless quantity. This is assured by the proportionality constant 2π radians/cycle.

The energy lost per cycle for the magnetron consists of the energy delivered to the load and the energy dissipated in the internal losses. Therefore, the total energy lost per cycle is related to the peak power output, circuit efficiency, and resonant frequency by....

$$W_L = \frac{P_o}{\eta_c f_o} \tag{43}$$

For a value of loaded Q_L we have...

$$Q_L = 2\pi f_o \eta_c \frac{W_S}{P_o} = \frac{\omega_o \eta_c W_s}{P_o} \tag{44}$$

or

$$W_S = \frac{Q_L P_o}{\omega_o \eta_c} \tag{45}$$

In a coaxial magnetron the internally stored energy is located partially in the stabilizing cavity and partially in the anode vane system. As noted before, an experimental measurement of the internal Q_o made from the output port of the tube gives only a composite value. But the interest in the present application is concerned only with effects in the stabilizing cavity which is

-33-

where the tuning diodes will be located. Information from other experiments based upon interpretation of measured changes in tuning curves of a stabilizing coaxial cavity with a smooth central coaxial conductor compared to one with an actual anode system shows that typically the fraction of the total internally stored energy (K) in the stabilizing cavity is about 85% (K = .85). Hence, the stored energy, W_P, contained only in the equivalent circuit primary resonator is given by...

$$W_P = \frac{KQ_L P_o}{\omega_o \eta_c} \qquad (46)$$

By equating (46) to the previously derived value for the stored energy in the equivalent rectangular cavity (equation 14), we determine a value for the peak of RF electric field strength in the cavity; e.g.

$$E_o = \left(\frac{8KQ_L P_o}{\varepsilon_o \eta_c \omega_o w\ell h}\right)^{1/2} \qquad (47)$$

The peak RF voltage across the center of the cavity and across the equivalent cirucit primary is...

$$V_P = E_o h = \left(\frac{8KQ_L P_o h}{\varepsilon_o \eta_c \omega_o w\ell}\right)^{1/2} \qquad (48)$$

Similarly, by substituting the value for the energy stored in the primary resonator (equation 46), a value for the primary circuit equivalent peak current is obtained from equation 23.

$$I_P = \left(\frac{\varepsilon_o \omega_o K Q_L w \ell}{2 \eta_c h} P_o \right)^{1/2} \qquad (49)$$

4.2   The Tuning Range Obtainable with Diode Switching

The tuning of the primary cavity caused by a change of impedance of the coupled circuit brought about by switching diodes can now be calculated. The equivalent circuits shown in Figure 6 are used. The closed loop impedance of the primary equivalent resonant circuit with a single coupled secondary circuit is given by[5]:

$$j\omega L_P + \frac{1}{j\omega C_P} + R_P + \frac{(\omega M_S)^2}{R_S + j\omega L_S + \frac{1}{j\omega C_S}} = 0 \tag{50}$$

$$j(\omega L_P - \frac{1}{\omega C_P}) + R_P + \frac{(\omega M_S)^2}{R_S + j(\omega L_S - \frac{1}{\omega C_S})} = 0 \tag{51}$$

$$j(\omega L_P - \frac{1}{\omega C_P}) + R_P + \frac{(\omega M_S)^2}{R_S + jX_S} = 0 \tag{52}$$

$$j(\omega L_P - \frac{1}{\omega C_P}) + R_P + \frac{(\omega M_S)^2 R_S}{R_S^2 + X_S^2} - j\frac{(\omega M_S)^2 X_S}{R_S^2 + X_S^2} = 0 \tag{53}$$

$$R_P + \frac{(\omega M_S)^2 R_S}{R_S^2 + X_S^2} + j(\omega L_P - \frac{1}{\omega C_P} - \frac{(\omega M_S)^2 X_S}{R_S^2 + X_S^2}) = 0 \tag{54}$$

The condition for resonance is taken to be that frequency for which the reactance term is zero. Hence,

$$\omega^2 (L_P - \frac{\omega M_S^2 X_S}{(R_S^2 + X_S^2)}) - \frac{1}{C_P} = 0 \tag{55}$$

$$\omega^2 = \frac{1}{L_P C_P} (1 - \frac{\omega M_S^2 X_S}{L_P(R_S^2 + X_S^2)})^{-1} \tag{56}$$

-36-

But

$$\omega_o^2 = (L_P C_P)^{-1} \text{ and } M_S = a L_P$$

Hence

$$\omega = \omega_o \left(1 - \frac{a^2 \omega L_P X_S}{R_S^2 + X_S^2}\right)^{-1/2} \qquad (57)$$

For the small frequency changes to be obtained with each coupled secondary circuit of the electronic-tuned magnetron, ωL_P can be taken to be the same as $\omega_o L_P$, which is the primary resonator inductive reactance, X_{LP}, at the initial resonant frequency. Furthermore, the voltage breakdown restriction on the diodes will limit, in practice, the tolerable values of mutual inductance between the two systems in the case of high values of RF field in the primary cavity, such as exists in a magnetron. Therefore, values for the coupling factor, a, will be significantly less than unity. Hence, the term in brackets can be written as a series expansion, and neglecting higher order terms we have....

$$\omega = \omega_o \left(1 + \frac{1}{2} \frac{a^2 \omega_o L_P X_S}{R_S^2 + X_S^2}\right) \qquad (58)$$

$$= \omega_o \left(1 + \frac{1}{2} \frac{a^2 X_{LP} X_S}{Z_S^2}\right) \qquad (59)$$

In the proposed tuning scheme there will be some number (n) of secondary cirucits employed. The total frequency shift from the initial resonant frequency of the unperturbed

-37-

cavity can be approximated by....

$$\omega = \omega_o \left(1 + \frac{n_1}{2} \ \frac{a^2 X_{LP} X_{S1}}{Z_{S1}^2} + \frac{n_2}{2} \ \frac{a^2 X_{LP} X_{S2}}{Z_{S2}^2}\right) \tag{60}$$

where

n_1 = total number of secondary circuits in the reverse biased state

n_2 = total number of secondary circuits in the forward biased state

$n = n_1 + n_2$

A net negative reactance ($X_s = -X_C$) in a secondary circuit lowers the resonant frequency and a net positive reactance ($X_S = X_L$) raises the resonant frequency.

For diode tuning, a secondary circuit is switched from one equivalent circuit to another; i.e., from Z_{S1} to Z_{S2}. Therefore, for a single circuit change...

$$\frac{\Delta f}{f} = \frac{1}{2} a^2 X_{LP} \left(\frac{X_{S2}}{Z_{S2}^2} - \frac{X_{S1}}{Z_{S1}^2}\right) \tag{61}$$

For a rigorous calculation of the tuning obtained with multiple secondary circuits coupled to the primary circuit, it would be necessary to calculate a new set of equivalent circuit parameters after each switching operation taking into account the change of reflected impedance into the primary circuit, but again the frequency excursion planned for this tuning technique is small

-38-

(less than 2%). Therefore, it is reasonable to assume, to a first order, that n identical secondary circuits, each producing a small frequency shift, will lead to a total frequency shift that will be very nearly n times that calculated above.* At the very least, this viewpoint allows the equivalent circuit model to be used for consideration of the various trade-offs that can be made between operational and physical parameters to obtain the best compromise for performance with an electronically-tuned magnetron.

The resistive component of impedance in a secondary circuit changes with diode switching. In the reverse biased state, the total resistive losses consist of the skin resistance of the bias leads, the solder joint contact losses, and the large shunt leakage resistance across the diode. As noted before, the shunt leakage resistance can be replaced by an equivalent series resistance which would have a very low value. The sum of these resistances is represented by R_{rb}. In the forward biased state, a secondary circuit resistance consists of the skin resistance of the bias leads, the solder joint contact losses, and the forward RF dynamic resistance of the diode. The sum of these resistances is represented by R_{fb}. In either case, the losses of the secondary circuits will contribute to a reduction in Q_o of the composite resonant circuit which will have a direct influence on the degradation of peak power output across the tunable bandwidth as the frequency is changed. The internal Q_o of the uncoupled primary resonant circuit is given by....

_____
*Mutual interaction effects between secondary circuits have not been considered.

-39-

$$Q_o = \frac{\omega L_P}{R_P} \qquad \qquad (62)$$

The rigorous calculation of Q_o as a function of frequency as the secondary circuits are diode switched would require consideration of both the change of the effective inductance caused by the coupled reactance as well as the change in coupled resistive components. The change in effective inductance, of course, alters the total stored energy. However, again, since the total frequency shift to be expected is small, we can neglect the effect of the small changes of L_P on Q_o and consider only the effect of the coupled resistive components. The value for the modified Q_o' of the cavity including the secondary coupled circuit can be written in terms of Q_o for the unmodified cavity as follows...

$$Q_o' = \frac{\omega L_P}{R_P + n_1 \left(\frac{a X_{LP}}{Z_{S1}}\right)^2 R_{rb} + n_2 \left(\frac{a X_{LP}}{Z_{S2}}\right)^2 R_{fb}} \qquad (63)$$

$$= \frac{Q_o}{1 + n_1 \left(\frac{a X_{LP}}{Z_{S1}}\right)^2 \frac{R_{rb}}{R_P} + n_2 \left(\frac{a X_{LP}}{Z_{S2}}\right)^2 \frac{R_{fb}}{R_P}} \qquad (64)$$

Equation 64 predicts the degradation in Q_o due to the secondary circuit losses reflected into the primary circuit of the equivalent circuit model. It is conceivable that additional factors could exist in the actual microwave cavity leading to further reduction in

-40-

Q_o that the equivalent circuit model does not take into account. For example, additional energy losses could occur as a result of mode conversion caused by mode shape perturbation as the secondary circuits are added to the cavities and/or are switched to produce a change of resonant frequency. Also, differential tuning effects could result since the diode tuning circuits will most likely not tune all cavity modes in the same way. Overlapping interfering modes that might result could be a serious problem, but these factors can only be evaluated by further examination of the actual microwave structure.

4.3   Operating Parameters of the Coupled Secondary Tuning Circuits

The magnitudes of the peak voltage and current induced
in a secondary circuit when the magnetron is operating are calcu-
lated by the following equations:

$$V_{PS} = I_P \omega M_S = I_P a \omega L_P = a I_P X_{LP} \tag{65}$$

$$I_{PS} = \frac{V_{PS}}{Z_S} = \frac{I_P \omega M_S}{Z_S} = \frac{I_P a \omega L_P}{Z_S} = \frac{a I_P X_{LP}}{Z_S} \tag{66}$$

The peak RF voltages developed across the diode junction capaci-
tance (V_C) and lead inductance (V_L) in the reverse biased state
(Condition 1) are given by...

$$V_{CS-1} = I_{PS-1} \, X_{CS-1} = \frac{I_P a X_{LP}}{Z_{S-1}} \, X_{CS-1} \tag{67}$$

$$V_{LS-1} = I_{PS-1} \, X_{LS-1} = \frac{I_P a X_{LP}}{Z_{S-1}} \, X_{LS-1} \tag{68}$$

In the forward biased state (Condition 2) the voltage developed
across the diode lead inductance loop (V_L) is given by...

$$V_{LS-2} = I_{PS-2} \, X_{LS-2} = \frac{a I_P X_{LP}}{Z_{S-2}} \, X_{LS-2} \tag{69}$$

In these equations (65-69) the convenient assumption is made that
the current in the primary circuit, I_P, remains essentially

-42-

unchanged for a secondary circuit coupled to the primary as it is switched from one condition to another. This approximation is reasonable for a single secondary circuit since its perturbing influence will be kept small by design. However, a more rigorous analysis for multiple secondary would have to take into account the total impedance coupled into the primary circuit which will alter the primary current as the frequency is changed. In essence, the whole problem would have to be solved for each switching condition. This can be tedious and is not essential for an initial intuitive understanding of the quantitative interplay between the circuit parameters.

For reasons given elsewhere, the switching sequence for the secondary circuits when the magnetron is delivering power is always from a reverse biased condition to a forward biased condition. In the reverse biased condition, the resistive losses of the diode are very small since the equivalent series resistance (R_{SHeq}) of the high impedance shunt leakage path across the diode (R_{SH}) is small. The predominant resistive loss of the circuit for this condition will be that of the solder joints, the skin resistance of the connecting leads and that of the cavity wall or end plate. The peak power, P_{d1}, dissipated in the diode in Condition 1 will be given by....

$$P_{d1} = \frac{1}{2} I_{PS-1}^2 R_{SHeq} \tag{70}$$

In the forward biased state, the predominant resistive component will be that of the diode RF dynamic resistance (R_{SD}). This

-43-

conclusion is based upon the current state-of-the-art diodes where RF dynamic resistances are of the order of one ohm. The peak power dissipated (P_{d2}) in the diode in Condition 2 is given by....

$$P_{d2} = \frac{1}{2} \; I_{PS-2}^2 \; R_{SD} \tag{71}$$

These quantities must be multiplied by the magnetron duty factor to get the average power dissipated.

These equations can now be used to consider the trade-offs that can be made to optimize the performance obtainable with diode tuning. The design of the magnetron cavity is determined from tube considerations and cannot be considered as a variable. Therefore, the attention must be directed to the secondary circuit parameters and the coupling impedance between the two systems. Equations 67 and 69 show that for any operating power level corresponding to a primary circuit current, I_P, the RF voltage developed across the diode is proportional to $\frac{aX_S}{Z_S}$. The coupling factor, $\underline{a}$, and the secondary circuit impedance, Z_S, can be adjusted to limit the value of RF voltage to which the diode is subjected. However, equation 61 shows that the obtainable frequency shift is proportional to $\frac{a^2 X_{LP} X_S}{Z_S^2}$. Therefore, decreasing the coupling between the two systems or increasing the secondary circuit impedance to decrease the RF voltage applied to the diode will also reduce the obtainable frequency shift for a coupled secondary circuit. On the other hand, equation 64 shows that the added reflected resistive loss in

-44-

primary circuit leading to a reduction in Q_o' is proportional
to $(aX_{LP}/Z_S)^2$. Hence, the coupled losses increase or decrease in
proportion to the frequency shift obtained. This means that the
circuit parameters can be adjusted to limit the RF voltage applied
to the diodes in the reverse biased state without sacrifice in
total frequency shift obtainable. It would just be necessary
to add additional secondary circuits to make up for the smaller
frequency shift obtained per circuit. The total resistive loss
coupled to the primary circuit will be about the same. The only
added complexity is the need for additional diode switching circuitry.
This will be discussed elsewhere.

Equation 61 shows that the tuning shift for a secondary
circuit is also influenced by the change in the secondary circuit imped-
ance as the diodes are switched. In each case, the net impedance
in the circuit should be reactive. If the secondary circuit should
happen to be purely resistive, as it would be at the series resonant
condition, there is no tuning effect on the cavity. The secondary
circuit would simply be a load on the cavity and dissipate power
without contributing to the tuning effect. Furthermore, the voltage
across the diode would be very large since the secondary loop
current would be limited only by the small resistive losses. This
is not desirable from RF breakdown considerations. On the other
hand, the obtainable tuning range can be large also if the net
complex impedance is small, but this leads to a greater reduction
in Q_o' because the I^2R losses in the secondary circuit will become

-45-

large. Consequently, it is apparent that a variety of considerations must be made in designing the secondary circuit impedance. Preferably the net reactance in each state should be large compared to the value of series resistance. In that case, equation 61 can be written...

$$\frac{\Delta f}{f} = \frac{1}{2} \; a^2 X_{LP} \; (\frac{1}{X_{S2}} - \frac{1}{X_{S1}}) \qquad (72)$$

The net reactance in the forward biased state, with the diode capacitance short circuited, will always be inductive; hence, $X_{S2} = X_L$. By a judicious choice of lead inductances and diode junction capacitance, the net reactance in the reversed biased state can be made capacitive and $X_{S1} = -X_C$. This combination is desirable since equation 14 shows that the reduction in Q_o' depends inversely upon the magnitude of Z_S^2; hence, the algebraic sign of the reactance term is not important. Equation 72, on the other hand, shows that this choice of reactances of opposite algebraic sign leads to a higher frequency shift than would occur if both net reactances were inductive. Further yet, it is also possible to deliberately select the lead inductance so that the net reactance in both states is a large value of inductive reactance. This, too, limits the value of RF voltage across the diode in the reversed biased state, but at the expense of a lower frequency shift for secondary circuit change. But, this also leads to a lower reflective loss to the primary circuit.

-46-

Furthermore, it will be seen that this secondary circuit design may also have some specific advantages for intrapulse tuning. It is apparent, therefore, that several options can be considered. Some sample calculations to be presented will show the predicted results for several design selections.

4.4   Tuning Rates with Diode Switching

The program objectives list two tuning range-rate
options. These include Option A, 300 MHz tuning range tuned at
a 50 MHz per millisecond tuning rate, and/or Option B, 100 MHz
tuning range at a 100 MHz per microsecond tuning rate. Both
are for a tube designed for 16.3 GHz. It is desirable for the
tube to have the capability of performing both tasks. Option A
can be accomplished with present state-of-the-art electromechanical
tuning schemes, such as Varian's Dither[R] tuned coaxial magnetrons,
but these are not purely electronic tuned devices and have other
limitations. Present tubes of this type at Ku-band can tune across
a 250 MHz tuning range at a 200 Hz rate. A 300 MHz tuning range
at the same tuning rate could be developed. These tubes cover the
full tuning range twice during each tuning cycle. This corresponds
to a 100 MHz per millisecond tuning rate. These electromechanical
tuning schemes dither the frequency in a sinusoidal manner, and
the frequency agility performance follows a prescribed format on
a pulse-to-pulse basis.

In all cases the diode switching sequence for tuning
will proceed, as stated previously, by switching the diodes from
the reverse to the forward biased state. The required switching
time will be limited in part by the diode properties but will be
limited primarily by the properties of the diode switching modulator.
These factors are discussed elsewhere. This diode switching sequence
is selected because the diodes can be switched from the reverse to

-48-

forward biased states in a time interval less than that required
to turn the diodes off. For the pulse-to-pulse frequency agility
mode of operation, the appropriate diodes required to tune the
stabilizing cavity to a particular available frequency will be
switched to the forward biased state prior to cathode pulsing
the magnetron. The diodes are then reset to a reverse biased
state, if necessary, after the magnetron is turned off and during
the inter-pulse period. This inter-pulse period is typically
much longer than the time required to reverse bias the diodes and
to allow them to fully recover to an "off" state. In other words,
all diode switching is done when the secondary tuning circuit is
not being driven by microwave energy in the coaxial cavity. With
this electronic tuning technique, the selected frequency can be
chosen at random or in any prescribed sequence from among those
frequencies obtainable in the tuning range, dependent upon the
logic circuitry used to control the diode switching modulator.
It is clear therefore that the diode switched tuning technique
can easily obtain the required tuning rates of Option A.

The tuning rate objectives of Option B are well beyond
the state-of-the-art for any electromechanical tuning technique
currently employed or envisioned for any type of pulsed magnetron
oscillator. These requirements can only be met by some form of
electronically tuned tube. A tuning rate of 100 MHz per micro-
second is much faster than necessary for ordinary magnetron
operation. Therefore, it is assumed that the objective is intra-
pulse frequency tuning, leading to the possibility of using a

-49-

magnetron in a pulse compression radar or some other sophisticated signal processing application. In this case the diodes will have to be switched during magnetron operation while the stabilizing cavity is driving all of the coupled secondary circuits. Several factors must be taken into account. A change of resonant frequency of a cavity is accompanied by a change of stored energy in the system. In the equivalent circuit model the stored energy subject to modification is that in the coupled secondary circuit. The question naturally arises as to whether the diode switched tuning technique has any significant tuning rate limitations. A complete analysis of the transition is complex because of the non-linear nature of the problem, but much insight to the phenomena can be obtained by considering several facets separately.

From conventional a.c. circuit theory, the peak real power dissipated in a circuit is $VI \cos \emptyset$ and the peak reactive power flowing in the system is $VI \sin \emptyset$ where $\emptyset$ is the phase angle between the peak voltage and peak current. The peak reactive power (P_R) in a coupled circuit is related to the stored energy (W_{SC}) in the coupled circuit by...

$$W_{SC} = \frac{P_R}{2\pi f_o}$$
(73)

The change in reactive power flow that accompanies a frequency change is...

$$\Delta P_R = P_{R1} - P_{R2}$$
(74)

In most cases, the circuit elements in the coupled secondary circuits will be selected so that the reactances are very much larger than the resistances. Hence, the phase angle will be very nearly $\pm 90°$,

-50-

dependent upon whether the reactance is inductive or capacitive. Therefore, the magnitude of the change in the average value of reactive power flow between the main cavity and the coupled secondary circuit can be written...

$$\Delta P_R = (I_P \omega_o M_S)^2 \quad (\frac{X_{S2}}{Z_{S2}^2} - \frac{X_{S1}}{Z_{s1}^2}) \tag{75}$$

$$= (I_P \omega_o M_S)^2 \quad (\frac{1}{X_{S2}} - \frac{1}{X_{S1}}) \tag{76}$$

$$= (I_P \omega_o a L_P)^2 \quad (\frac{1}{X_{S2}} - \frac{1}{X_{S1}}) \tag{77}$$

$$= 2 I_P^2 \omega_o L_P \quad \frac{a^2 \omega_o L_P}{2} \quad (\frac{1}{X_{S2}} - \frac{1}{X_{S1}}) \tag{78}$$

Substituting equation 49 for I_P, equation 22 for L_P, and using equation 72, this becomes...

$$\Delta P_R = \frac{\epsilon_o \omega_o K Q_L w \ell P_o}{\eta_c h} \quad \omega_o \quad \frac{4h}{\epsilon_o \omega_o^2 w \ell} \frac{a^2 \omega_o L_P}{2} \quad (\frac{1}{X_{S2}} - \frac{1}{X_{S1}}) \tag{79}$$

$$\Delta P_R = \frac{4 K Q_L P_o}{\eta_c} \quad (\frac{\Delta f}{f}) \tag{80}$$

From equations 73 and 80 we have....

$$\Delta W_S = \frac{\Delta P_R}{2 \pi f} = \frac{4 K Q_L P_o}{\omega_o \eta_c} \quad \frac{\Delta f}{f} \tag{81}$$

$$= 4 W_P \frac{\Delta f}{f} \tag{82}$$

-51-

This result is the same as that predicted by the perturbation formula derived by Slater[6,7] for the relationship between the change of stored energy and frequency shift of a microwave cavity due to insertion of a small perturbing object. His result was obtained by calculations based upon the electromagnetic field equations within a microwave resonator whereas the result here was obtained based upon an equivalent circuit analysis. In both derivations the change in resonant frequency and in stored energy must be small for the approximations that were used to be valid.

The change of stored energy in the system predicted by equation 82 must be dissipated in some manner. It is of interest to note where this is done and what, if anything, this implies about the diode operation. The stabilizing cavity functions as a driving generator and the coupled secondary circuits operate as a load with a complex impedance. Since the secondary circuits are not series resonant, there is an exchange of the reactive power between the load and generator each RF cycle. The switching time for the diode going from reverse bias to forward bias condition will be determined primarily by the diode switching modulator capability. In any event, several nanoseconds will be required for completion of the switching operation. During this time several tens of RF cycles will occur for a Ku-band magnetron. Hence, reactive power will be transferred between the generator and load many times during this interval. During the switching sequence the diode RF dynamic resistance in the lumped element equivalent circuit representation changes progressively from a

-52-

very large value shunt leakage resistance in parallel with the junction capacitance to a very low value resistance in series with the lead inductance. This change of resistance alters the Q of the cavity during the transition. Figure 10 illustrates this effect.

Figure 10 shows the detected signal of a swept frequency RF power source reflected from an S-band cavity resonator as the diode forward bias current is progressively increased from zero to its final value. The equipment used for this measurement was that shown in Figure 1. The shift in frequency and change in the internal Q_o as the bias current was changed is shown in Figure 11. Note that the shift in the resonant frequency is completed at a current level far below that of the final value of bias current. Also note that the internal Q_o drops considerably in value at low values of current for this experiment, but then recovers as the diode resistance approaches the final value at full forward biased conditions. Because of this, one might question the stability of the oscillator during this transition. But note also that nearly full recovery has been obtained at less than 1% of the final bias current level. If we assume that the bias current is applied by a linear saw-toothed current pulse from zero to one hundred milliamps over a period of 10 nanoseconds, this data would show that the major variation in Q_o lasts for a period of less than 2 RF cycles. The transition would last an even shorter time if the diode modulator delivers a bias current pulse having a steeper rise time. Based upon intuitive reasoning, it does not seem likely that the magnetron will cease to oscillate as the result of such a short lived transient.
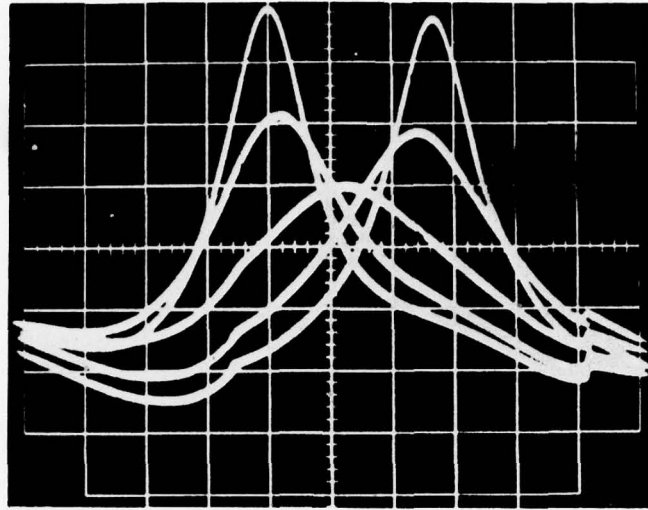
-53-

<u>FIGURE</u> 10

THIS FIGURE SHOWS THE OSCILLOSCOPIC DISPLAY OF DETECTED
SIGNALS FROM A SWEPT FREQUENCY SIGNAL SOURCE REFLECTED
FROM AN S-BAND DIODE-TUNED CAVITY. THE RESPONSE SHOWN
IS FOR FIVE DIFFERENT VALUES OF FORWARD BIAS CURRENT.
AN INCREASE IN RESONANT FREQUENCY OF 4 MHz IS SHOWN PRO-
GRESSING FROM LEFT TO RIGHT. AT VERY LOW BIAS CURRENTS
THE FREQUENCY SHIFT IS SMALL, BUT A SIGNIFICANT REDUCTION
IN LOADED Q OCCURS. INCREASING THE BIAS CURRENT STILL
FURTHER LEADS TO PROGRESSIVE FREQUENCY SHIFT WITH THE
LOADED Q RECOVERING IN VALUE TO A FINAL VALUE SOMEWHAT
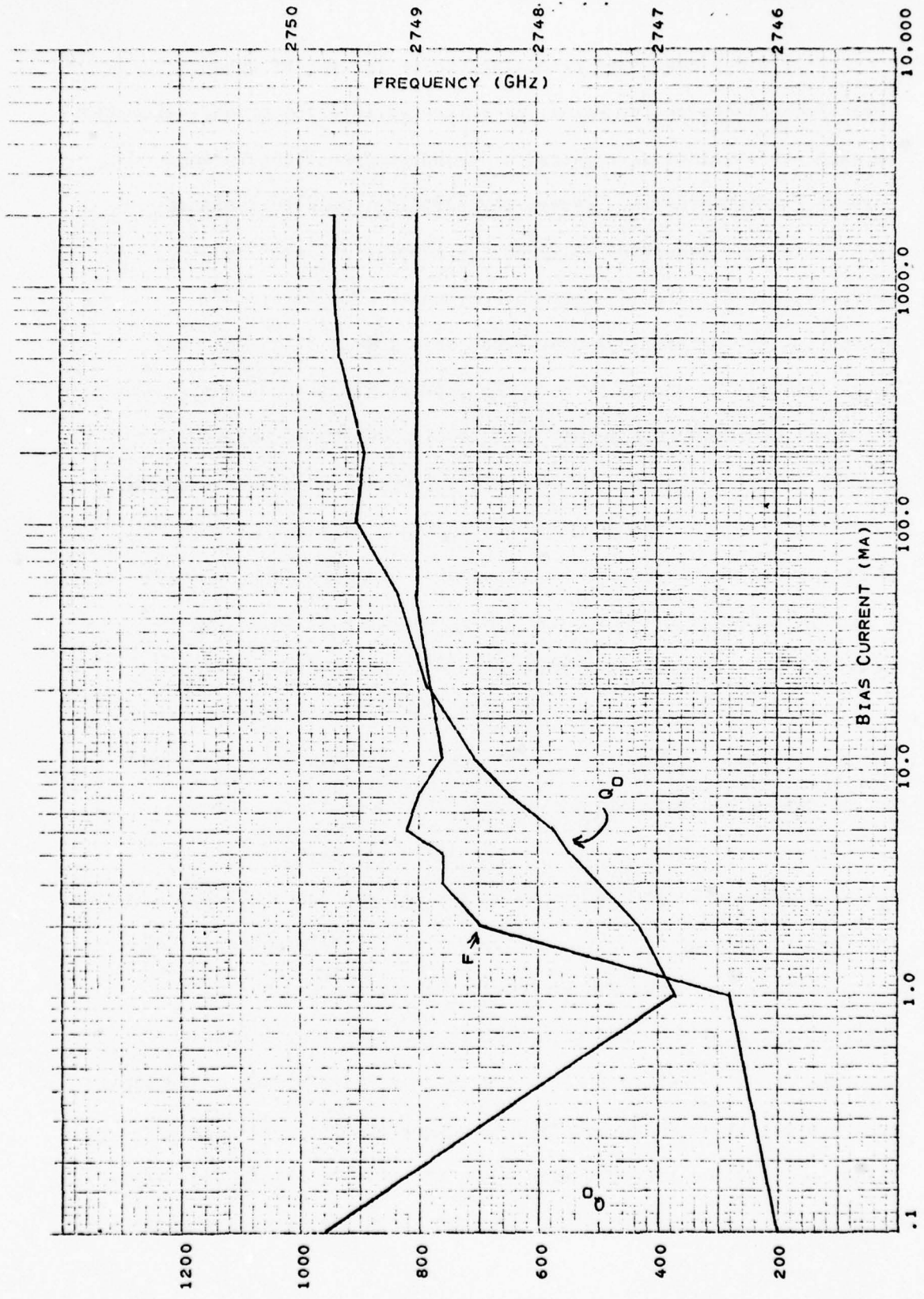LOWER THAN THE INITIAL VALUE.

-54-

FIGURE 11 - VARIATION OF RESONATOR FREQUENCY AND Q0 WITH CHANGE IN FORWARD BIAS CURRENT IN A COUPLED CIRCUIT.

In any case, the transitory value for the RF dynamic

resistance, whatever its value, is reflected into the primary circuit

to some other values of resistance dependent upon the coupling

between the two systems. Hence, the coupling could be designed

to minimize the reduction in Q_o at the expense of less frequency

shift per diode-switched, secondary circuit. The internally

stored energy that must be dissipated as a result of a switching

operation will be shared by both the primary and secondary circuits.

The exact division will depend upon the instantaneous circuit pro-

perties as the transition occurs. In any event, the thermal effect

on the diode can be calculated conservatively by assuming that all

of this power is dissipated in the diode. Clearly, this predicts

a much more severe impact on the diode than it will encounter in

in practice. Some sample calculations will be presented later.

Another approach to the design of the secondary circuit

can also be made to minimize the change in Q_o during the transition

as the diodes are switched during magnetron operation. It was

noted previously that the frequency shift could be maximized per

switched secondary circuit by having the net reactance be capacitive

for Condition 1 and inductive for Condition 2. This selection is

quite satisfactory when the circuit switching can be done in the

interpulse period when the magnetron is not operating. However,

when the diode is switched from reverse to forward biased conditions,

during a magnetron pulse, the junction capacitance passes through

all vales from the initial value of C_j to infinity and X_{CS} decreases

from its initial value to zero. At some value the secondary circuit

-56-

will be series resonants and, in principle, the $I^2 R_S$ losses can become very large with an attendant large reduction in Q_o. This can be avoided by selecting the secondary circuit parameters such that the net reactance is inductive in both Condition 1 and Condition 2. Then, as the diode is switched, the secondary circuit complex impedance will increase progressively in value from its initial to its final state without becoming series resonant. It can be seen, therefore, that the design of the coupled secondary circuits may be different dependent upon the kind of tuning to be accomplished.

Yet another question that can be considered for intra-pulse tuning is the ability of the cavity to change frequency with sufficient rapidity to follow the transition dictated by the coupled circuits. It is assumed that the change of the circuit reactance can be accomplished by the change of reactance elements since they are charged and discharged each RF cycle. However, it is also necessary that the excess stored energy be dissipated within the transition period. This can be accomplished easily. The energy stored in a resonant cavity will decay upon removal of the driving source according to the equation:

$$W_P(t) = W_P(o)\ e^{-\frac{\omega t}{Q_L}} \tag{83}$$

This equation shows that 63% of the internal stored energy will be dissipated in a time period of $Q_L/2\pi$ RF cycles. This is much more dissipation than required as a result of diode switching a secondary circuit. In practice, each intrapulse frequency shift

-57-

will only be a few MHz. Hence, in one switching operation we have....

$$\Delta W_P = W_P \ (o) - W_P \ (\Delta t) = W_P(1 - e^{-\frac{\omega \Delta t}{Q_L}}) \qquad (84)$$

Be equating equation 82 and 84 we have...

$$\frac{4\Delta f}{f} = (1 - e^{-\frac{\omega \Delta t}{Q_L}}) \qquad (85)$$

From equation 85 we obtain the time in RF cycles to dissipate the necessary stored energy for a frequency change to occur; i.e.,

$$\Delta t = \frac{Q_L}{2\pi} \ln \left(1 + \frac{4\Delta f}{f}\right) \text{ RF cycles} \qquad (86)$$

Even though the diode-tuned magnetron will shift only a few MHz per switching operation, *for sake of illustration*, we assume that a shift across the full intrapulse tuning bandwidth (100 MHz) occurs in one switching operation for a tube with a loaded Q_L of 750 at 16.3 GHz. Equation 86 shows that the excess stored energy could be dissipated in such a free running cavity in less than 3 RF cycles; i.e.,

$$\Delta t = \frac{Q_L}{2\pi} \ln \left(1 + \frac{4\Delta f}{f}\right) \qquad (87)$$

$$= \frac{750}{2\pi} \ln \left(1 + 4 \times \frac{100}{16300}\right) \qquad (88)$$

$$= 2.89 \text{ RF cycles} \qquad (89)$$

-58-

Since there are 16.3 RF cycles per nanosecond for the magnetron and since much smaller frequency shifts will actually be obtained during a switching operation requiring a time interval of several nanoseconds to accomplish, it is clear that properties of the microwave circuit will not be a limiting factor. It is believed intuitively that this will be true even though it is not a free running resonator, but continues to be driven by the magnetron electronic interaction mechanism. The rate at which the magnetron can shift frequency will be limited in practice only by the rate at which the diodes can be switched.

4.5   Diode Switching Power Requirements

        The d.c. power requirements for switching the operating

condition of the diodes in the coupled secondary circuits is quite

modest compared with that consumed by other electromechanical

systems used for obtaining frequency agility. The diode power

requirements consist of two components. The first is the charging

energy necessary to reverse bias the diodes each time they are

reset to this state. This amounts to $CV^2/2$. This stored energy

must be removed and dissipated each time when a diode is switched

to a forward biased state. The second requirement is the d.c.

power necessary to forward bias the diodes for the period of time

that the magnetron is operating. It is not necessary of course

to supply a forward bias current when the tube is not operating.

PIN diodes have a contact potential difference of approximately

0.6 volts that must be overridden by the forward bias power supply.

There are some resistive losses in the connecting leads so that

a 1 volt source may be required with enough forward bias current

to get the RF dynamic resistance of the diodes as low as possible.

This could require some value between 0.1 and 1.0 amps. Hence,

each diode in a forward biased state could require as much as

1 watt of d.c. power supplied at the same operating duty as the

magnetron, e.g. typically du = 0.001. Assume that there are 100

secondary circuits in a Ku-band cavity, each containing two diodes,

and assume that each obtainable frequency has an equal probability

of utilization. This means that on the average 50 secondary

circuits and 100 diodes would be in the forward biased state during

-60-

the magnetron operation, requiring as much as 100 mw of average

forward biasing power. We can also assume that all diodes are

reset to the reverse bias state during the inter-pulse period,

although this is certainly not necessary and probably would

not be done in practice. As an extreme case we can assume that

the diodes each require a reverse bias voltage of 1,000 volts,

although it is anticipated that much lower values will be satis-

factory for long lifetime diodes. Initial calculations indicate

that diode chips with a junction capacitance of 0.1 pfd will be

used for a Ku-band magnetron. We assume the magnetron operates

at 1,000 cps repetition. Therefore, the reset power required is

$\frac{1}{2}$ CV^2 x 100 x prf = 5 mw average. Hence, the total average modu-

lation power required to operate the diodes for tuning is 105 mw.

This is quite small compared with the 20 to 50 watts required

for tuning electromechanical frequency agile magnetrons.

The diode switching modulator and logistical drive

circuitry will require some d.c. power, but this is not expected

to be large. This will be discussed elsewhere. Also, the RF

power lost in the coupled secondary circuits does not effect

the tuning modulation power requirements. That power is supplied

indirectly by the magnetron's cathode pulse modulator.

4.6 Calculations of Electronic Tuning Parameters for a Ku-Band, Coaxial Magnetron

4.6.1 Coaxial Cavity Equivalent Circuit Elements

The equations derived in the previous sections will now be used to calculate the electronic tuning parameters for a 60 kW, Ku-band, coaxial magnetron. The dimensions of the stabilizing coaxial cavity are shown in Figure 12a together with typical values for Q's for such tubes. The equivalent rectangular cavity dimensions are shown in Figure 12b. The cross section of the rectangular cavity is the same as the cross section of any sector of the coaxial cavity and the rectangular cavity height, h, is equal to the mean circumference around the inside volume of the coaxial cavity. Figure 13 shows a Ku-band, coaxial magnetron with the top cover plate of the tube removed.

The capacitance for the lumped element equivalent circuit of the rectangular cavity without coupled secondary circuits is obtained from equation 20.

$$C_p = \frac{\epsilon_o w \ell}{4h} = 4.10 \times 10^{-15} \text{ Fd}$$

The lumped element inductance is obtained from equation 22.

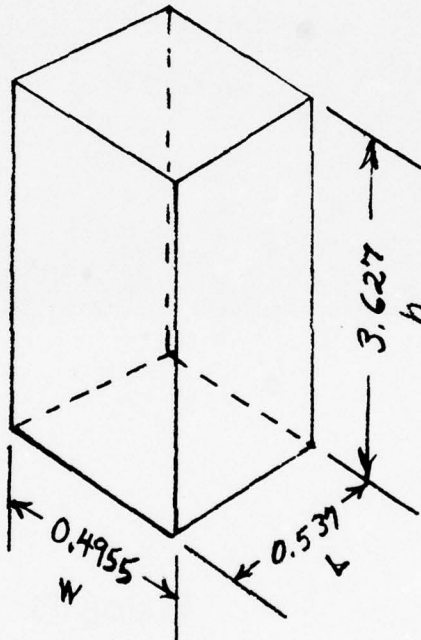$$L_p = \frac{1}{\omega_o^2 C_p} = 2.325 \times 10^{-8} \text{ H}$$

The primary inductive reactance of the equivalent circuit at 16.3 Ghz is 2381 ohms. The value for Q_o of the coaxial cavity given in Figure 12 is typical of the composite Q_o measured from the

-62-

TE$_{011}$ COAXIAL CAVITY

0.537

0.659
D$_1$

1.650
D$_2$

(A)

F$_O$ = 16.3 GHz

Q$_O$ = 3000

Q$_E$ = 1000

Q$_L$ = 750

ALL DIMENSIONS IN INCHES.
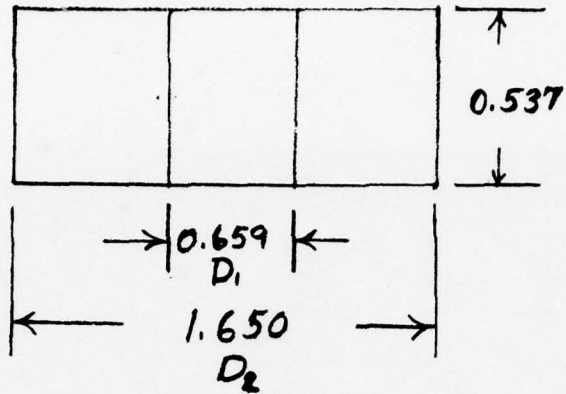
RECTANGULAR CAVITY EQUIVALENT OF TE$_{011}$ COAXIAL CAVITY.

(B)

3.627
h

0.4955
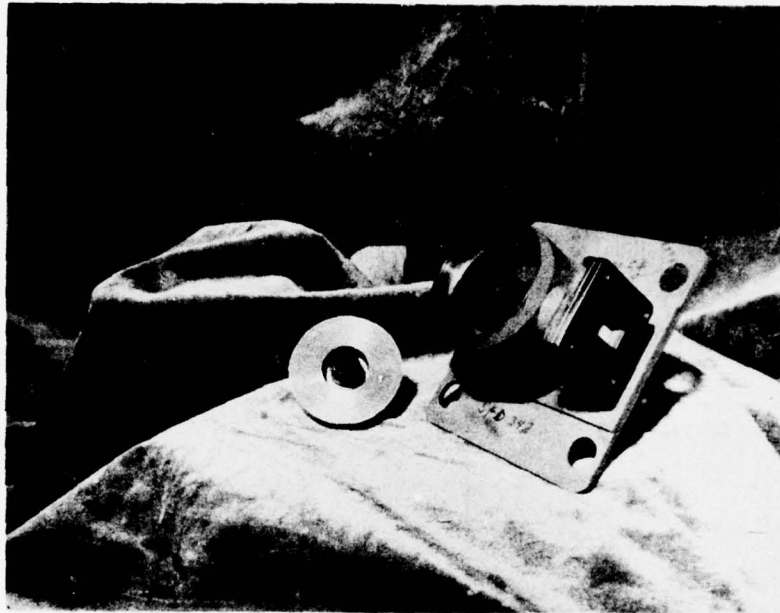W

0.537
L

FIGURE 12

RESONATOR DIMENSIONS

FIGURE 13

PHOTOGRAPH OF KU-BAND MAGNETRON - TOP REMOVED

-64-

output port of the magnetron. Since a measured value for Q_o of the coaxial cavity alone is not available; i.e., sans anode, the value for the equivalent series resistance of lumped element circuit is obtained using the estimated value given by equation 26.

$$R_p = \frac{\omega_o L_p}{2Q_o} = 0.4 \ \Omega$$

Equation 48 gives the peak voltage across the equivalent circuit primary (assume K = .85, η_c = .75).

$$V_p = \left(\frac{8KQ_L P_o h}{\epsilon_o \eta_c \omega_o w\ell}\right)^{1/2} = 2012 \ Po^{1/2} \quad \text{volts}$$

The peak primary current without coupled secondary circuits is given by equation 49.

$$I_p = \left(\frac{\epsilon_o \omega_o K Q_L w\ell P_o}{2\eta_c h}\right)^{1/2} = 0.845 \ Po^{1/2} \quad \text{amps}$$

4.6.2   Coupled Circuit Parameters

The properties of the secondary circuits depend upon the diodes, the bias lead connections, and the actual mounting configuration that is utilized. The equations for calculating the secondary circuit properties do not indicate a unique solution, but instead show that many possible combinations exist. Insight to the best approach can be obtained by considering a family of curves portraying the functional dependence of the significant parameters.

Tuning is accomplished by having a significant difference in the coupled circuit impedance in the two biased states for the diode. Consequently, the diode should have a significant amount of reactance at Ku-band and the self inductive reactance of the bias lead/coupling loop configuration should be large enough to yield a significant change when the diode is switched. As a practical matter, this dictates that PIN diodes with a reverse biased, junction capacitance value of the order of 0.05 to 0.2 pF be selected. For example, a capacitance of 0.1 pF has a reactance of about 100 ohms at Ku-band and two diodes in series for the coupled secondary loop will have a net capacitive reactance of 200 ohms. Since the diodes will have a resistive loss of the order of one ohm each, these values satisfy the requirement that the net reactive impedance be much larger than the resistance in the coupled circuit. Significantly larger values of junction capacity lead to net reactance values that are too small and diodes with significantly smaller junction capacitance are more difficult to fabricate. In addition,

-66-

the resistive losses may increase too much if the diode capacitance becomes too small.

The self inductance of the coupling loop between the two diodes is a function of the conductor cross section dimensions and the mounting configuration. From practical fabrication considerations, a rectangular loop geometry, as shown in Figure 5, is attractive. The low frequency, self inductance for a rectangular loop of a rectangular conductor can be calculated by[8]:

$$
L = 0.02339 \left[(S_1+S_2) \log \frac{2S_1S_2}{b+c} - S_1 \log (S_1+g) - S_2 \log (S_2+g) \right] + 0.01016 \left[2 g - \frac{S_1+S_2}{2} + 0.447 (b+c) \right] \mu H \tag{90}
$$

where

b = conductor thickness

c = conductor width

S_1 = height of the rectangular loop

S_2 = width of the rectangular loop

g = diagonal length of the rectangular loop

$\quad = (S_1^2 + S_2^2)^{1/2}$

All dimensions are in inches.

This equation is valid at low frequencies where current flow is essentially uniform throughout the conductor. At very high frequencies the skin effect causes the RF current to crowd into thin layers near the conductor surface and this can lead to a slightly lower value of self inductance. However, for the small dimensions of the conductor to be used here, the difference will not be significant.

-67-

Also, the formula was derived for a loop with a conductor of uniform cross section around the periphery whereas in the proposed mounting configuration the cavity wall forms part of the conductor path of the coupling loop. However, the wall currents in the TE_{011} mode flow in concentric circles, hence no significant radial spreading of current flow on the wall between the diodes is expected to occur. Also, to preserve this feature the coupling loops size should be kept small so that RF magnetic field lines associated with coupled circuit current flow will not have a circumferential component which could lead to energy conversion to non-resonant, non-circular electric mode components. This would cause additional unwanted loss to occur. Large loops should be made arcuate in form to avoid this by conforming to the field shape of the RF electric field lines. However, large loops are not likely to be used since they would result in too much coupling between the systems possibly leading to excessive voltage applied to the diodes. For all these reasons, the above expression is believed to give a reasonably accurate value for the self inductance for the loops that will be used.

Table I gives values of self inductance for several rectangular loop configurations formed from conductors with a cross section of 0.001 X 0.005 inches. It will be noted that, for a given perimeter of the loop, the maximum value of self inductance is obtained with a square shape. Hence for a specified value of self inductance, a square loop leads to the least amount of additional surface area for current flow and, therefore, to the least additional amount of bias lead resistive losses in the cavity.

-68-

TABLE I

SELF INDUCTANCE OF RECTANGULAR LOOPS OF RECTANGULAR CROSS SECTION (0.001 X 0.005 INCHES). SIDE DIMENSIONS OF LOOP IN INCHES, SELF INDUCTANCE IN NANOHENRIES.

S_1 \ S_2	0.010	0.020	0.030	0.040	0.050	0.060	0.070	0.080	0.090	0.100
0.010	0.279	0.495	0.703	0.910	1.115	1.320	1.525	1.730	1.935	2.139
0.020	0.495	0.812	1.102	1.385	1.664	1.942	2.220	2.496	2.772	3.048
0.030	0.703	1.102	1.451	1.784	2.111	2.434	2.755	3.075	3.394	3.713
0.040	0.910	1.385	1.784	2.159	2.523	2.881	3.235	3.587	3.938	4.287
0.050	1.115	1.664	2.111	2.523	2.919	3.306	3.688	4.066	4.443	4.817
0.060	1.320	1.942	2.434	2.881	3.306	3.719	4.125	4.527	4.925	5.321
0.070	1.525	2.220	2.755	3.235	3.688	4.125	4.554	4.976	5.394	5.809
0.080	1.730	2.496	3.075	3.587	4.066	4.527	4.976	5.417	5.854	6.286
0.090	1.935	2.772	3.394	3.938	4.443	4.925	5.394	5.854	6.307	6.755
0.100	2.139	3.048	3.713	4.287	4.817	5.321	5.809	6.286	6.755	7.218

The coupling factor between the main cavity and a secondary coupled cricuit with a rectangular loop when located in the optimum position is given by equation 40.

$$a = \frac{h'}{h} \sin \frac{2\pi \ell'}{\ell}$$

Table II shows the calculated coupling factor for several rectangular loop configurations. For small rectangular coupling loops, inspection of Table II, or equation 40, shows that a square loop also gives the largest coupling factor for a specified perimeter or conductor length. Hence, square shaped coupling loops will be used.

The presence of the bias lead feeding through a hole in the cavity end plate should cause no interfering effects if the coupled circuit impedance parameters are truly symmetrical about it. The balanced configuration will make the input bias lead an RF neutral conductor and will not contribute any detrimental effects.

Figure 14 shows the calculated self inductance (in nanohenries) of square loops of conductor (cross section = 0.001 X 0.005 inches) as a function of the side dimension (in mils) of the loop over the size range of interest. Figure 15 shows the calculated inductive reactance for the secondary circuit inductance at 16.3 GHz as a function of coupled loop size. Figure 16 shows the functional variation of the coupling factor with square loop size.

-70-

TABLE II

COUPLING FACTOR FOR RECTANGULAR LOOPS IN RECTANGULAR KU-BAND CAVITY
(ALL VALUES TO BE MULTIPLIED BY 10^{-4}).

$$a = \frac{h'}{h} \sin \frac{\ell'}{\ell} \times 180°$$

$\ell = 0.537$
$h = 3.627$

h' ↓ \ ℓ' →	0.010	0.020	0.030	0.040	0.050	0.060	0.070	0.080	0.090	0.100
0.010	1.612	3.219	4.814	6.393	7.950	9.480	10.978	12.438	13.855	15.225
0.020	3.224	6.437	9.628	12.786	15.901	18.961	21.956	24.876	27.711	30.451
0.030	4.836	9.656	14.442	19.180	23.851	28.441	32.934	37.314	41.566	45.676
0.040	6.448	12.874	19.257	25.573	31.802	37.921	43.912	49.751	55.421	60.901
0.050	8.060	16.093	24.071	31.966	39.752	47.402	54.889	62.189	69.276	76.127
0.060	9.673	19.312	28.885	38.359	47.702	56.882	65.867	74.627	83.132	91.352
0.070	11.284	22.530	33.699	44.752	55.653	66.362	76.845	87.065	96.987	106.577
0.080	12.897	25.749	38.513	51.146	63.603	75.843	87.823	99.503	110.842	121.802
0.090	14.509	28.967	43.327	57.538	71.553	85.323	98.801	111.941	124.698	137.028
0.100	16.121	32.186	48.141	63.932	79.504	94.803	109.779	124.379	138.553	152.253

$$L = 0.02339 \left[2S_l \log \frac{2S_l^2}{b+c} - 2S_l \log (1+\sqrt{2}) S_l \right] + 0.1016 \left[(2\sqrt{2} - 1) S_l + 0.447 (b+c) \right]$$

L (nH)

LOOP SIZE (MILS)
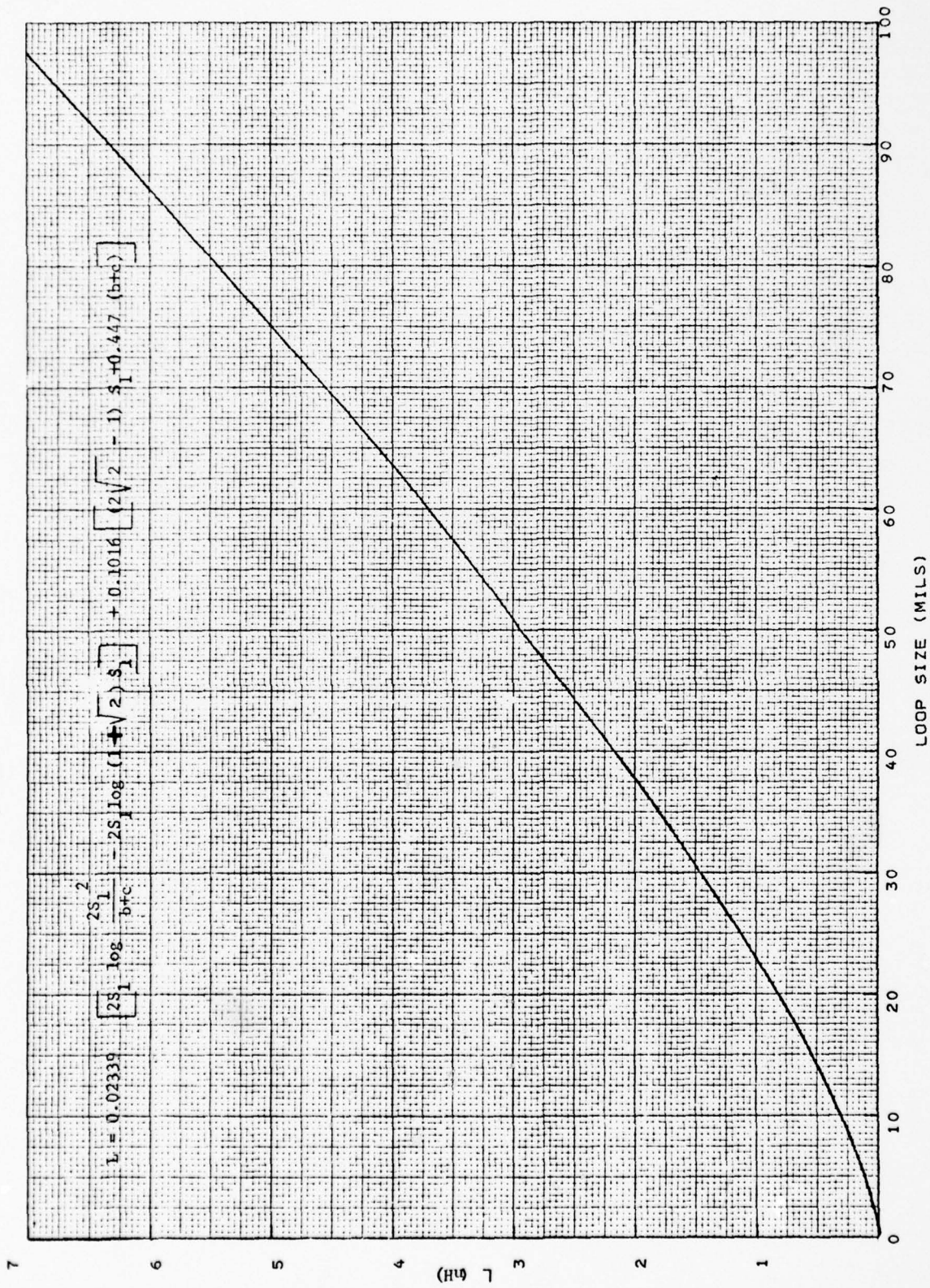
FIGURE 14 - CALCULATED SELF-INDUCTANCE OF SQUARE LOOP.

-72-
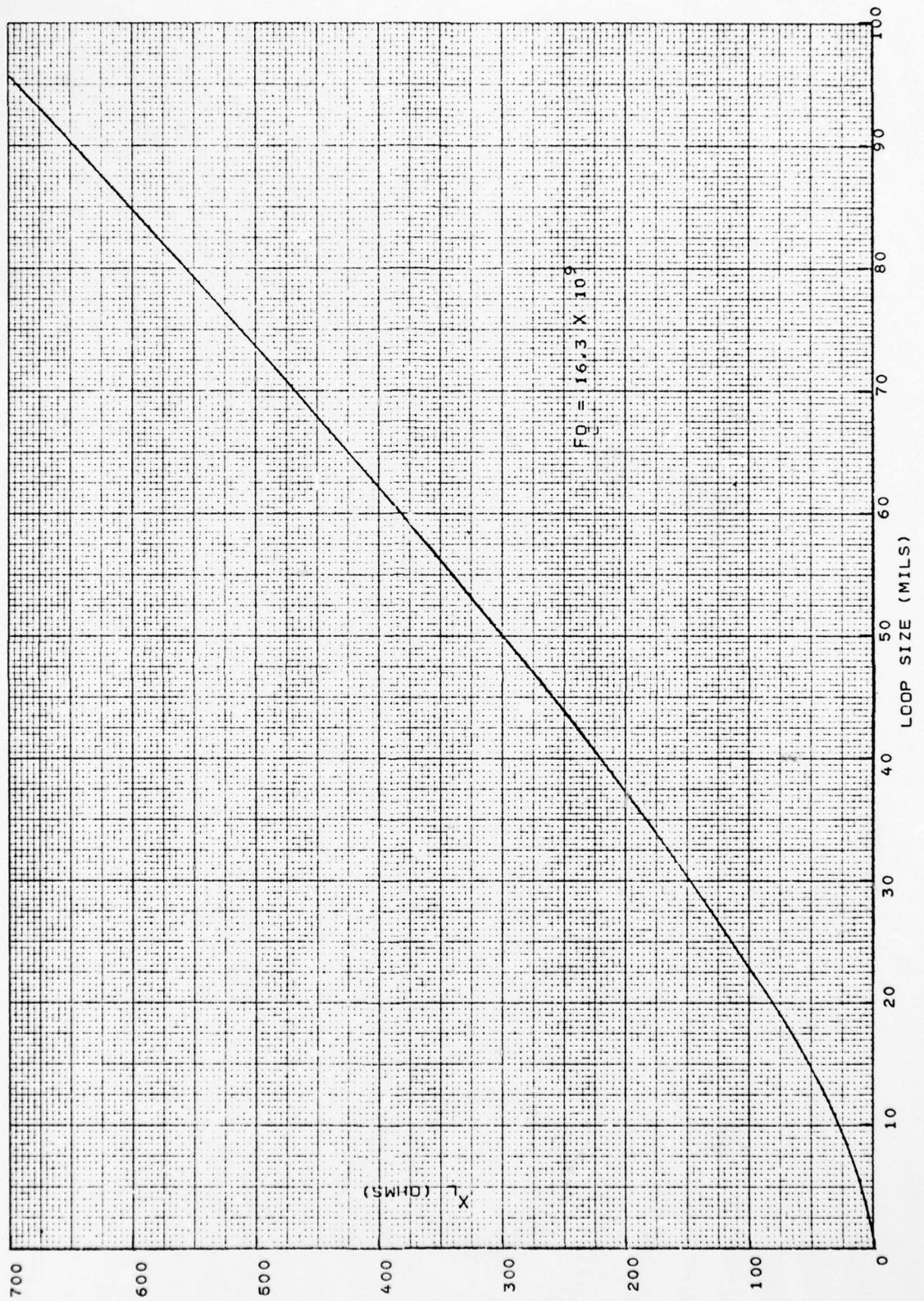
FIGURE 15 - SELF-INDUCTANCE OF SQUARE LOOP AT 16.3 GHz.

$FQ = 16.3 \times 10^9$

LOOP SIZE (MILS)

X_L (OHMS)
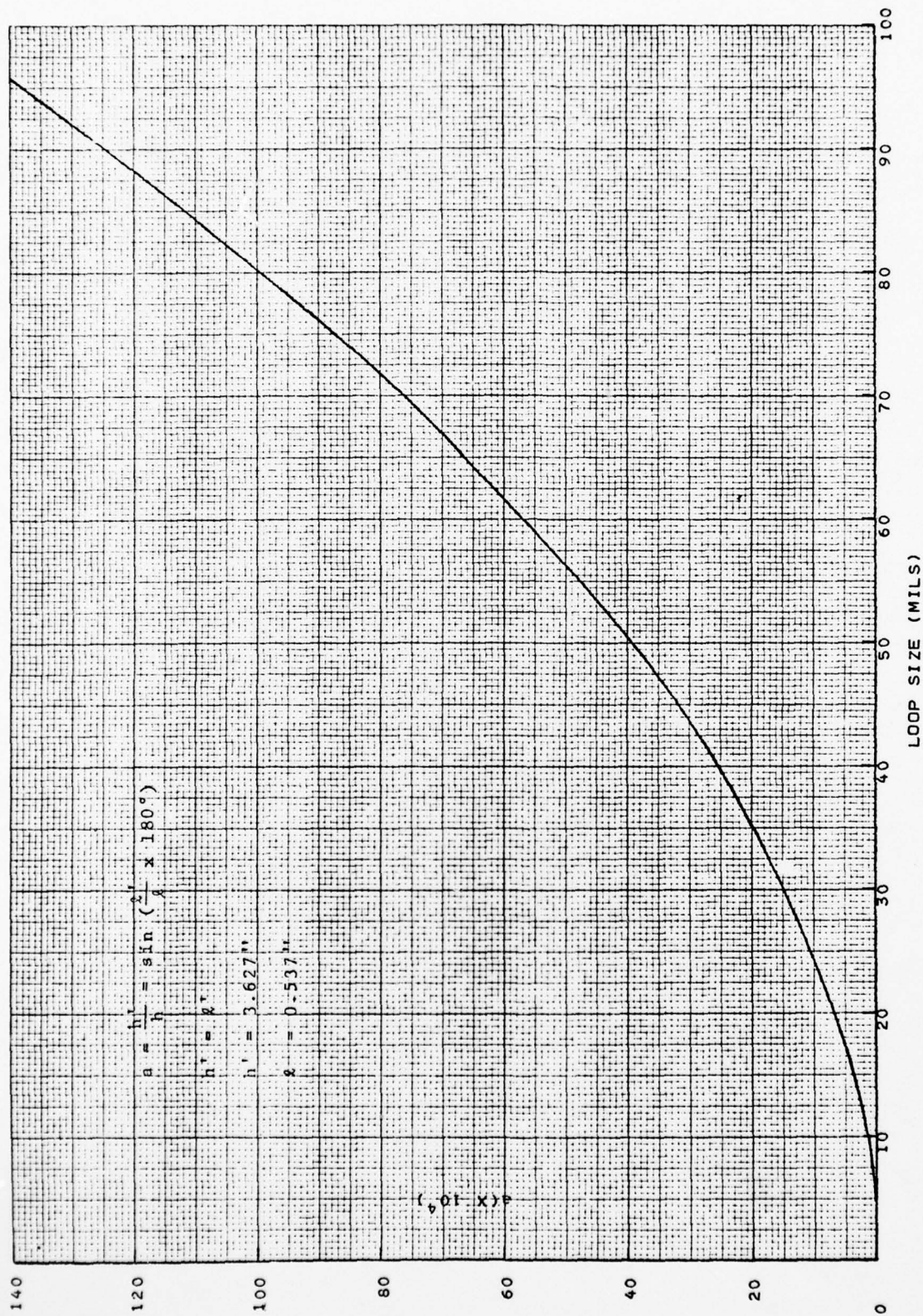
FIGURE 16 - COUPLING FACTOR FOR SQUARE LOOPS IN DU-BAND RESONATOR.

LOOP SIZE (MILS)

$a = \frac{h^1}{h} = \sin\left(\frac{\ell^1}{\ell} \times 180^\circ\right)$

$h^1 = k^1$

$h^1 = 3.627''$

$\ell = 0.537''$

-74-

4.6.3   Calculated Tuning Shifts

The predicted tuning shift of the cavity resonant frequency
with coupled circuit switching was calculated by assuming the use
of two similar diodes with specific values of secondary circuit
capacitive reactance at 16.3 GHz. For this calculation the diodes
were assumed to be lossless so that the change of frequency could
be calculated more easily using equation 72 instead of equation
61. The secondary circuit inductive reactance was taken as
a variable parameter. The large tuning values obtained near
series resonant conditions for the secondary circuit are not
correct, but values more remote from this condition (where the
net reactance values are large compared with the secondary circuit
resistance) will be reasonably accurate. Figure 17 shows the cal-
culated tuning shifts at 16.3 GHz that result from switching from
a reversed biased to a forward biased state for the diode. Note
that both the magnitude of the frequency shift and the direction
can change. Equation 59 shows that a secondary circuit with a
net capacitive reactance shifts the resonant frequency below that
of the unperturbed cavity. Whereas one with a net inductive
reactance raises the resonant frequency above that of the unperturbed
cavity. Consequently, when the net reactance in the coupled circuit
is capacitive in the reverse biased state (below series resonance
in Figure 17) and is switched to the forward biased state which
will always be inductive, the net frequency shift is upward or
positive in algebraic sign. Contrarily, when the net reactance
is inductive in the reverse biased state (above series resonance
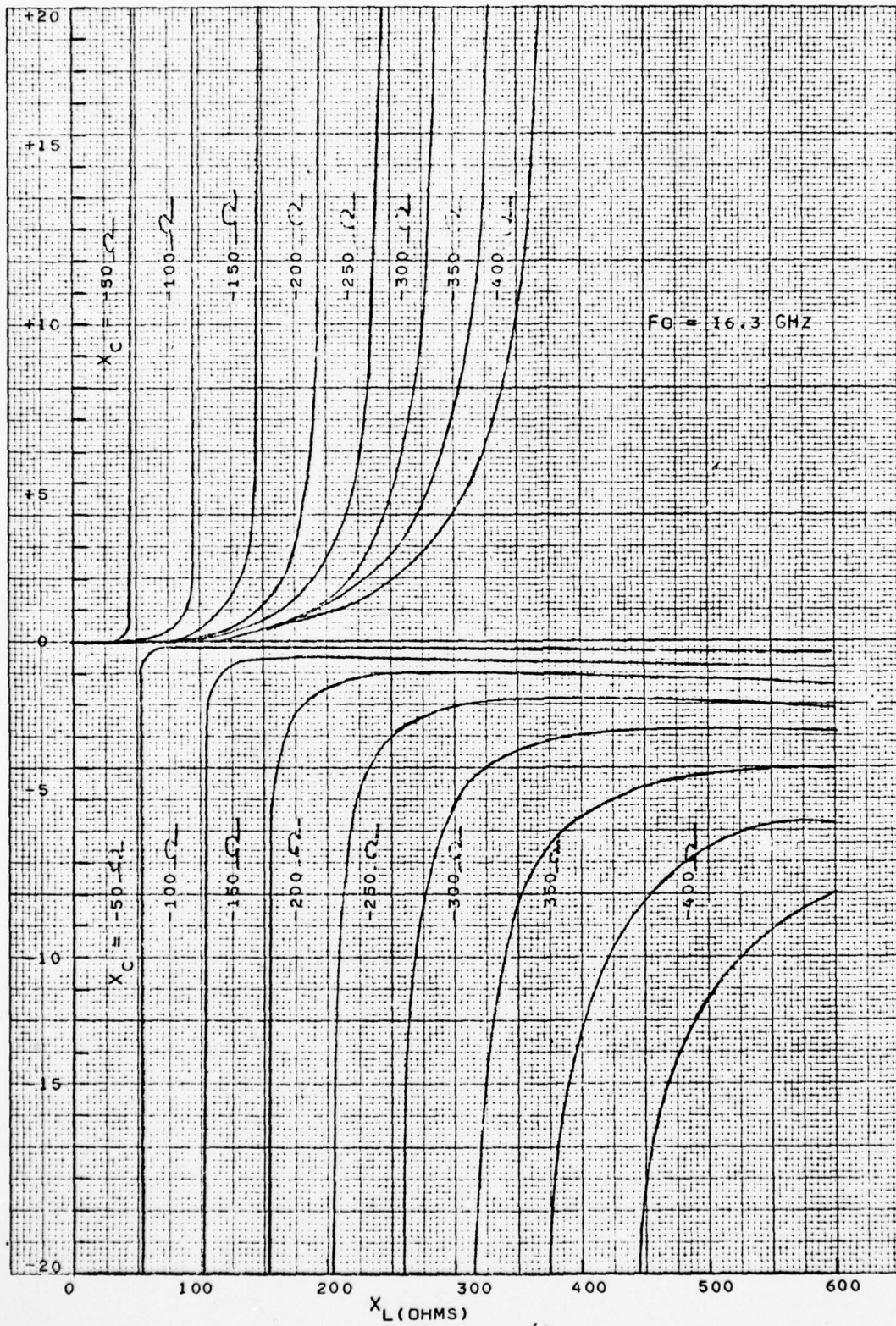in Figure 17) the resonant frequency will be above that of the

-75-

FIGURE 17 – CALCULATED ELECTRONIC TUNING SHIFTS.

unperturbed cavity in both cases. However, the resonant frequency
will be higher in the reverse biased state than when forward
biased leading to a downward shift in frequency and a negative
algebraic sign for the frequency change.

Practical tuning shifts are intimately related to the
secondary circuit element voltages. The total induced voltage
in the secondary coupled circuit is calculated using equation
65. Assuming an operating frequency of 16.3 GHz, peak power
output of 60 kW, and the other parameters given in Figure 12,
the calculated secondary circuit induced voltage is shown in
Figure 18 as a function of secondary circuit inductive reactance.
The voltage increases with reactance because of the associated
increase of loop size and coupling factor. The RF current flow
in the secondary circuit in the reverse biased state is calculated
using equation 66. The voltage across the total capacitive
reactance in the reverse biased state is given by equation 67.
The voltage across each diode is half of this amount. The frequency
shift resulting from diode switching a coupled circuit and the
RF voltage across a single diode in the reversed biased state for
several assumed capacitive reactances are shown in Figures 19 - 26.
as a function of coupled circuit inductive reactive impedance.
The RF voltage across the diode capacitance is, of course, zero
in the forward biased state. Note that the ordinates are not
the same for all figures. The absolute values of peak voltage
across the diode is plotted since magntiude only is the important
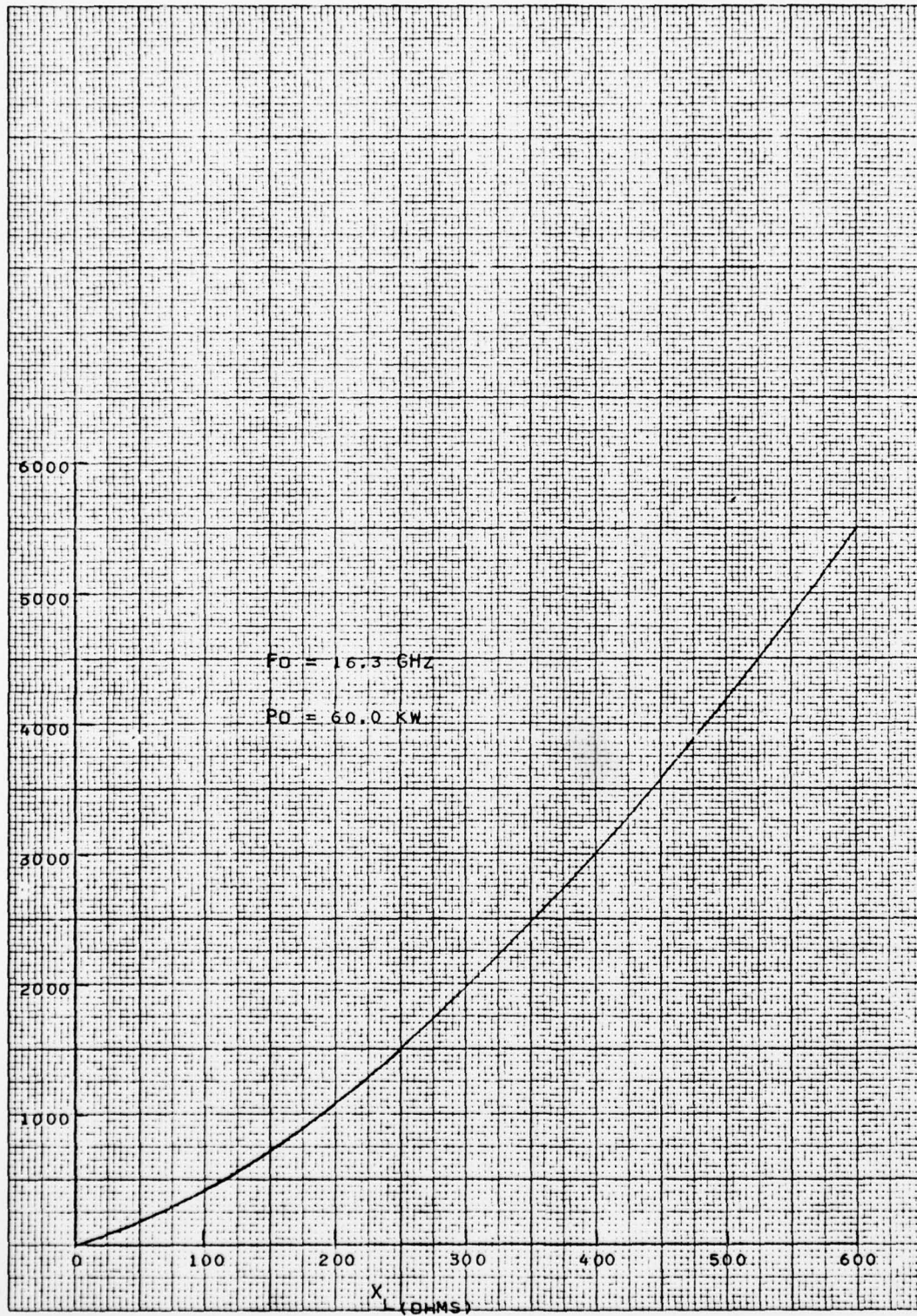parameter so far as voltage breakdown is concerned. Actually, the

-77-

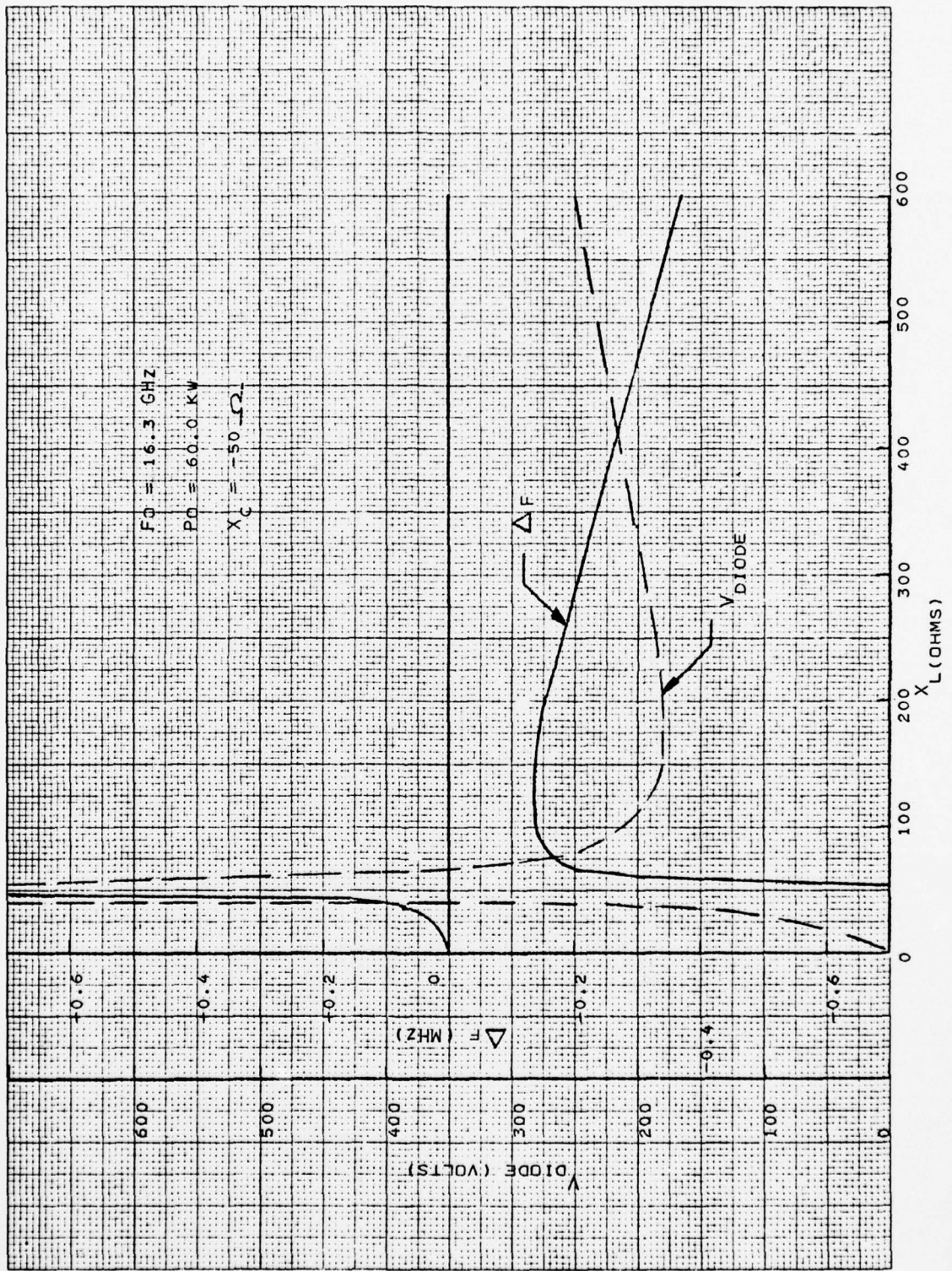FIGURE 18 – CALCULATED INDUCED VOLTAGE IN A COUPLED
CIRCUIT.

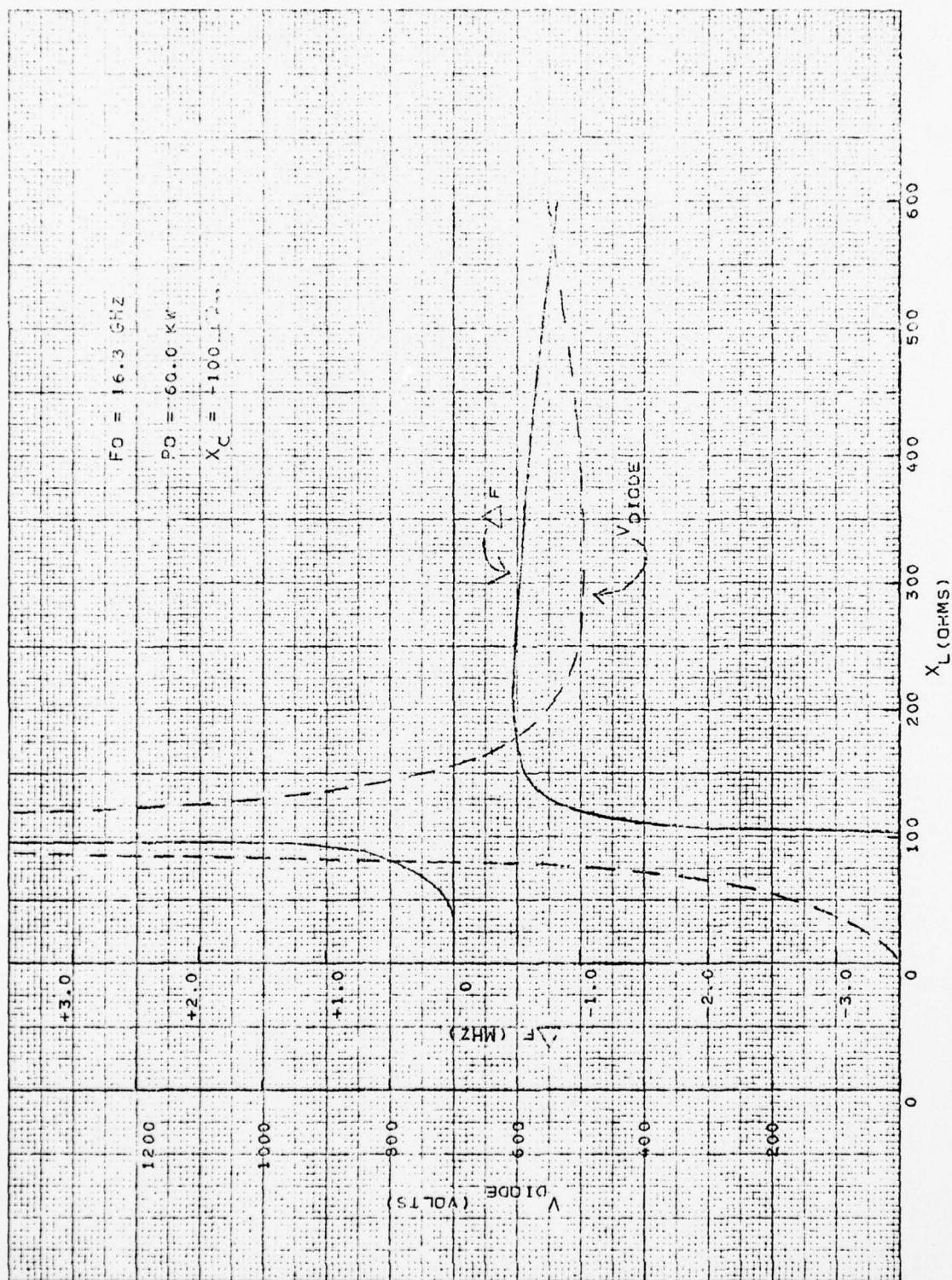FIGURE 19 - CALCULATED ELECTRONIC TUNING CHARACTERISTICS

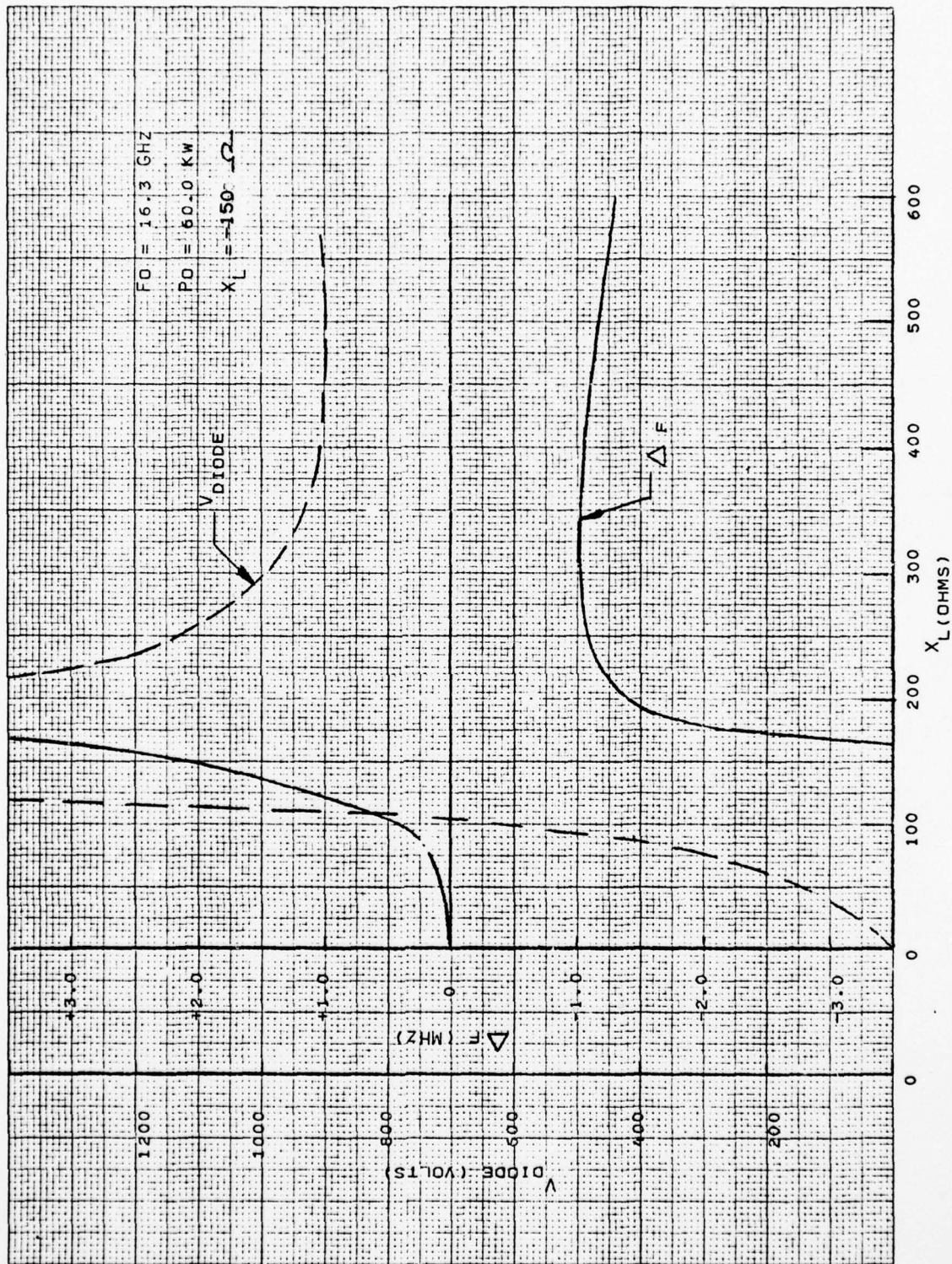FIGURE 20 – CALCULATED ELECTRONIC TUNING CHARACTERISTICS

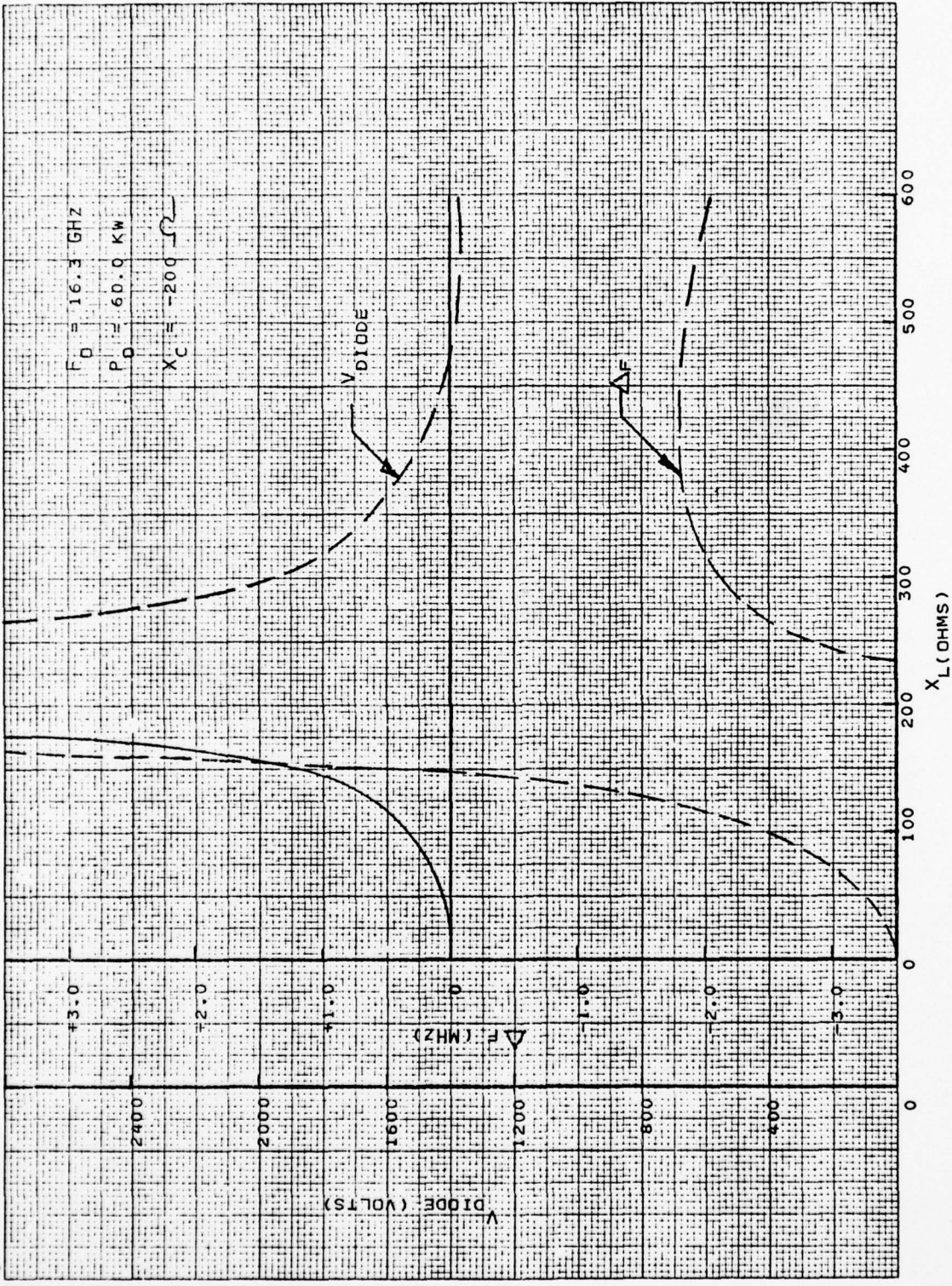FIGURE 21 - CALCULATED ELECTRONIC TUNING CHARACTERISTICS

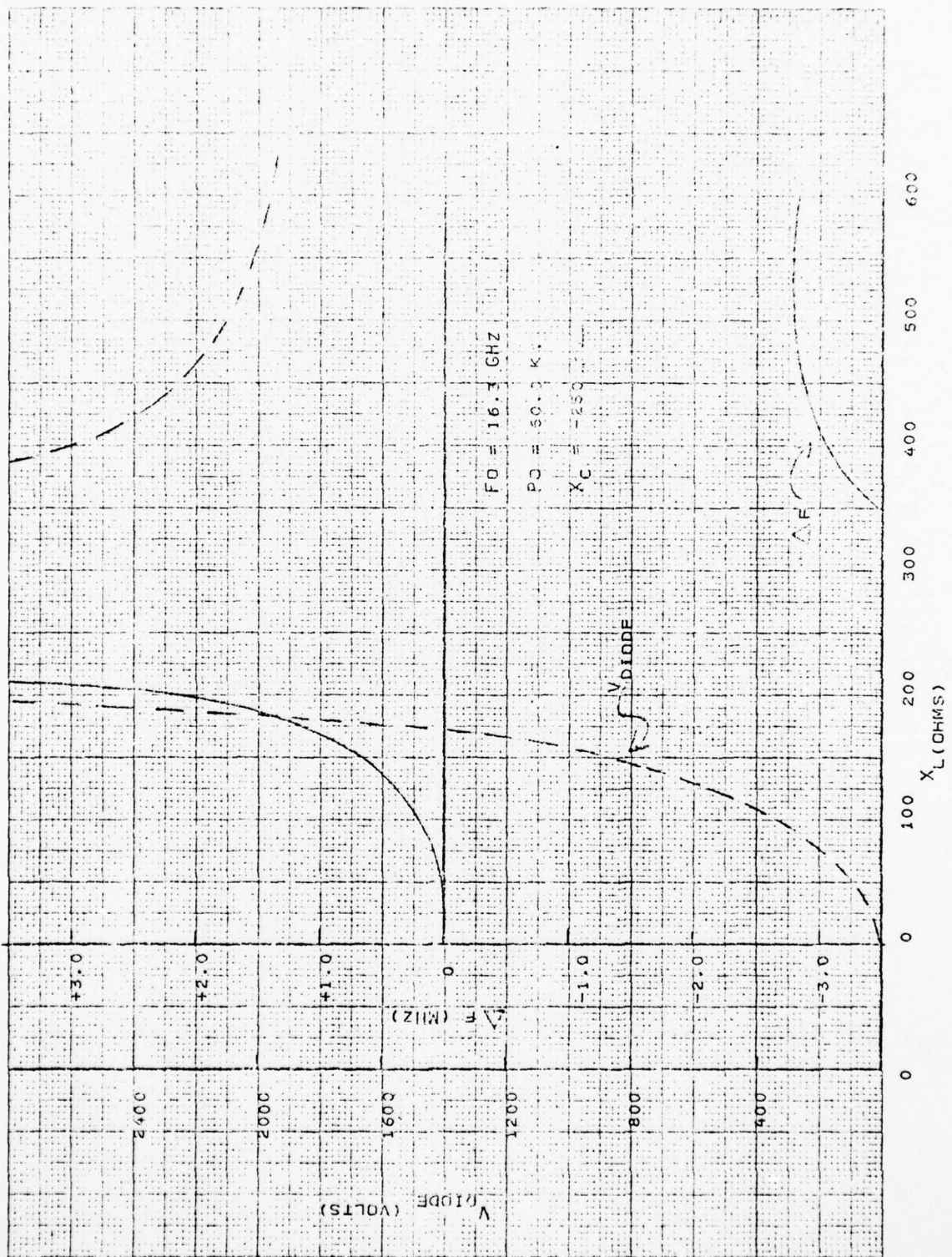FIGURE 22 - CALCULATED ELECTRONIC TUNING CHARACTERISTICS

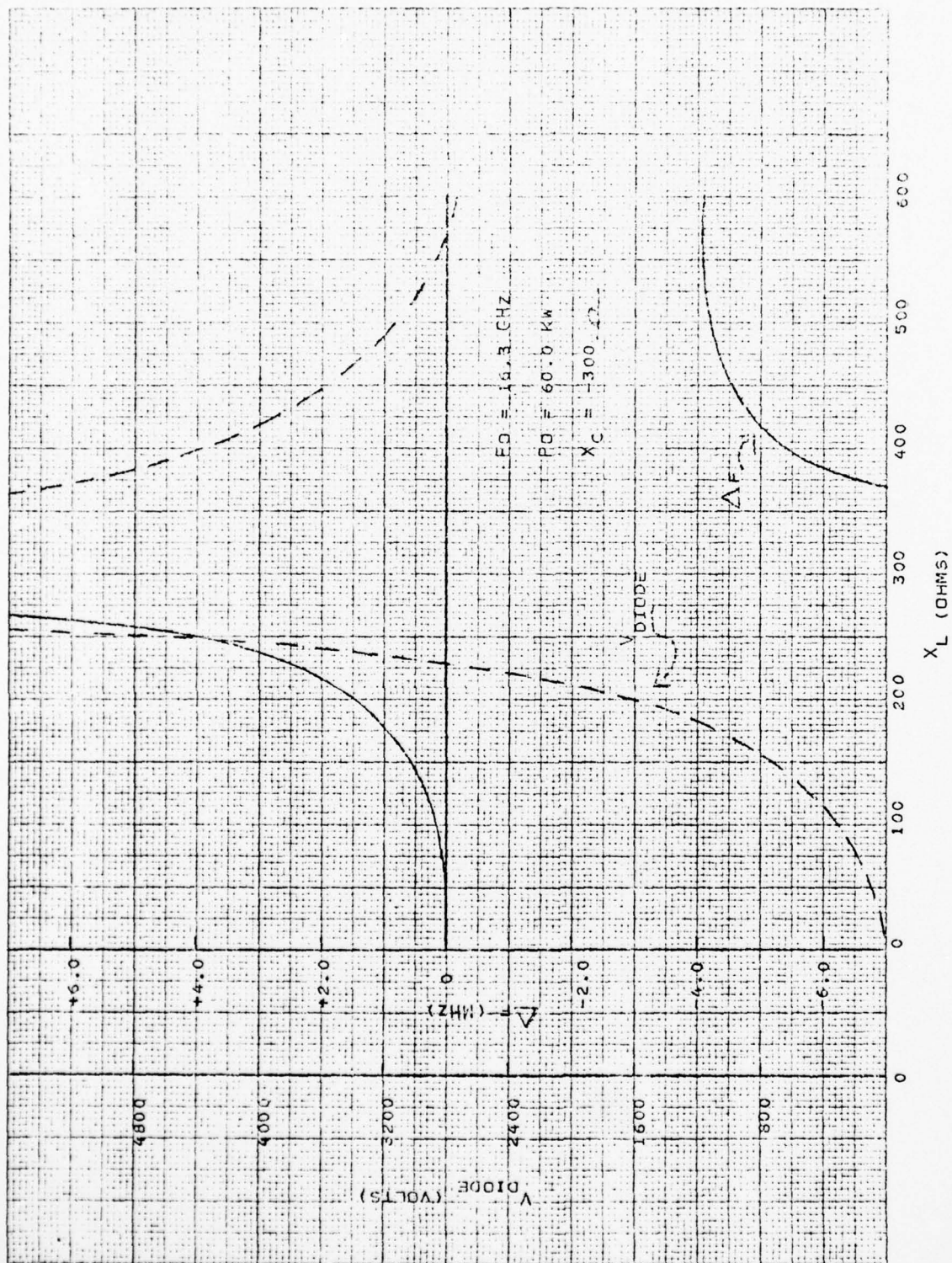FIGURE 23 - CALCULATED ELECTRONIC TUNING CHARACTERISTICS
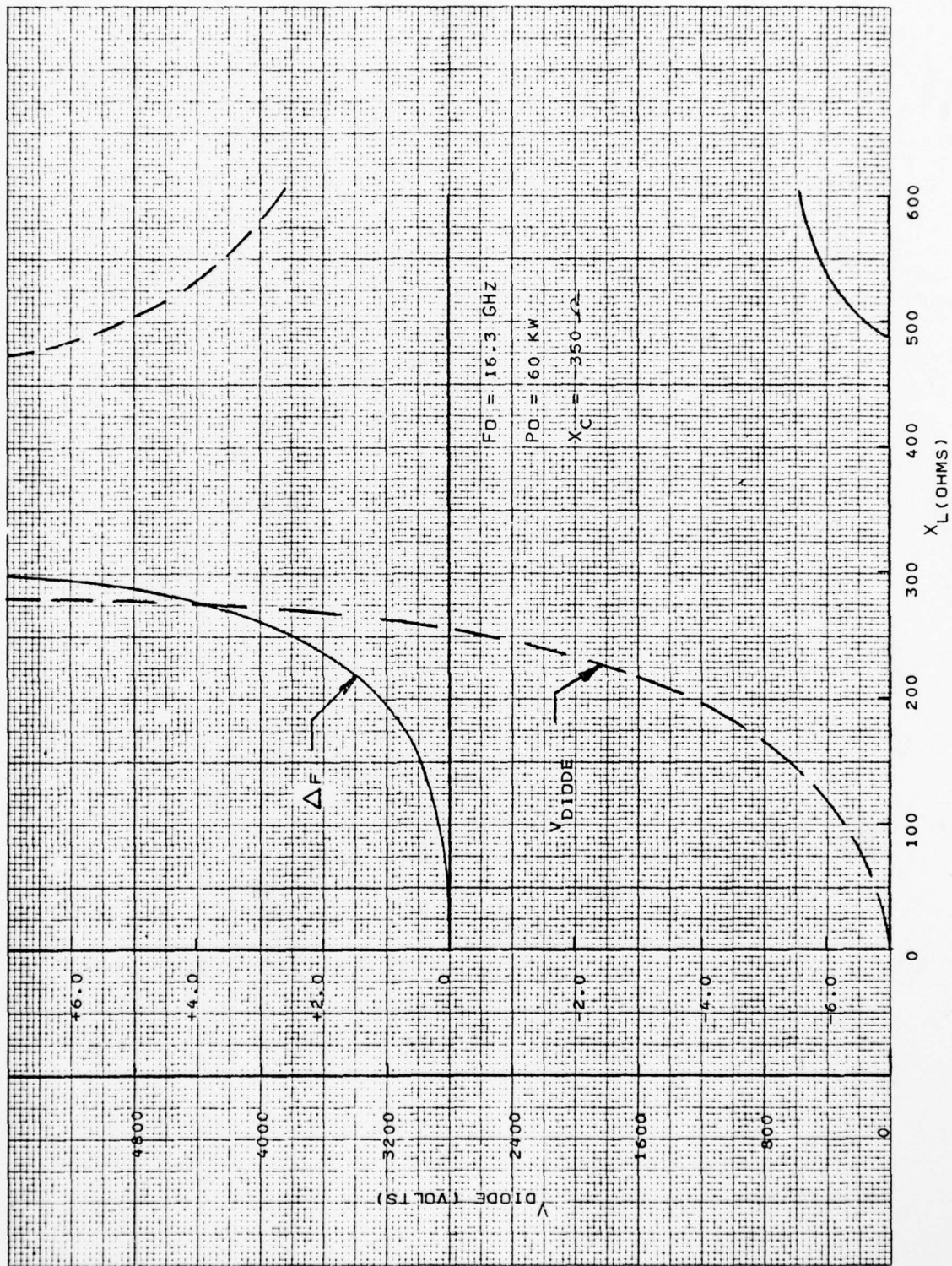
FIGURE 24 - CALCULATED ELECTRONIC TUNING CHARACTERISTICS

FIGURE 25 - CALCULATED ELECTRONIC TUNING CHARACTERSIICS
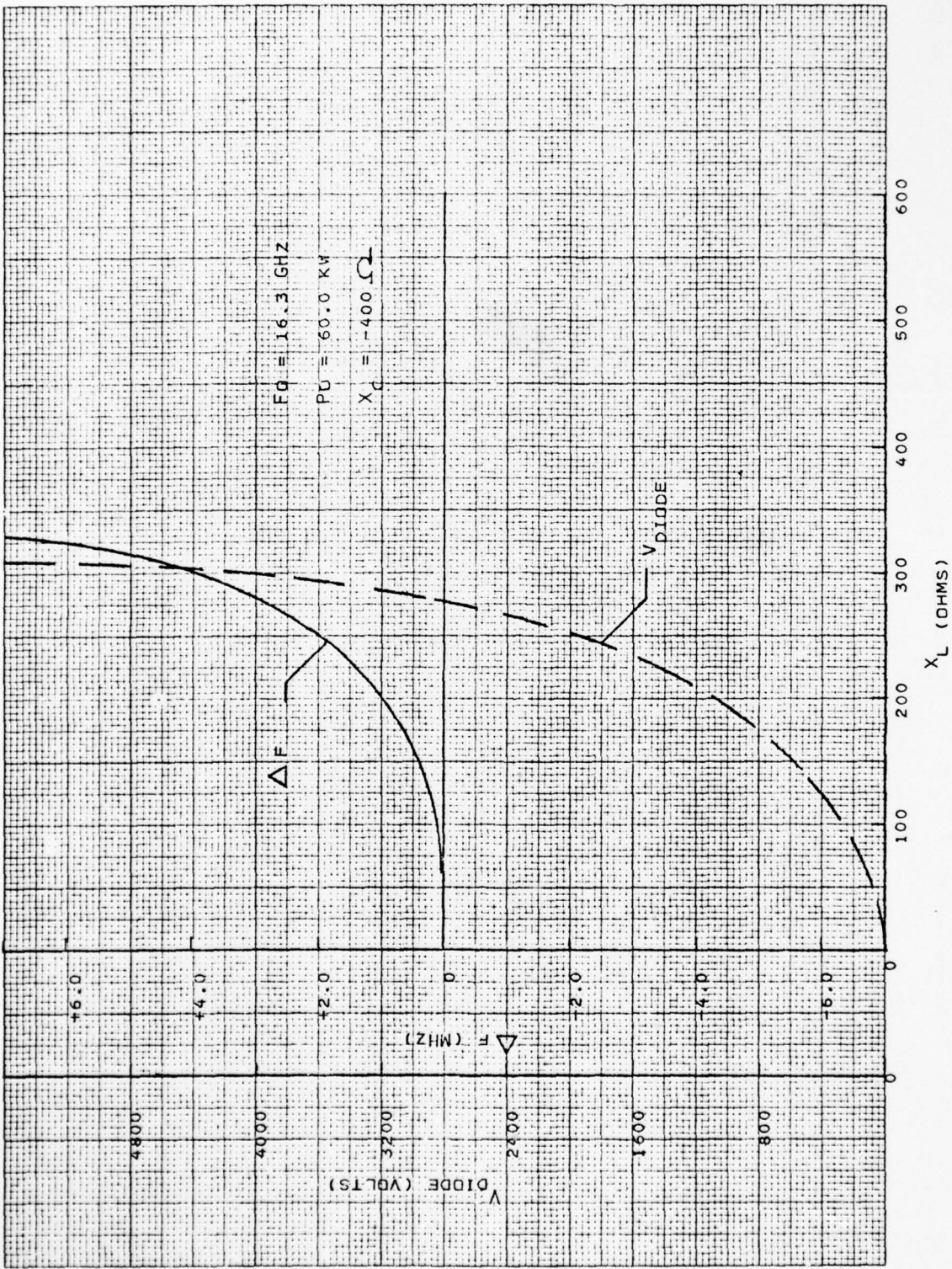
FIGURE 26 - CALCULATED ELECTRONIC TUNING CHARACTERISTICS
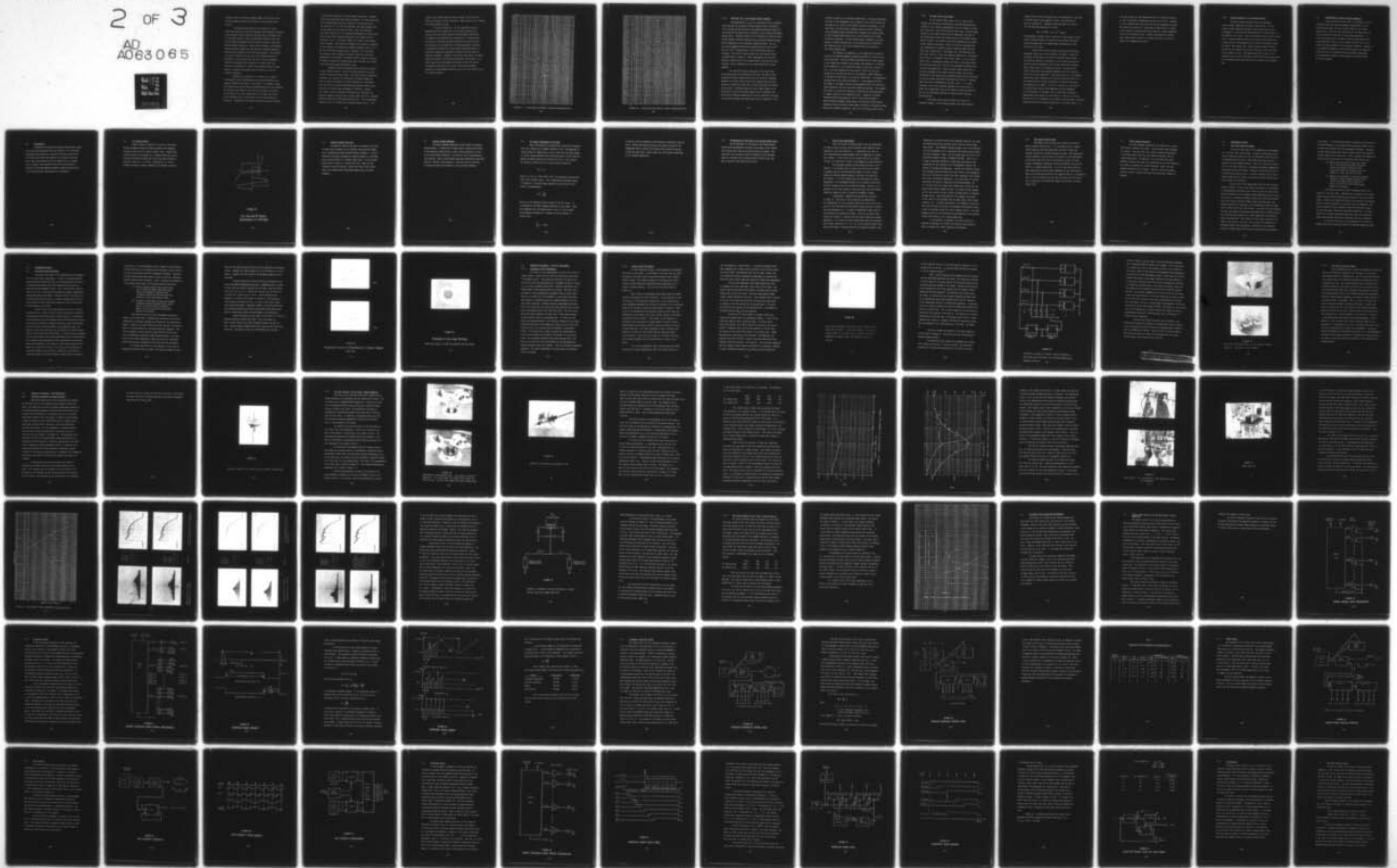
algebraic sign of the diode voltage changes on each side of the
series resonant condition in reference to the secondary loop
current.

The general trend shown by the curves for a fixed
capacitive reactance is that the frequency shift increases initially
with secondary circuit inductive reactance which corresponds also
to increased coupling. Both the obtainable frequency shift and
the RF voltage developed across the diode become very large near
series resonant conditions. Above series resonance, the frequency
shift and diode voltage first decrease with increased inductive
reactance then reverse the trend and both increase. The reversal
in trend is caused by the fact that the secondary inductance
approaches a linear change with the size of the loop dimension
whereas the coupling factor continues to increase with the
loop cross sectional area. Hence, the secondary induced voltage
begins to increase more rapidly than the build up of the net
secondary impedance.

Examination of Figures 19 - 26 shows that a variety
of secondary circuit configurations are possible dependent upon
assumed tolerable conditions for the diodes. For example, assume
that diode chips can be fabricated satisfactorily that can withstand
RF voltages across them of about 1500 volts together with appro-
priate reverse d.c. bias voltage while at the same time having
an RF resistance that is sufficiently low to avoid excessive Q
reduction. In addition, the circuit parameters should be selected

to allow some tolerance to circuit element variations. Consider

first those conditions above series resonance. As noted previously,

these configurations are most suitable for intrapulse tuning.

For values of X_c = 50, 100, and 150 ohms, the diode voltage curve

is very steep in the vicinity of 1400 - 1600 volts implying

that small variations in the coupling loop geometry or diode capac-

itance could lead to large differences in the coupled circuit

operation. For X_c = 200 ohms, however, the slope of the voltage

curve is modest. This region corresponds to an inductive reactance

in the vicinity of 400 ohms and a negative frequency shift of 1.8

MHz for a switched coupled circuit. Moreover, it is seen that

the change in diode voltage and frequency shift are relatively

insensitive to any change in secondary circuit inductive reactance.

At values of capacitive reactance much above 200 ohms, the voltage

across the diode becomes excessively large.

Consider now those configurations below series resonance

for the coupled circuits. Recall that these geometries are most

suitable for pulse-to-pulse tuning. For small values of capacitive

reactance, the variation of tuning shift and diode voltage are

much too rapid with changes of either inductance or capacitance.

This could lead to difficult manufacturing procedures where repro-

ducibility of tube-to-tube performance is required. However,

for a larger value of capacitive reactance; e.g., 400 ohms, the

computed voltage across the diode is about 1500 volts for a secondary

inductive reactance of 225 ohms (see Figure 26). The corresponding

frequency shift is 1.35 MHz for a switched coupled circuit. The

-88-

change of the tuning range and diode voltage is not great with
change of secondary circuit inductance. Hence, this too is a reason-
able tuning geometry to use.

In each of Figures 19 - 26 the capacitive reactive
impedance was held constant and the inductive reactance was
varied so that the curves indicate the performance sensitivity
to changes in the coupling loop configuration. Variations will
also occur in the diode junction capacitance from chip-to-chip.
An indication of the sensitivity to diode capacitance variation
is obtained by plotting the tuning range and diode voltage as a
function of capacitive reactance variation for fixed values of
inductive reactance. Figures 27 and 26 show the results for fixed
inductive reactance of 225 ohms and 400 ohms; respectively. The
diode chips can be fabricated and selected so that the spread
in capacitive reactance will be only a few percent maximum.
Therefore, the performance variation will not be very large in the
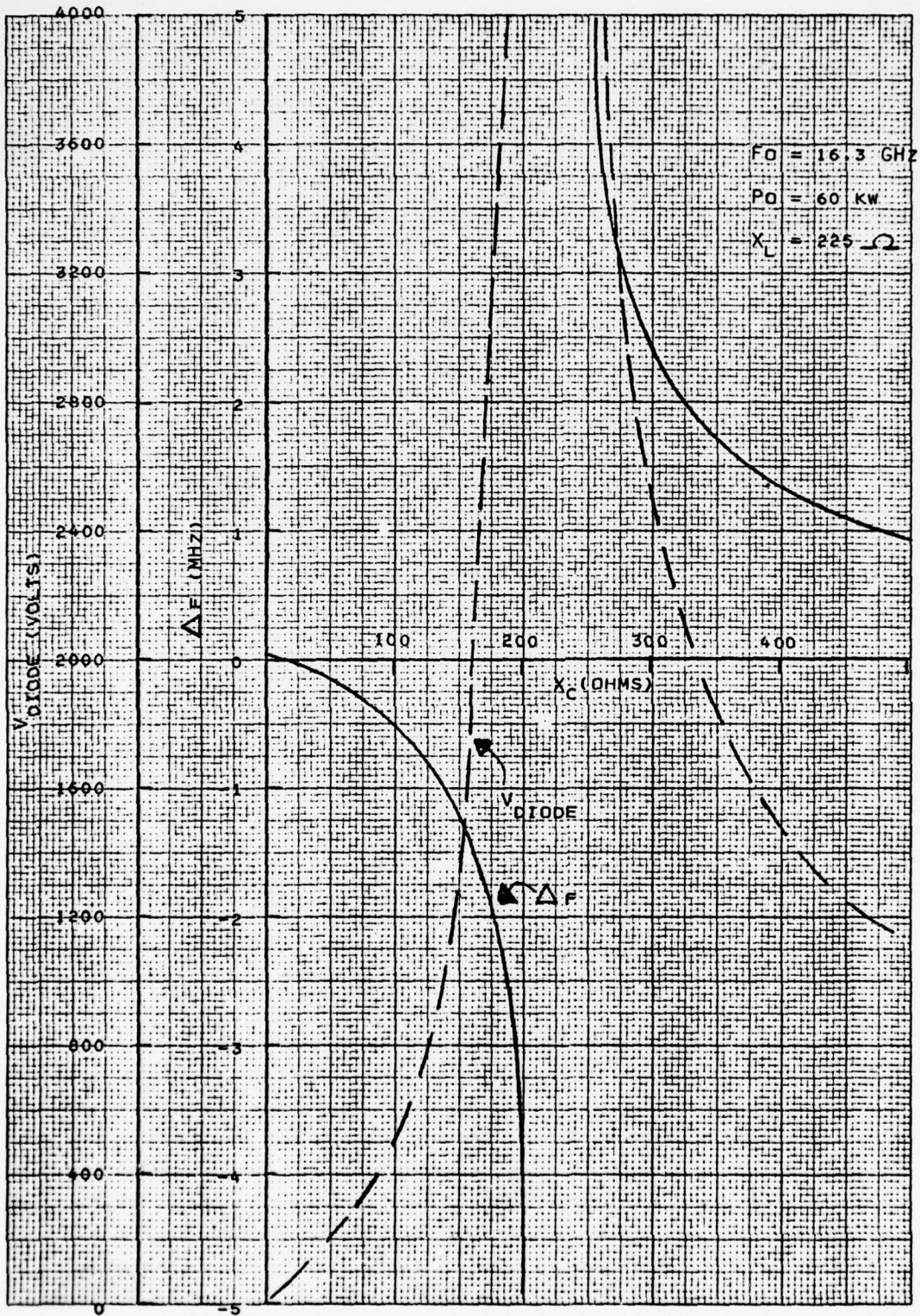two selected regions.

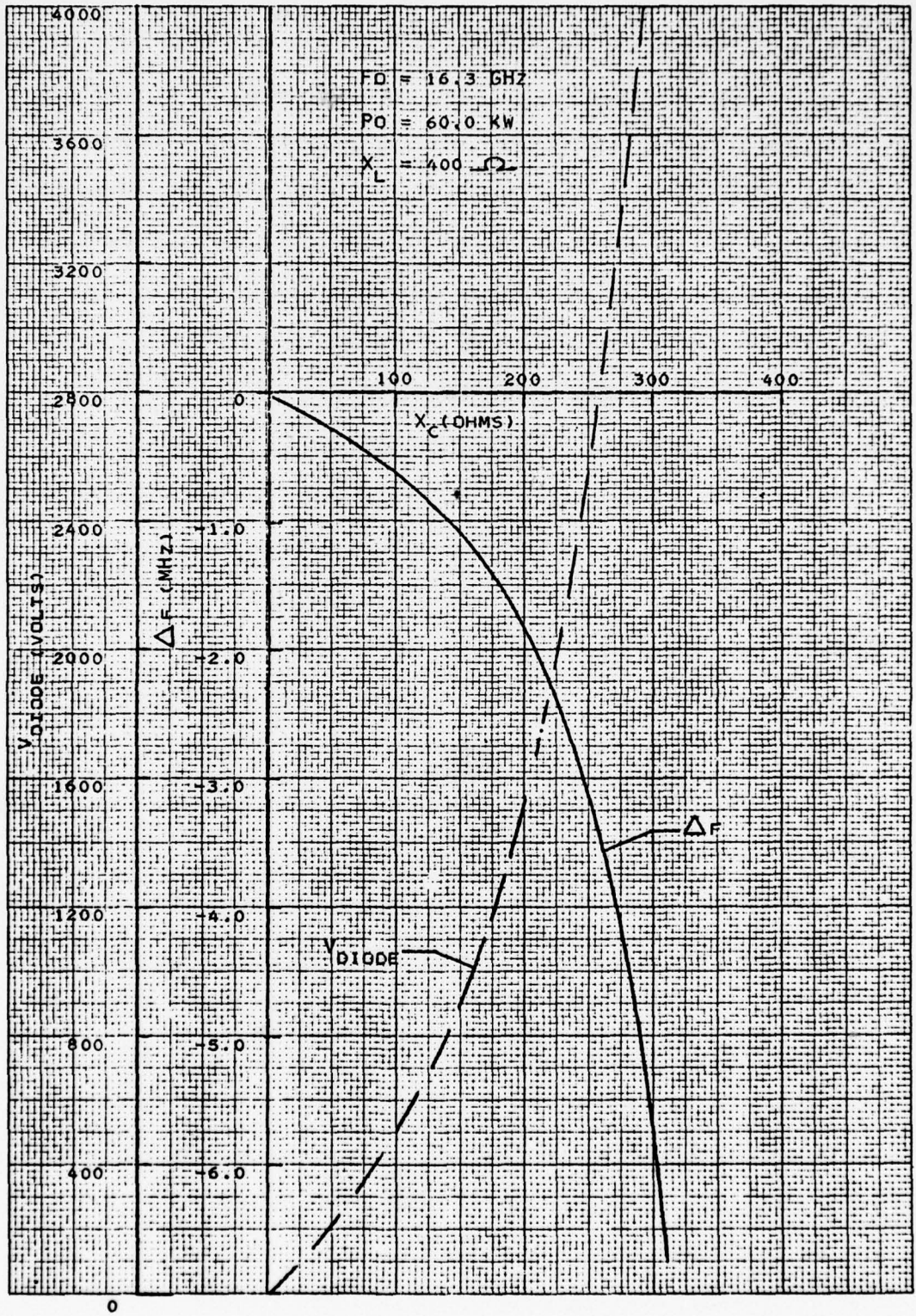FIGURE 27 - CALCULATED ELECTRONIC TUNING CHARACTERISTICS

FIGURE 28 - CALCULATED ELECTRONIC TUNING CHARACTERISTICS

-91-

4.6.4   Variation of Q_o' with Coupled Circuit Geometry

The degradation of Q_o for the unperturbed cavity resonator

resulting from the inclusion of known coupled circuit reactances

can be calculated from equation 64 provided quantitative values are

also known for the diode series resistance in the reverse and forward

biased states. Different effects can be obtained for below and above

series resonant operation because of the resulting impedance change

and the magnitude of the associated coupling factors. For the

two cases considered before the coupling factors are 26.2×10^{-4}

and 61.2×10^{-4}; respectively for 225 and 400 ohms inductive

reactance. The resistive loss coupled into the primary circuit

is proportional to $(a/X_{S2})^2$. Hence, degradation in Q for each

switched coupled circuit can be significantly lower for the below

resonance circuit dependent upon the diode resistance for each

geometry.

The equivalent series resistance of the diode chips

and coupling loops are anticipated to be about the same in both

reverse and forward biased states since the losses are composed

primarily of contact losses which do not change with bias state.

Therefore, equation 64 shows that it would be possible to produce

tuning across a frequency range with only a small change in Q_o'.

This would be done by selecting coupled circuit parameters for

below series resonance operation with the net capacitive reactance

in the reverse biased state being about equal in magnitude to the

-92-

inductive reactance in the forward biased state. For these conditions, the terms in the denominator are the same for both circuit states and no change of Q_o' occurs as the coupled circuits are switched. On the other hand, for above series resonance operation the net secondary circuit impedance always increases when changing from reverse biased to fully forward biased states and Q_o' will increase as the diode circuits are switched. In both of these cases, therefore, the total number of coupled circuits that can be utilized will be limited by the reduction in Q_o' that can be tolerated with all circuits in the reverse biased state.

For purposes of comparison, it is assumed that a reduction of Q_o for the Ku-band magnetron stabilizing cavity by a factor of two can be tolerated. Since the losses associated with the anode system do not change with coupled circuit tuning, this amounts to a reduction of the composite Q_o of the anode and cavity of less than a factor of two. It is also assumed that each coupled circuit has a series resistance of two ohms and that the net secondary circuit impedance is 200 ohms for both cases in the reverse biased state. The appropriate coupling factors are taken from Figure 14. Using equation 64 shows the number of tolerable circuits is approximately 209 in the below resonance operation, and 38 in the above resonance operation. This assumes that there is no physical limitation to mounting the specified number of coupled circuits in the magnetron cavity. Using the calculated frequency shifts from Figures 22 and 26, these results predict a pulse-to-pulse obtainable tuning range of 275 MHz for below resonance operation, and an obtainable tuning range of 68 MHz for interpulse tuning using above resonance operation. Both are at 60 kW peak power output.

4.6.5   RF Power Loss in the Diodes

In the forward biased state, the d.c. bias current through the diode must be sufficient to provide enough minority carriers in the intrinsic semiconductor layer to support the peak RF current flow. More will be said of this later. The RF voltage induced in the coupled circuit will be essentially the same in both biased states since the tuning effect on the primary circuit driver is small. The current flow will be limited by the coupled circuit inductive reactance. Hence, for the two configurations just considered the secondary induced voltage is 3000 volts and 1250 volts; respectively. (See Figure 16.) The resulting peak RF current flow is 7.5 and 6.25 amperes; respectively. The diodes will be able to accommodate these values easily. In the reverse biased state, displacement current only flows in the diode chips. The calculated values are 15.0 and 7.4 peak amperes; respectively, for these two geometries. Using the peak current values and an accurate knowledge of the diode resistive losses, the RF power dissipated in the diodes during a magnetron pulse can be calculated for the two biased conditions using equations 70 and 71. Average power loss will be determined by the duty factor. If a diode resistance of one ohm is assumed together with a duty factor of 0.001, the average power loss in the diodes is much less than one watt for all operating conditions in pulse-to-pulse frequency agile operation.

Some other factors must be taken into account for intrapulse tuning. It was noted previously that diode switched

-94-

tuning during a pulse as proposed must be accompanied by a decrease
in stored energy in the magnetron cavity. This decrease is
given by equation 82. Assuming a frequency shift of 2 MHz at
16.3 GHz and using equation 46 we have...

$$\Delta W = 4 \ W_p \ \frac{\Delta f}{f} = 2.44 \ X \ 10^{-7} \ joules$$

Even assuming, contrary to fact, that all of this energy is dissi-
pated in the two diodes of a coupled circuit during a ten nano-
second switching time, the average power dissipation at 0.001
duty factor is trivial.

Another factor must be taken into account also during
intrapulse tuning that is more difficult to assess. During the
transition of the diode from reverse to forward biased states,
the junction capacitance increases to a very large value and low
reactance and the equivalent circuit shunt resistance decreases
from a large value to an ultimate low value. The main cavity
couples energy into this changing impedance which is a function
of the bias current magnitude. The detailed nature of the impedance
change during this transition is not known specifically and it is
not possible without further information to calculate the power
loss absorbed by the diode. It will, of course, be a function of
the applied bias current pulse magnitude and time dependence.
It is well known, for instance, that in some other intrapulse
applications where diodes are used solely as a switch in a trans-
mission line, it is possible for the diodes to pass through a resistive
value that serves as a matched termination to the power source. If

-95-

the diode remains at this impedance level for a sufficient period
of time, catastrophic overheating and burn out can occur. However,
it is not believed that this will occur in this application because
the diodes will always be in series with a large value of coupled
circuit inductive reactance which will limit the current regardless
of the diode resistance value. However, experimental Q measure-
ments using coupled circuits in a cavity will have to be made to
assess this phenomenon more fully.

4.6.6   Voltage Gradients in the Coupled Circuits

The peak voltage developed across the equivalent
circuit primary capacitance is given by equation 48. For the
Ku-band coaxial magnetron designed for 60 kW peak output, this
corresponds to a peak electric field gradient of 136 volts/mil in
the middle of the cavity. Tubes of this kind have been built success-
fully. Voltages developed across the coupled circuit gives rise
to peak electric field gradients of less than 50 volts/mil between
the ends of the coupled loop. Hence, voltage breakdown between
the ends of the coupling loop or from the loop to the cavity wall
are not likely to occur. The maximum electrical stress in the
secondary circuit will be developed across the PIN diode capacitance
in the reverse biased state which must be designed to accommodate
this.

5.0 CONSIDERATION OF OTHER PIN DIODE PROPERTIES

It has already been noted that it is desirable to have
PIN diodes with high voltage breakdown characteristics in the
reverse biased state and low resistive losses in the forward
biased state. There are other properties of the diodes that are
also of concern for their use in this tuning application. It
is not the purpose here to present a detailed discussion of PIN
diode properties. That is a full subject in itself and is dis-
cussed at length elsewhere in the technical literature. However, it
is considered worthwhile to review briefly some of the character-
istics that will be influential in the successful achievement
of electronically tuning a coaxial magnetron using PIN diodes
as control elements.

5.1   Construction

PIN diodes can be made with either polarity with respect to the heat sink upon which they are attached. For a PIN diode the N-type semi-conductor is attached to the heat sink and for a NIP diode the P-type semi-conductor is attached to the heat sink. Both constructions will serve equally well for coupled circuit tuning. The selection of one over the other may be favored for achieving maximum breakdown voltage characteristics or for optimizing the tuning modulator requirements.

5.2   V-I Characteristics

Figure 29 shows a typical V-I curve for a PIN diode.
Reverse breakdown voltage is defined usually as the negative
voltage at which 10 µA of reverse current flows. Forward bias
current flows when the applied d.c. voltage exceeds the contact
potential difference between the P and N type semi-conductors;
typically, about 0.6 - 0.7 volts. The forward d.c. current
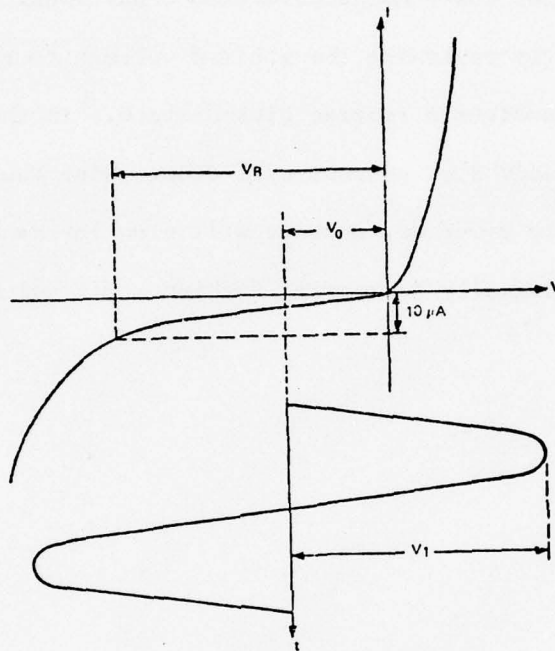through the diode is usually limited by the external circuitry.

-100-

FIGURE 29

D.C. BIAS AND RF VOLTAGE
RELATIONSHIP IN A PIN DIODE

-101-

5.3   <u>Minority Carrier Life Time</u>

The minority carrier life time is a measure of the rate
at which holes disappear in the intrinsic semi-conductor region
due to recombination under non-equilibrium conditions. It can be
measured by abruptly reversing the applied voltage to a PIN diode
from a forward biased to a reverse biased state. In the forward
biased state a steady d.c. current will flow. When the bias
voltage is abruptly reversed, current will flow in the reverse
state in an exponentially decreasing fashion until all holes
disappear.

5.4   Reverse Voltage Breakdown

The major breakdown mechanism for PIN diodes is avalanche
multiplication. A reverse bias voltage causes a high electric field
in the depletion region which, in turn, causes ionization to occur
in the semi-conductor material. For silicon, this is approximately
700 volts/mil. Hence, high voltage diodes will necessarily have thick
layers of intrinsic semi-conductor. Care must also be exercised
to design the diode chip geometry to avoid surface breakdown.

-103-

5.5   RF Current Limitations of the Diode

When a PIN diode is in forward bias, carriers are injected into the I region and it appears resistive to RF. The magnitude of the RF current is limited only to such a value that the total amount of carrier charge removed by the reverse RF current is less than the amount of charge stored in the junction by the d.c. bias current. The charge Q_o stored by the d.c. bias current is given by:

$$Q_o = I_o \tau$$

where I_o is the d.c. bias current and τ is the minority carrier life time in the intrinsic layer. For a superimposed sinusoidal signal of frequency f, the peak charge removed by one half cycle of RF current is approximately:

$$Q_1 = \frac{I_1}{2\pi f'}$$

where I_1 is the amplitude (zero-to-peak) of the RF current. It is assumed that the shunt leakage resistance is very large. Under the assumption that the charge stored by the d.c. bias current is the maximum available to be removed by the RF current, it follows that...

$$\frac{I_1}{I_o} = \leqslant 2\pi f \tau$$

-104-

So long as there is sufficient stored charge, rectification does not occur. Diodes with minority carrier life times in excess of 100 nanoseconds will be used as will forward bias currents of 100 mA or more per diode chip. Hence, there are no RF current limitations in the proposed application.

5.6 <u>RF Resistance of PIN Diode in the Forward Biased State</u>

The RF resistance of the diode in the forward biased state varies approximately inversely proportional to the forward bias current until some low saturation value is reached. This saturation value increases with the thickness of the intrinsic layer and decreases with increased minority carrier life time. Hence, long life time diodes will be used.

5.7   Reverse Bias Requirements

When a PIN diode is reverse biased, there are essentially
no charge carriers stored, and the intrinsic semi-conductor layer
appears as a low loss dielectric. In some diodes, the value of
this capacitance may change somewhat with the magnitude of reverse
bias voltage. If this occurs for the diodes used in the coupled
circuits, it could have an effect on the magnetron output frequency.

For high power operation other points also must be con-
sidered. It is evident that so long as the reverse bias voltage
is greater than the zero-to-peak RF voltage, the total voltage
across the junction remains negative, and hence the diode does
not conduct. It is also evident that the diode does not conduct
appreciably if the breakdown voltage is not exceeded by the sum of
the bias voltage and the zero-to-peak RF voltage. However, it is
possible for the total voltage to make excursions into the forward
conduction region and also to exceed the breakdown voltage.

A qualitative explanation can be given by reference
to Figure 29. The bias V_o can be less than the amplitude V_1
and consequently the total voltage across the junction can be posi-
tive but, the diode does not necessarily conduct because of carrier
life time phenomena; i.e., it takes a considerably longer time tha
the RF period for conduction to begin. Thus, the intrinsic layer
retains its dielectric character and the circuit equivalent remains
capacitive. It is found in certain applications that the excursions
into forward conduction; i.e., $V_1 - V_o$, can be several hundred volts
with low RF losses. Excursion beyond the breakdown voltage at high

-107-

frequencies is possible because the breakdown values are not sharp for diodes having thick intrinsic layers that are used in high power diodes. The breakdown voltage rating is not a true avalanche (or Zener) breakdown, but is associated with surface states rather than bulk phenomena. Hence, current runaway does not occur if the specified breakdown voltage is somewhat exceeded. There can be so many interacting parameters in high power applications that frequently the most practical way of determining a proper bias voltage is through experimentation. Besides the breakdown voltage, bias voltage, peak RF voltage and circuit losses, other parameters that come into play are carrier life time, frequency, pulse length, duty cycle, and ambient temperature. As a side effect to voltage excursions into positive conduction and beyond breakdown, the d.c. reverse bias power supply must deliver more current than the normal diode reverse leakage current. The normal reverse leakage will be less than 10 μA when a diode is biased below its breakdown voltage rating. Under high power RF, the leakage can increase to the order of 1 mA depending upon the power level, bias voltage, frequency, etc. In pulsed applications, the leakage is observed to vary over the time of the pulse; the maximum value obtained during a pulse is generally called the "pulse leakage current". The pulse leakage current and its stability are good measures of how adequate a given bias voltage is for a given application.

It was desired, if possible, that these features be employed to advantage to minimize the necessary bias voltage in order to simplify the control modulator requirements.

5.8   PIN Diode Switching Times

PIN diodes can be switched very rapidly from reverse bias to forward biased states. It is necessary first to remove stored energy in the diode capacitance and then to drive the required forward bias currents through the diode. With appropriate control modulator circuitry this can be done in a few nanoseconds. On the other hand, the value of the minority carrier life time places a fundamental limitation on the time required to return the diode to a reverse biased state. It is for this reason that all reset operations to reverse bias conditions for the diode must be done in the interpulse periods of the magnetron when it is inoperative. This is also the reason why chirp mode operation during the pulse must be obtained by switching the diodes from reverse to forward biased state.

5.9   Diode Leakage Resistance

The shunt leakage resistance of the diode in the reverse
bias state is normally very large. Values greater than 20 megohms
are typical. Care will have to be taken to prevent contamination
of the diode chips inside the tube caused by material from the
cathode when heated. In addition, it is also known that photo
produced, electron hole pairs can be generated in the semi-conductors
as a result of exposure to optical radiation. Hence, the shunt
leakage resistance can be lowered. This may occur in the magne-
tron as a result of optical radiation from the heated cathode and
filament.

6.0   EXPERIMENTAL RESULTS

6.1   High Power Diode Development

        The goal of this phase of the program was the development
of a low loss, high voltage diode. In order to withstand environ-
mental conditions within the tube, the individual diode chip had to
be thermally passivated with a high temperature SiO_2 layer for
stability and low leakage currents. Also, the electrical contacts
had to be of such a nature as to withstand the bakeout temperatures
encountered during tube exhaust. Minority carrier life time was to
be sufficiently long (>1 μsec.) to prevent rectification at the RF
levels inside the tube cavity with relatively little reverse bias
voltage applied to the diode.

        Initial work on this phase began with the use of Inverse
Epitaxial Silicon. Bulk N type silicon was used with a resistivity
of approximately 1000 ohm/cm, and a grown N+ layer of 0.001 ohm/cm.
With this material and the standard Varian PLESA fabrication process,
we were able to fabricate thermally passivated, bulk silicon diodes.
Early test results indicated higher series resistance (R_S), low
minority carrier life time (T_L), and a variation of forward voltage
(V_f) at 100 ma across the silicon wafer. To lower the R_S and lengthen
the life time values, slow cooling experiments prior to metallization
were conducted upon completion of these experiments and additional
wafers were generated. Test results of these wafers indicated life
times in the order of 2.25 μsec., but the R_S and V_f remained sub-
stantially higher than anticipated. Evaluation of the material
being used showed a poor N/N+ interface causing these fluctuations

-111-

in R_S and V_f. A second problem, which is common to the fabrication of most PIN diodes, was obtaining Inverse Epitaxial Silicon with an N+ layer more heavily doped than customarily available. Typically, the more heavily doped layer would be lower in loss and, therefore, provide reduced series resistance. After a complete re-evaluation of this process and its goals, the following points became clear:

(1) While a heavily doped N+ layer would reduce R_S, it would also grade during SiO_2 passivation and subsequent diffusion steps. A process by which the junctions were both formed at a later time would be ideal.

(2) Because of the problem in using and obtaining repeatable Inverse Epitaxial Silicon, fabrication of the diode would be difficult; hence, the use of pure bulk silicon would improve the situation.

With these key points in mind, development effort was shifted to this type diode. Problems were encountered in the early stages such as thinning, handling, and flatness of the bulk silicon wafers. However, once these difficulties were overcome, the development of a process suitable for the goal listed was completed. The first successful run was completed in May 1976 with three slices for each individual capacitance range being fabricated. All three slices in the lowest capacitance range were diced into individual diode chips and made available for microwave cold test evaluation.

In dicing these slices, it was important to note that in dealing with chips in excess of 1000 V the distance between the mesa

-112-

6.0   EXPERIMENTAL RESULTS

6.1   High Power Diode Development

The goal of this phase of the program was the development
of a low loss, high voltage diode. In order to withstand environ-
mental conditions within the tube, the individual diode chip had to
be thermally passivated with a high temperature SiO_2 layer for
stability and low leakage currents. Also, the electrical contacts
had to be of such a nature as to withstand the bakeout temperatures
encountered during tube exhaust. Minority carrier life time was to
be sufficiently long (>1 μsec.) to prevent rectification at the RF
levels inside the tube cavity with relatively little reverse bias
voltage applied to the diode.

Initial work on this phase began with the use of Inverse
Epitaxial Silicon. *Bulk N type silicon* was used with a resistivity
of approximately 1000 ohm/cm, and a grown N+ layer of 0.001 ohm/cm.
With this material and the standard Varian PLESA fabrication process,
we were able to fabricate thermally passivated, bulk silicon diodes.
Early test results indicated higher series resistance (R_S), low
minority carrier life time (T_L), and a variation of forward voltage
(V_f) at 100 ma across the silicon wafer. To lower the R_S and lengthen
the life time values, slow cooling experiments prior to metallization
were conducted upon completion of these experiments and additional
wafers were generated. Test results of these wafers indicated life
times in the order of 2.25 μsec., but the R_S and V_f remained sub-
stantially higher than anticipated. Evaluation of the material
being used showed a poor N/N+ interface causing these fluctuations

-111-

in R_S and V_f. A second problem, which is common to the fabrication of most PIN diodes, was obtaining Inverse Epitaxial Silicon with an N+ layer more heavily doped than customarily available. Typically, the more heavily doped layer would be lower in loss and, therefore, provide reduced series resistance. After a complete re-evaluation of this process and its goals, the following points became clear:

(1) While a heavily doped N+ layer would reduce R_S, it would also grade during SiO_2 passivation and subsequent diffusion steps. A process by which the junctions were both formed at a later time would be ideal.

(2) Because of the problem in using and obtaining repeatable Inverse Epitaxial Silicon, fabrication of the diode would be difficult; hence, the use of pure bulk silicon would improve the situation.

With these key points in mind, development effort was shifted to this type diode. Problems were encountered in the early stages such as thinning, handling, and flatness of the bulk silicon wafers. However, once these difficulties were overcome, the development of a process suitable for the goal listed was completed. The first successful run was completed in May 1976 with three slices for each individual capacitance range being fabricated. All three slices in the lowest capacitance range were diced into individual diode chips and made available for microwave cold test evaluation.

In dicing these slices, it was important to note that in dealing with chips in excess of 1000 V the distance between the mesa

-112-

edge and the nearest metallic object was very important in preventing arcing. Assuming the field strength in air of 30 KV/cm for a 1.5 KV diode, a distance of 0.020" would be the necessary separation from mesa edge.

Parallel evaluation of these devices was performed in the Diode Development Engineering Laboratory. Breakdowns were in excess of 1000 volts and could be measured in chip form. Life time varied from 1.0 to 1.5 μsec. at a forward bias current (I_f) of 60 mA, and a reverse bias current (I_R) of -40 μA. Series resistance was measured at a forward bias current of 100 mA on a chip mounted in a N20 package and ranged from 0.8 - 0.9 ohm for the lowest capacitance diodes fabricated. Additional diodes are now being fabricated with breakdown voltage and junction capacitance values being determined by evaluation of diode chip performance in the magnetron.

Figure 30a shows the video input current pulse to a diode for measuring minority carrier life times. Figure 30b shows the diode reverse current pulse used to measure minority carrier life time. Figure 31 shows a single diode chip of the size and type being developed. The graticule scale is 0.02 millimeter per division.
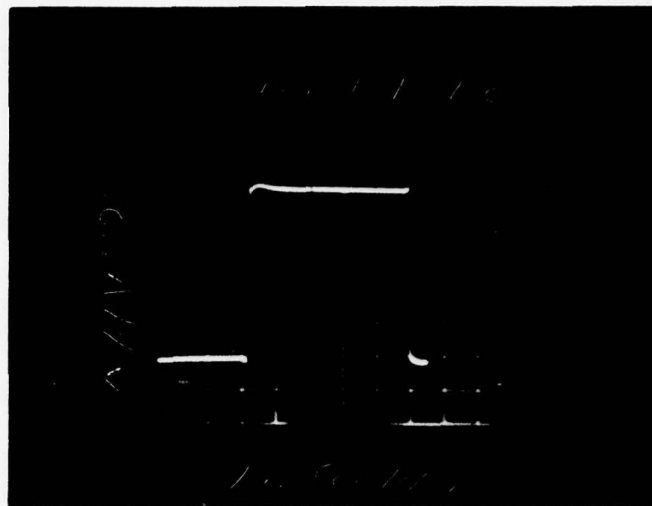
(A)
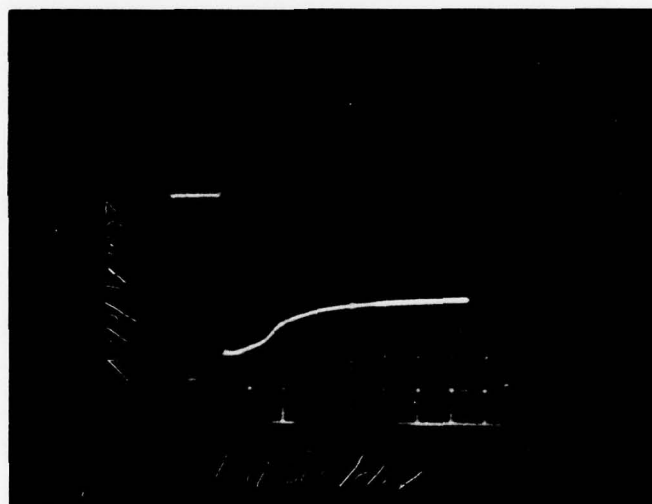
(B)

FIGURE 30

OSCILLOSCOPE DISPLAY FOR MEASUREMENTS OF MINORITY CARRIER
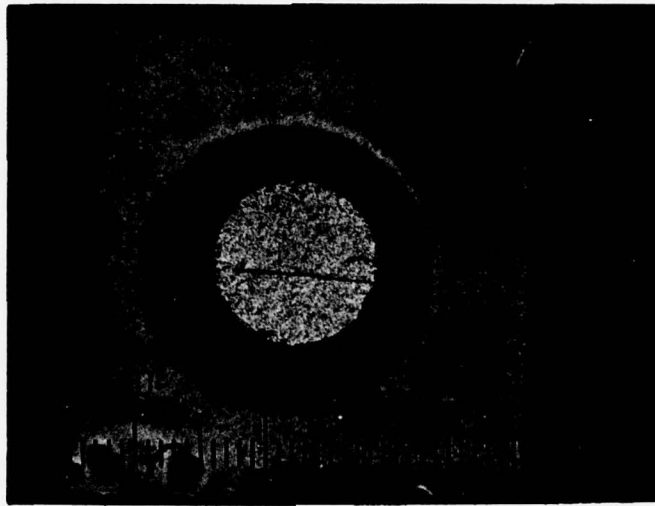LIFE TIME

-114-

FIGURE 31

PHOTOGRAPH OF HIGH POWER PIN DIODE

GRATICULE SCALE IS 0.02 MILLIMETER PER DIVISION.

-115-

6.2   Magnetron Development - Cold Test Experiments

6.2.1   Rectangular Cavity Experiments

The first cold test measurements to verify the concept of
lumped element, coupled circuit tuning at Ku-band were made using
a rectangular cavity. The reasons for this were the same as for
the initial cold test experiments in a rectangular cavity at S-band;
e.g., by using a dominant mode cavity, potential interfernce from
nearby higher order resonant modes was avoided. The first tests
were made by spot welding small rectangular loops of gold ribbon
(0.001 in. X 0.005 in.) to the middle of a flat cavity end plate.
This simulates a coupled circuit with lossless diodes in the for-
ward biased condition. Resonant frequency measurements were made
with a flat plate only as a cavity end plate and then with the flat
plate and attached loop as the cavity end plate. The first loops
were quite small intended to produce only 1-3 MHz tuning similar
to what would be used in an operating tube. It turned out that
there was enough difference in the resonant frequency of the cavity
caused by variations in the mechanical clamp up of the cavity that
the effect due to the coupled loops was masked by experimental
errors. To overcome this a larger coupling loop (approximately
0.120 X 0.200 inches) was attached to the middle of a cavity end
plate. The calculated frequency shift when changing from a flat
plate to one with this loop was +285 MHz and the experimentally
measured frequency shift was +250 MHz. This was considered reasonable
agreement. No further measurements were made using a rectangular
cavity at Ku-band.

-116-

6.2.2   Coaxial Cavity Experiments

A fixed frequency, Ku-band, coaxial magnetron was modified for use as a cold tester. It was found at cold test that the cavity end plate of the tube could be removed and replaced quite readily without change. The resonant frequency of the TE_{011} mode as well as that of other modes were repeatable within measurement error using a standard wavemeter. The cold test vehicle is shown in Figure 13.

Next a series of measurements were made using this coaxial tester for evaluation of several features. It was desirable to test the accuracy of the predicted tuning shifts in the coaxial cavity since reasonable agreement would increase confidence in the calculated values of RF voltage to which the diodes would be subjected. Next, it was to be determined if the balanced circuit and bias lead configuration of the coupled circuit did, indeed, inhibit the coupling of radiation from the cavity. And finally, it was important to determine if the inclusion of a large number of coupled circuits would degrade the cavity Q_o because of excessive losses or because of mode conversion. For these experiments, square coupling loops (0.065 in. X 0.065 in.) were formed from the same gold ribbon used previously. These were spot welded to a circular flat plate that could be inserted into the coaxial tester to close up the cavity.

In the first experiments twelve loops without bias leads attached were located symmetrically about the cavity end plate at

-117-

the mid diameter of coaxial cavity. A calculated frequency shift

when changing from a normal cavity end plate to one with the twelve

loops was 24 MHz. The measured value was 19.5 MHz. Again, this

was considered reasonable agreement considering the accuracy with

which the loops could be made and attached in these early experiments.

For the next experiment, bias leads formed from 0.003

in. diameter wire were connected to the center of the loops. The

twelve loops had previously been mounted to straddle holes drilled

through the circular flat plate. The bias leads passed through

ceramic tubing contained in the holes. They extended about a quarter

of an inch or so beyond the surface of the plate and could serve

as antennas if RF were present on the exposed wires. The cavity

end plate was then replaced in the Ku-band tester. No evidence of

radiation from the TE_{011} mode was observed.

The effect of a large number of coupled circuits was

evaluated by adding loops in a progressive fashion. A total of 102

loops were added in three concentric rings. At first, twelve

loops were attached to an inner ring over one third of its circum-

ference. Frequency shift and Q's were measured as the end plate

was rotated in the cavity with respect to the output port. Slight

differences in tuning and Q_o were observed. The experiment was

repeated after each third of a ring of loops was added until three

complete rings were attached. See Figure 32. The conclusion suggested

that the coupled circuits should be switched in a symmetrical sequence

in order to minimize variation in Q_o and Q_E over the tuning band.
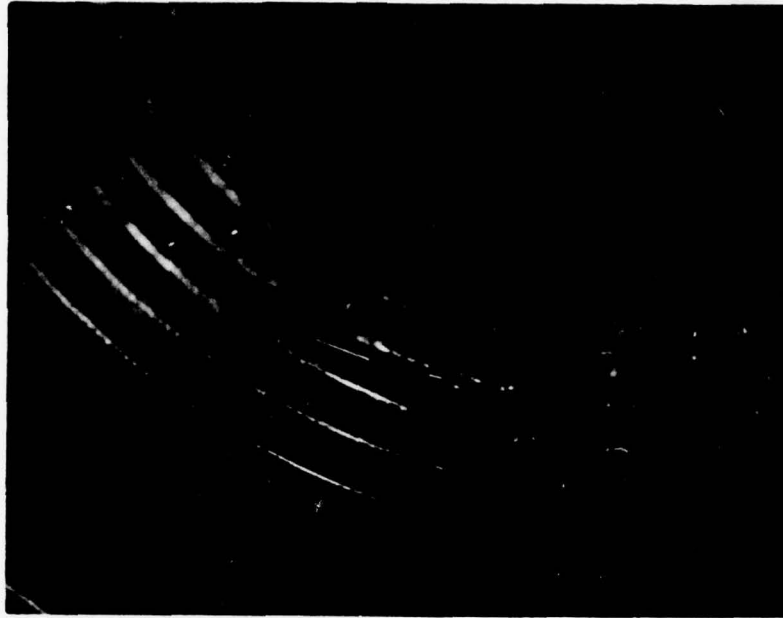
-118-

FIGURE 32

COLD TEST EXPERIMENT THAT SIMULATES FORWARD BIASED
STATE WITH PERFECT, LOSS-FREE DIODES, CALCULATED
TUNING SHIFT OF 180 MHz FOR 102 COUPLED CIRCUITS
COMPARES FAVORABLY WITH THE MEASURED SHIFT OF
150 MHz.

-119-

A total frequency shift of 151 MHz was measured compared to a cal-
culated shift of 185 MHz. Q_o degraded about 25% with the addition
of the 102 coupled circuits.

Next, a cavity end plate was assembled with four coupled
circuits including diodes and bias leads. The diodes were fastened
to the end plate in a circular groove with conductive epoxy and the
coupling loops were affixed to the diodes. Mechanical difficulties
were encountered in this first assembly and the coupled circuits
subsequently became unuseable. Nevertheless, some initial tests
were made. At reverse bias the resonant frequency was above that
of the unperturbed cavity and decreased about 6 MHz in frequency
as the diodes were switched to forward bias condition. In addition,
there was a slight increase in Q_o when the diodes were switched from
reverse to forward bias. All of these changes are in the direction
predicted by the analysis in Section 4.0. The diodes had a junction
capacitance of 0.1pF each and, in conjunction with 0.065 in. square
coupling loop, result in a geometry suitable for intrapulse tuning.
This corresponded to X_C = 200 ohms and X_L = 400 ohms. See Figure
22.

The bias voltages were applied to the diodes using the
circuit shown in Figure 33. Bias switch was done using manually
operated toggle switches.

Two additional cold testers were assembled with twenty-
four coupled circuits each. For these testers, the diodes were
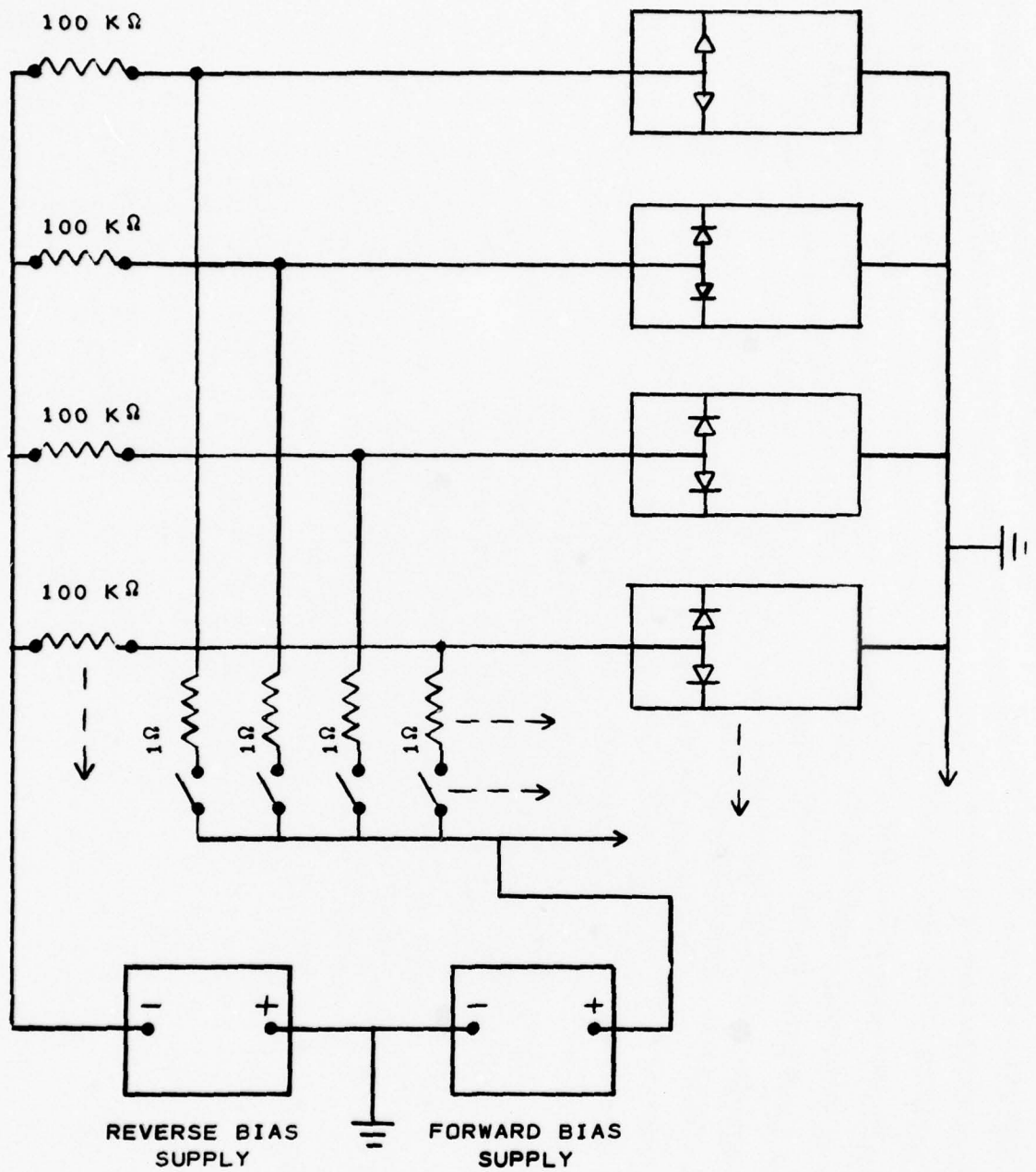recessed into circular spots machined into the cavity end plate.

-120-

FIGURE 33

SCHEMATIC DIAGRAM OF CIRCUIT USED FOR MANUALLY

SWITCHING BIAS VOLTAGES TO THE DIODE-CONTROLLED,

COUPLED CIRCUITS.

-121-

Figure 34 shows a close up view of the diode mounting arrangement
and a completed cavity end plate tuner assembly. One of the plugs
for connecting to half of the coupled circuits is not visible in
the figure. Both of these testers were assembled using experimental
diodes from the diode development program. Those used in the first
assembly were known to have higher resistive loss than desirable.
In both cases, difficulty was encountered in assembly and attaching
the diodes and coupling loops to the cavity end plates. These are
much larger than the pedestals upon which diode chips are usually
mounted. The assembly equipment was not well suited for this appli-
cation and some alteration of the diode properties may have occurred.
In any case, both of these testers gave significantly more tuning
than calculated. For one, a tuning range of approximately 50 MHz was
obtained and for the other nearly 100 MHz. The reason for these differ-
ences is not understood. For both testers, the tuning curves were
approximately linear with small deviations due to differences in
coupled circuit parameters.

Shortly after these experiments were performed, a new
fabrication procedure was adopted for mounting the coupled circuits.
This was selected to utilize fabrication techniques more customarily
used in assembling PIN diodes. Because of this, no further experi-
ments were performed with these two cold testers and the reason
for the higher tuning ranges was not resolved.
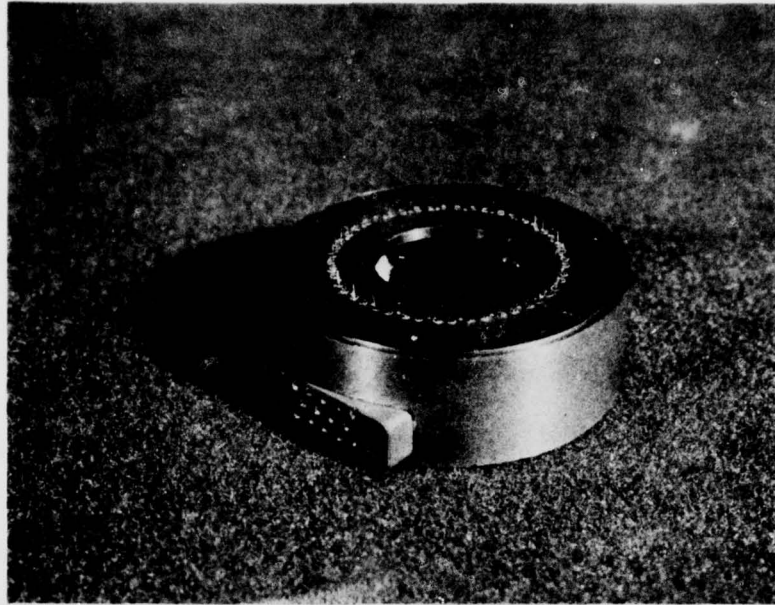
FIGURE 34

COLD TEST EXPERIMENT WITH 24 PIN DIODE, COUPLED

CIRCUITS.   OBTAINED 50 MHz TUNING.

-124-

6.2.3 Peak Power Testing of Diodes

Some attempts were made to assess the high power character-
istics of PIN diodes by mounting a pair of them on a flat plate
and joining them with a coupling loop. The flat plate was attached
to the output end of the waveguide replacing the absorptive load in
a magnetron test set. The reflected power from the end plate was
coupled by means of a high power circulator into an absorptive load.
The incident pulsed power from a magnetron was adjusted to provide
different peak power levels to the diode-coupling loop combination.
From the coupled circuit parameters, the peak RF voltage applied to
the diodes could be calculated. The d.c. bias to the diodes was
varied along with changes of incident peak power. Attempts were
made to determine the RF voltage level at which reverse breakdown
and/or rectification occurred. This was noted by the presence and
the polairty of d.c. current flowing in the bias lead. Initially,
it was thought that this procedure was giving meaningful results.
However, in view of some of the results obtained during hot test
operation of a diode-tuned tube, there is now some reservation about
the proper interpretation of these early experiments. During any
further development of the diode-tuned concept for a coaxial magnetron,
additional effort must be devoted to evaluating the diode properties
and tuning circuit characteristics exclusive of the operating tube
characteristics.

6.3   <u>Magnetron</u> <u>Development</u> - <u>Tube</u> <u>Experiments</u>

6.3.1   <u>Individual</u> <u>Mounting</u> <u>for</u> <u>Coupled</u> <u>Circuits</u>

   Fabrication difficulties were encountered when affixing the PIN diode chips to the relatively large resonant cavity end plate. The diodes were attached by thermal compression bonding and the available bonding equipment and tooling fixtures were not very suitable for this operation. In addition, once all of the diode chips were attached to the tuner plate, it would be very difficult to make any repairs if one or more diode chips or coupling loops should fail for any reason. Because of this a new fabrication technique was devised. In this arrangement, a separate mounting stud was used to which two diode chips, a coupling loop and a bias lead could be attached. See Figure 35. The mounting stud is comparable in size to the metal-ceramic package geometry used in production type PIN diodes and, therefore, presents much less difficulty in making the thermal compression bonds. In addition, this configuration permits test and evaluation of individual coupled circuits for satisfactory operation prior to assembly into a magnetron. Furthermore, individual circuits could be removed and replaced if necessary.

   The mounting studs were fabricated with a groove to accommodate the diode chips and two flat sides parallel to the groove. The coupling loop was attached to the two chips so that the plane of the coupling loop was along the center of the groove. The flat sides of the mounting set the orientation of the mounting

-126-

stud when placed in a groove in the cavity end plate. This assured

the proper position for maximum coupling to the radial RF magnetic
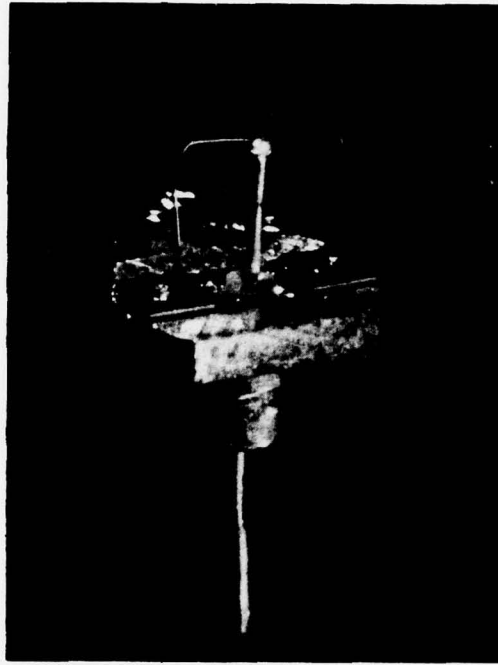
field lines of the TE_{011} mode.

FIGURE 35

CLOSE UP VIEW OF PIN DIODE COUPLED CIRCUIT TUNING STUD.

-128-

6.3.2   The First Coupled,-Circuit-Tuned, Coaxial Magnetron

The first test of the diode controlled, coupled circuit tuning principle in an operating tube was conducted at Ku-band. The test vehicle was a modified BLM-183 magnetron. This tube is rated at 35 kW minimum peak power output and has been tested at higher voltage to produce over 70 kW. The modification consisted of exchanging the conventional movable tuner plate with a fixed end plate for the cavity. In addition, an extension header was added that contained insulated feedthrough connectors for attaching the d.c. bias voltages to the diodes.

The heaters were fabricated prior to the completion of the initial cold test measurements. Twenty four connectors were used in anticipation of using twenty four coupled circuits. The feedthrough connectors were arranged around the periphery of the tube for convenience of attaching internal connecting leads to the bias terminals of the coupled circuits.

The first tube was assembled with six coupled circuits. This number was selected because it represented a compromise between demonstrable tuning range and potentially excessive degradation in Q_o if more were used, and because this was considered a reasonable number for a first test of a new configuration. Two views of the subassemblies of the first tube are shown in Figure 36. The completed experimental breadboard tube is shown in Figure 37.

Cold test measurements were made at each stage of the final assembly to determine if and when any damage occurred to the coupled circuits. For instance, cold test measurements of Q_o were
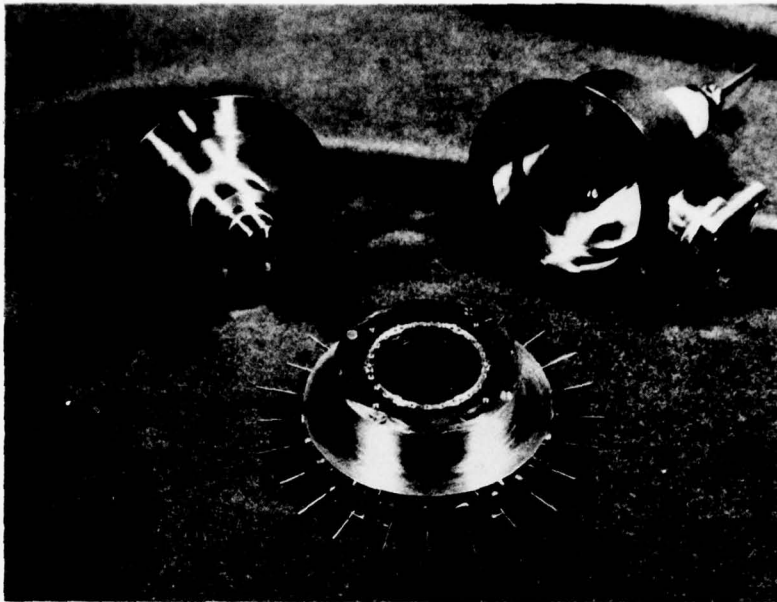
-129-
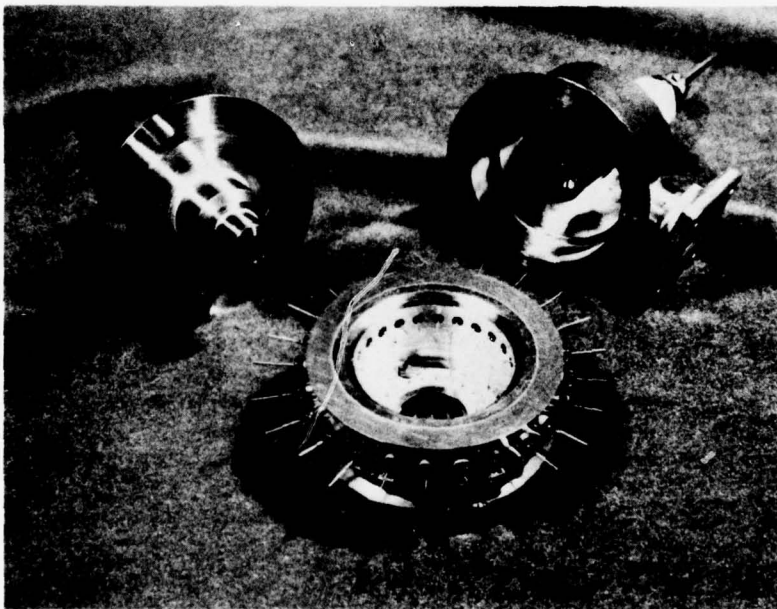
FIGURE 36

EXPERIMENTAL BREADBOARD TUBE. SIX COUPLED CIRCUITS
EMPLOYED. TOP VIEW SHOWS THE TUNER PLATE FROM THE
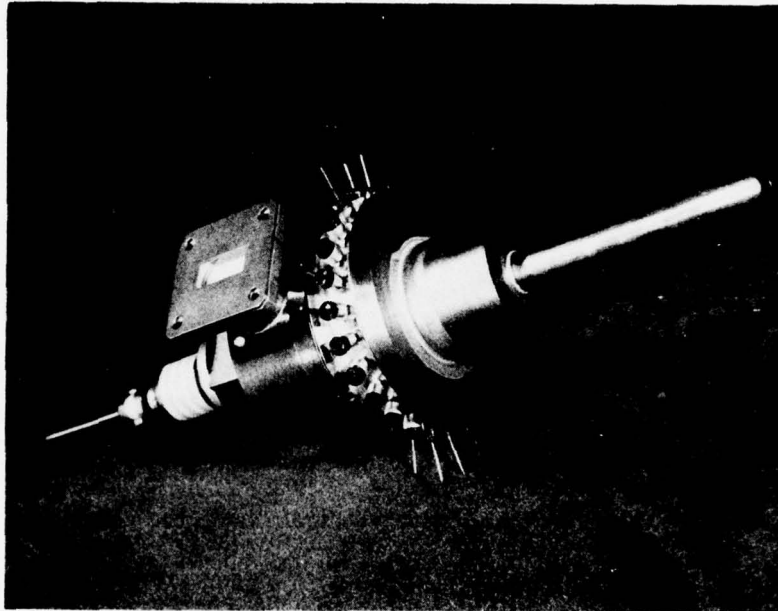CAVITY SIDE. BOTTOM VIEW SHOWS THE BIAS CONNECTIONS.

-130-

FIGURE 37

COMPLETE EXPERIMENTAL BREADBOARD TUBE

-131-

made in a clamp up of the subassemblies before the internal connection between the feedthrough connectors and bias terminals were made. Then they were made again after the connections were made; and again, after each of the heliarc welds to seal the tube. The coupled circuits survived without Q_o degradation, but it was observed after the first heliarc weld that the d.c. connection to two of the coupled circuits seemed erratic at times. One of these subsequently became short circuited.

The tube was baked out and exhausted in the usual fashion except that the heater was not activated on the exhaust station. This was done because it was desirable to determine if contamination of the diodes occurred during this procedure. Q measurements after exhaust showed some degradation in Q_o, but resistance measurements did not indicate any change in leakage resistance for the diodes.

On a bench test, the cathode heater was raised slowly to normal operating temperature. An appendage vac-ion pump was used to limit the internal pressure of the tube. Measurement of the leakage resistance of the diodes when the heater voltage was applied showed a decrease in leakage resistance to about 10-20 meg ohms. This does not seem serious. Q measurements made afterward did not show any significant change in Q_o. However, during these measurements one of the coupled circuits became short circuited. The reason is not known at this time since the tube has not been opened. The remaining five coupled circuits produced a down shift in frequency of 19 MHz. When all were switched from reverse bias (-125 V) to forward bias

-132-

(1 amp total current), the values for Q_o increased. The changes in Q's are shown below.

	fo	Q_E	Q_o	Q_L
All reverse bias	16365	906	2219	643
All forward bias	16346	849	2453	631

This tuning range is larger than calculated and larger than planned for five coupled circuits. It is believed that the reason is that the mounting studs for the coupled circuit are sealed in a groove in the end plate measuring 0.019 by 0.072 inches. It is speculated that this effectively lowers the cavity wall in the vicinity of the coupled circuits, and thereby increases the magnitude of the coupling factor. This increases the tuning range, but it also increases the induced voltage in the coupled circuit. This exposes the diodes in the reverse biased state to larger RF voltage than intended at 60 kW peak power output.

Prior to hot test operation of this tube, additional cold test data were taken to show the transitional characteristics during the switching of a coupled circuit. The change in frequency and Q_o was measured as the forward bias current was increased from zero in one coupled circuit to a full forward biased state while the other four circuits were kept fully reverse biased. The results are shown in Figures 38 and 39. This measurement reflects the same kind of change shown earlier in Figure 11 where less complete data were shown. The shape of these curves is explained by the diode character-istics. As the diode is forward biased, the capacitance progressively increases in value until it becomes infinite and the shunt leakage resistance decreases progressively until its final low value is
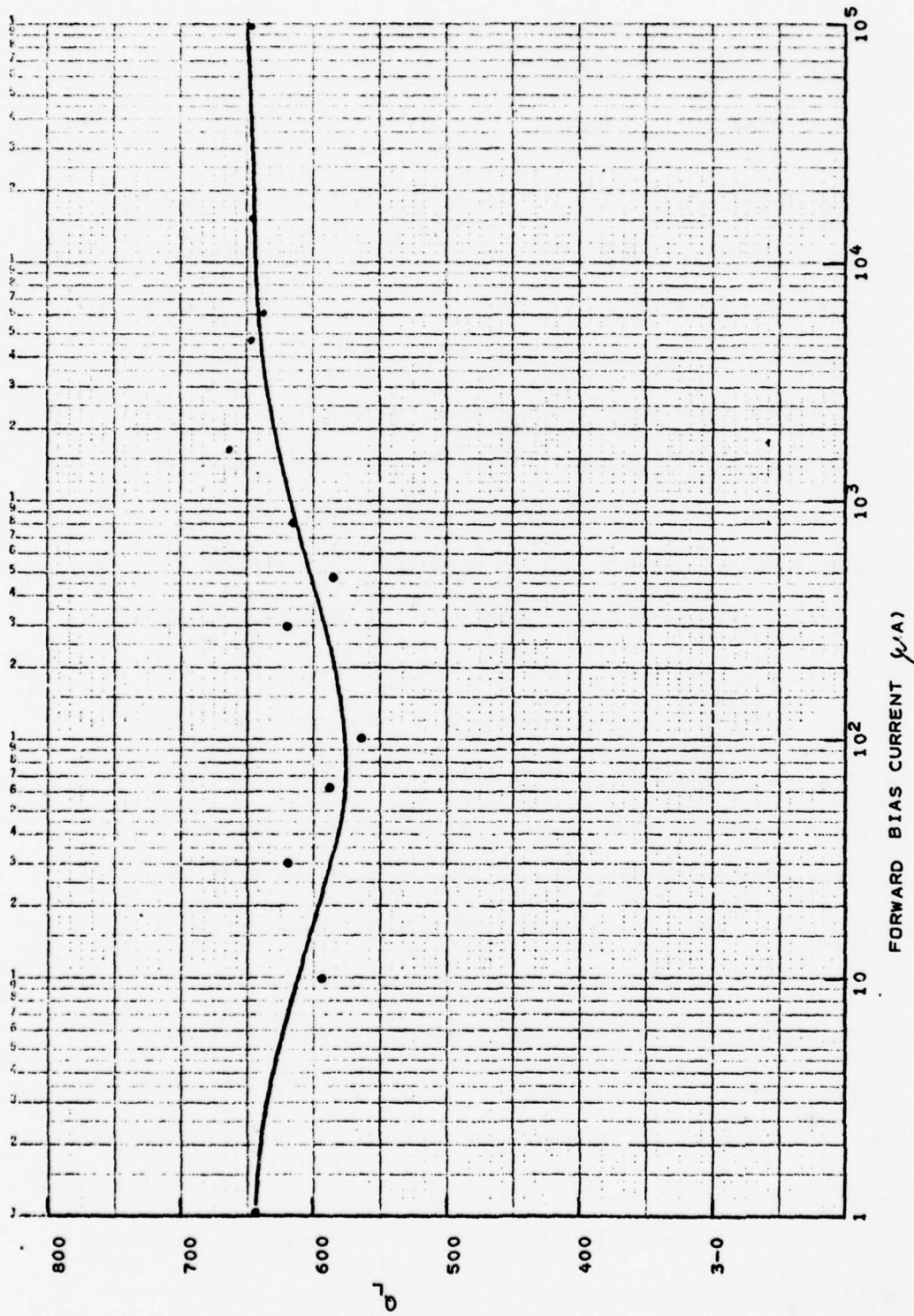
-133-

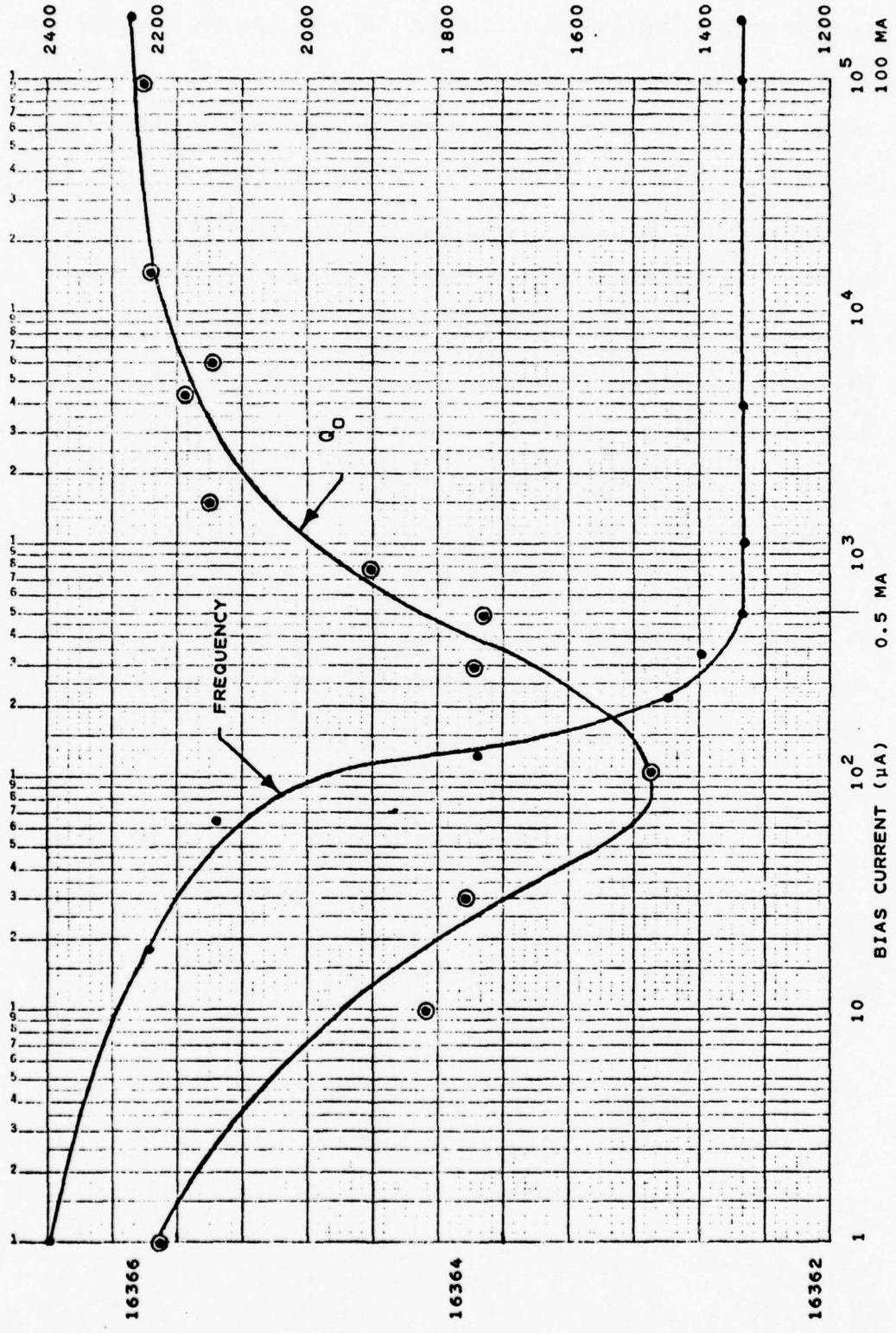FIGURE 38 - VARIATION OF Q_L WITH FORWARD BIAS CURRENT

-134-

FIGURE 39 - COUPLED CIRCUIT TUNING VERSUS PIN DIODE BIAS CURRENT

reached at full forward current bias. In other words, the diode has a variable complex impedance during the transition. The significant factor to note is that the full change in frequency and the major portion of Q_o degradation and recovery have already transpired when the forward bias current is less than one percent of the final bias current. This suggests that it may be possible to use only one coupled circuit geometry to obtain both intrapulse and interpulse tuning. Previously, it was suggested in Section 4.4 that a coupled circuit designed to always present a net inductive reactance would be used to avoid possible problems when passing through series resonance during intrapulse tuning. These data show, however, that the transition may be made to occur so quickly that problems may be avoided by an appropriately designed, fast response, driver circuit. This will need to be investigated further with other coupled circuit configurations. It this proves feasible it will aid in meeting the program goals of achieving both Option A and B with one vehicle.

The tube was evaluated using a conventional magnetron test set. The tube was operated in an electromagnet. Figure 40 shows two close up views of the tube. Figure 41 shows the test set with bias supplies and switching unit on an adjacent movable cart.

The tube was tested initially at low peak power output and -150 volts reverse bias. Tuning was demonstrated at a peak power level of 1-2 kW. The bias voltage was then adjusted to determine how low it could be set and still demonstrate tuning. It was found that the tube would operate and tune with reverse bias voltage as low
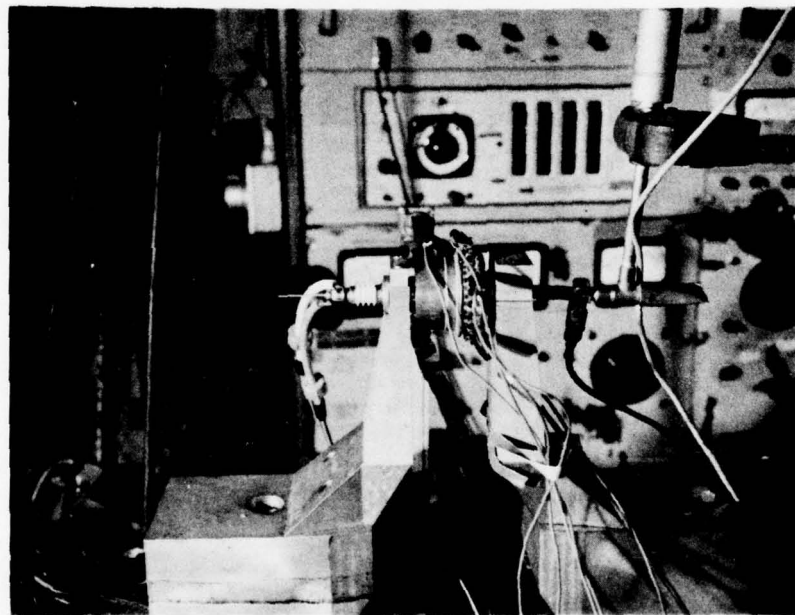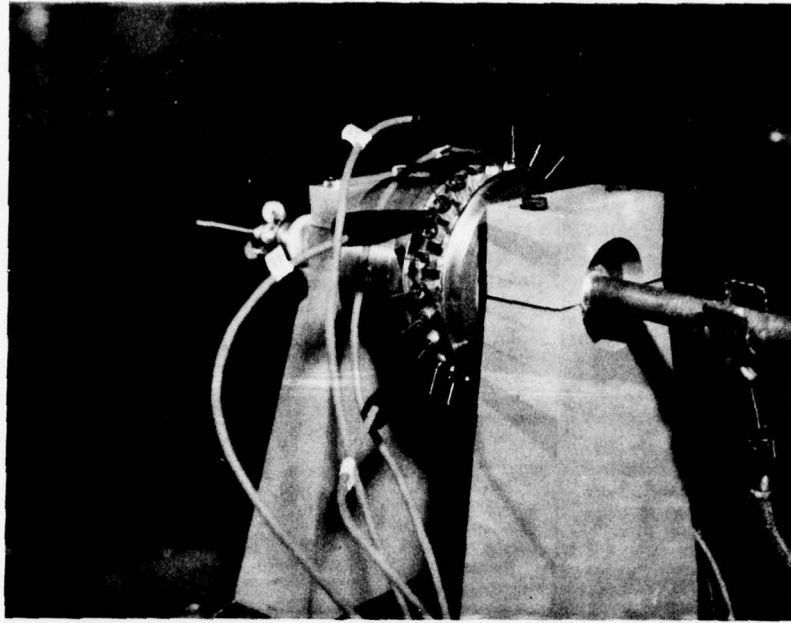
-136-

FIGURE 40

TWO VIEWS OF THE EXPERIMENTAL TUBE MOUNTED IN THE
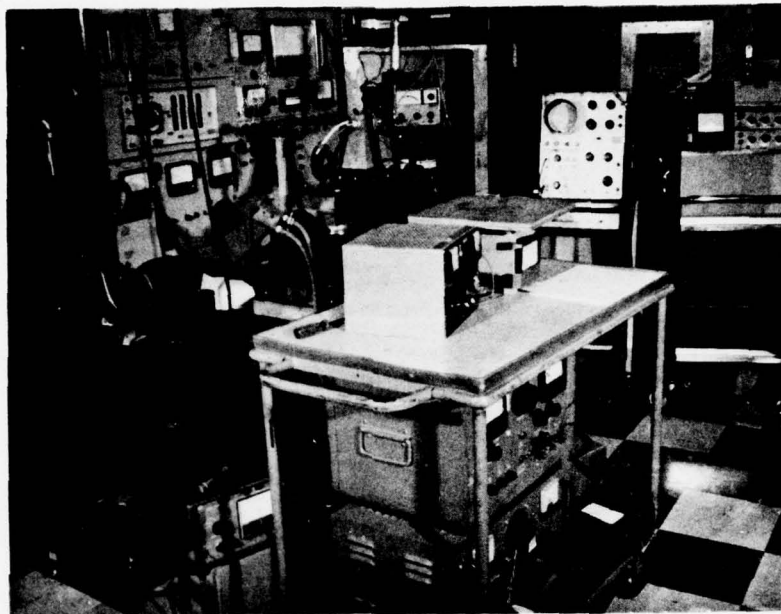ELECTROMAGNET

-137-

FIGURE 41

TUBE TEST SET

-138-

as as 10-20 volts. The bias power supply voltage was then set to
150 volts and the circuits set to forward bias with a total bias
current of 1.0 amps. The peak power output was increased to 50-55 kW
and the coupled circuits were switched. About 10 MHz tuning was
obtained and the power output changed by about 3 dB. These results
were not expected. The tuning range was less than that obtained at
cold test and the power variation was greater than the cold test
measured values of Q's would have predicted. Some time was spent
rechecking these results and it was observed that the tube peak
power output was decreasing with time. A complete set of measurements
were then made for power otuput and tuning as well as photographs of
the detected RF output pulse and pulse spectrum distributions. These
are shown in Figures 42-45.

The tube was then removed from the hot test set. Resistance
measurements were made of the diodes and the shunt leakage resistance
was found to have become lower. Q measurements showed degradation
in the internal Q_o, but the same low power tuning range of 19 MHz was
obtained as before. It was speculated that the diodes had become
contaminated during tube operation.

The conclusion from this first operational test was that
the feasibility of electronic tuning using PIN diode-controlled,
coupled circuits had been demonstrated. Tuning was also demonstrated
using relatively low values of reverse bias voltage. But discrepancies
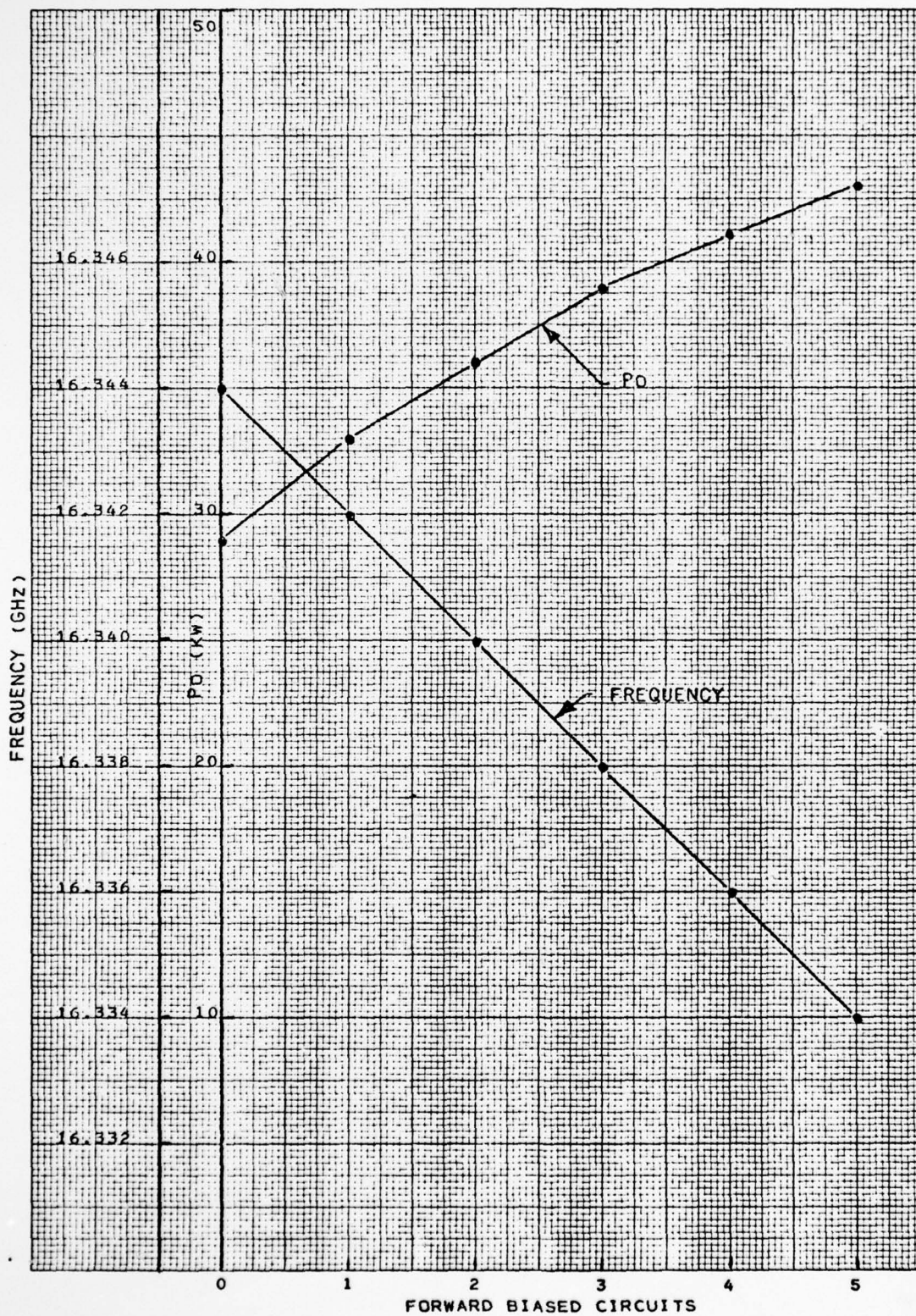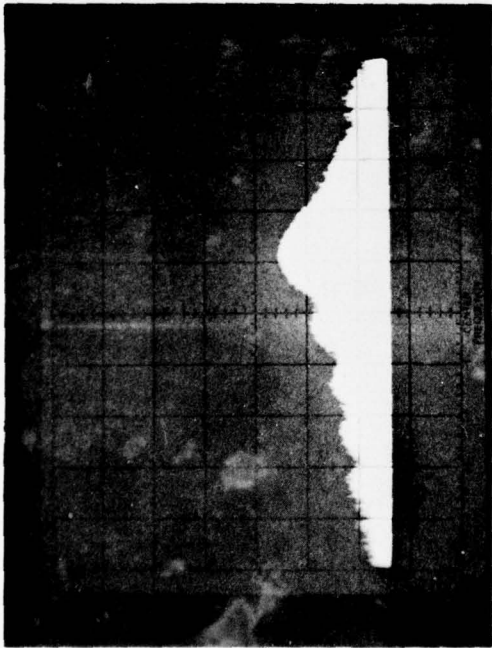existed between results observed at cold test and those at hot test.

-139-

FIGURE 42 - ELECTRONIC TUNED MAGNETRON CHARACTERISTICS

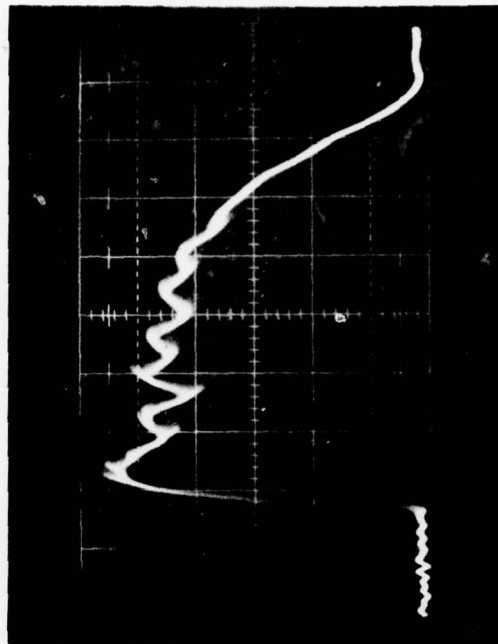ALL DIODES
ARE
REVERSE
BIASED

fo = 16344 MHz

Po = 29 kW

1 CIRCUIT
FORWARD
BIASED;

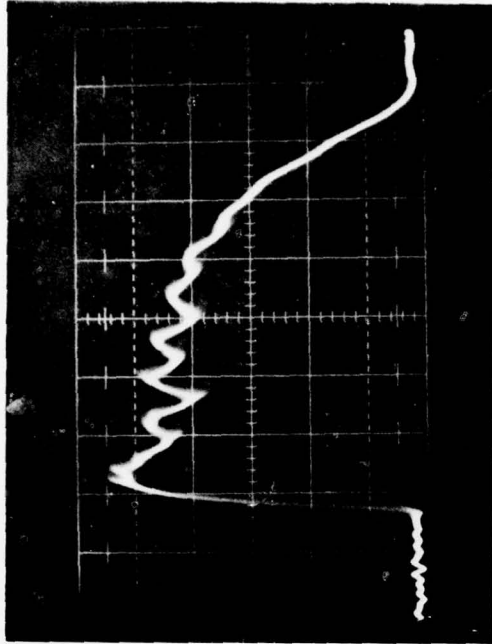4 REVERSE
BIASED

fo = 16342 MHz

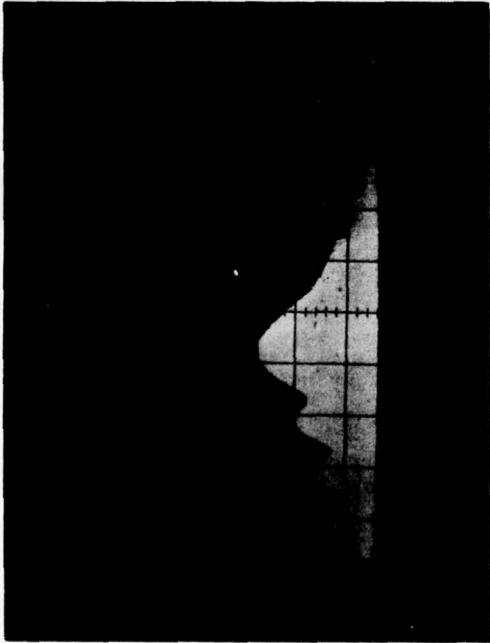Po = 33 kW

FIGURE 43

Spectrum degrades with all diodes are reverse biased because of Q degradation.
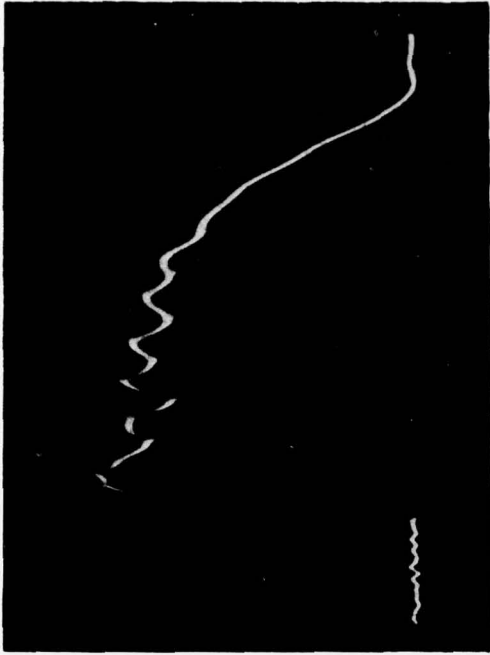
VERTICAL SCALE = 10 dB/cm

HORIZONTAL SCALE = 2 MHz/cm

2 CIRCUITS
FORWARD
BIASED;
3 REVERSE
BIASED

fo ≐ 16340 MHz

Po = 36 kW

3 CIRCUITS
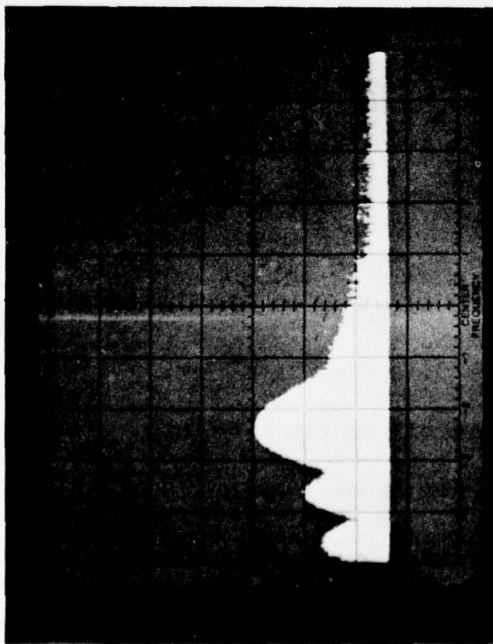FORWARD
BIASED;
2 REVERSE
BIASED

fo = 16338 MHz

Po = 39 kW

Spectrum degrades when all diodes are reverse biased because of Q degradation.

FIGURE 44

VERTICAL SCALE = 10 dB/cm

HORIZONTAL SCALE = 2 MHz/cm

4 CIRCUITS
FORWARD
BIASED;
1 REVERSE
BIASED

fo = 16336 MHz

Po = 41 kW
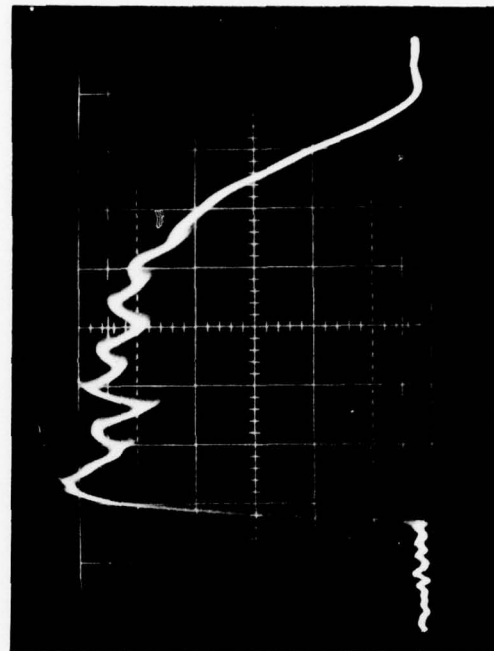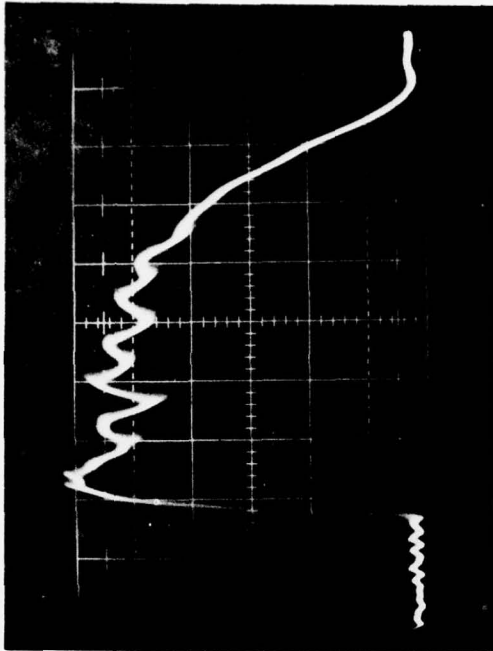
5 CIRCUITS
FORWARD BIASED;
ANALYZER CENTER
FREQUENCY
ADJUSTED TO
KEEP MORE OF
THE SPECTRUM
IN THE PICTURE

fo = 16334 MHz

Po = 43 kW

Spectrum degrades when all diodes are
reverse biased because of Q degradation.

FIGURE 45

VERTICAL SCALE = 10 dB/cm

HORIZONTAL SCALE = 2 MHz/cm

-143-

It was not known at this point whether the differences were due to change of diode characteristics between low and high power, or due to some other difficulty. Because of this and because the contractual time period was nearly over, a second tube was assembled with the identical coupled circuit design. However, this tube was assembled with 12 coupled circuits. While this tube was being completed for test, further analysis was made of the results obtained to try to understand the unanticipated differences between hot and cold test.

Upon further study, it was concluded that changes in leakage resistance alone could not account for the differences. The change was clearly associated with high power operation. Figure 46 shows an equivalent circuit of the tuning element and bias supply arrangement. The capacitance between the bias lead and ground is made up from the feedthrough insulator in the mounting stud and other stray capacitances. This equivalent circuit shows the tuning element has the same configuration as a full wave rectifier. Hence, once the diode starts to rectify a negative self bias will be developed across the capacitors which will, in turn, discharge through isolating resistors. The negative self bias will be almost equal to half the full voltage coupled into the secondary circuit. The differences will be just enough to allow a rectified current to replace the d.c. losses. Consequently, a small net average d.c. current will be flowing through the diode. Since the carrier life time is much greater than an RF cycle, the diode will not turn off on the reverse half cycle and the net effect will be as though the diodes were
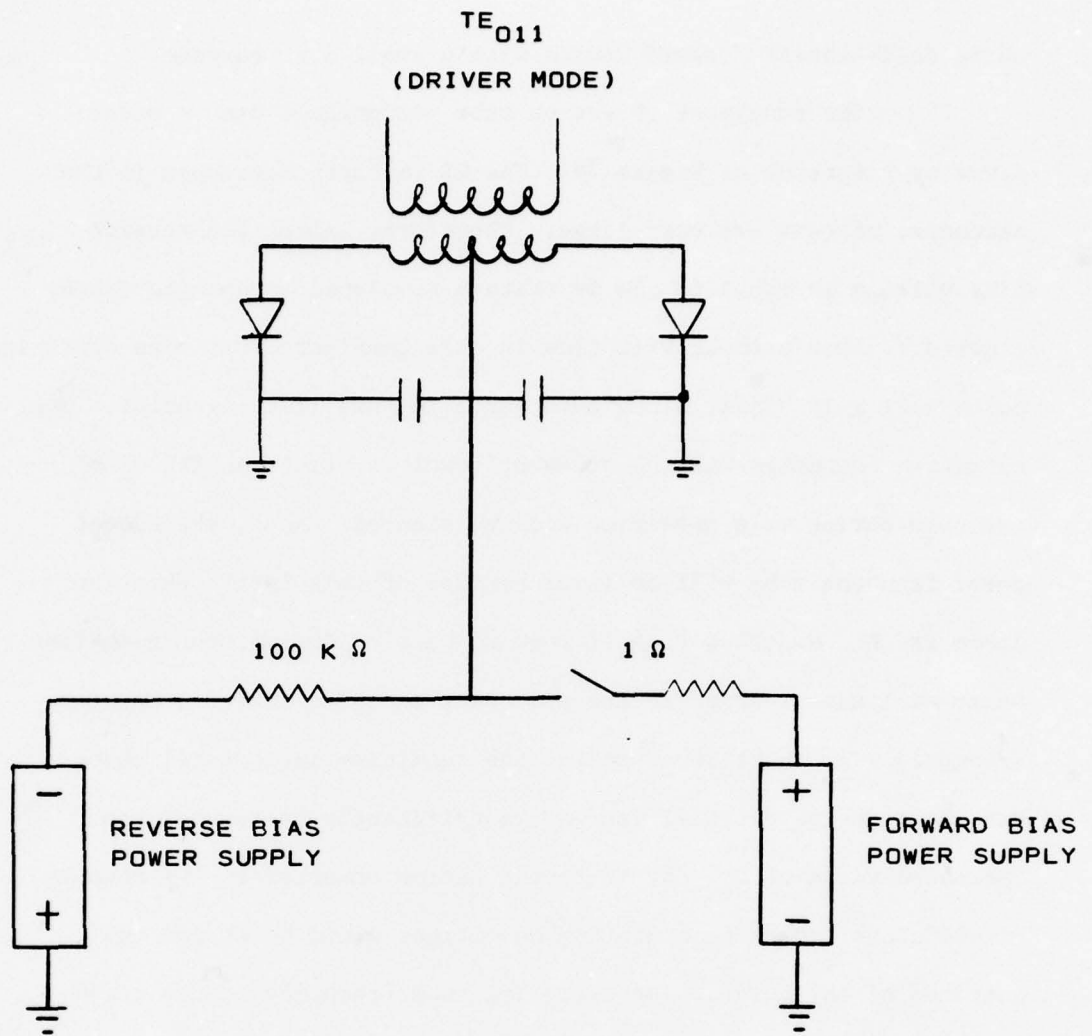
-144-

TE$_{011}$

(DRIVER MODE)

100 K Ω 1 Ω

REVERSE BIAS
POWER SUPPLY

FORWARD BIAS
POWER SUPPLY

FIGURE 46

SCHEMATIC DIAGRAM OF DIODE-CONTROLLED, COUPLED

CIRCUIT AND BIAS POWER SUPPLIES.

-145-

being deliberately forward biased with a small d.c. current.

The resultant effect on tube performance can be understood by reference to Figure 38. The RF voltages developed in the secondary circuit are very large. Therefore, unless the reverse bias voltage is equal to the RF voltage developed across the diode, a net d.c. bias current will flow in this configuration. The operating point will self adjust along this curve to some limiting point. The operating frequency will be somewhat lower in value and the Q_o of the tube during this operation will be reduced. Also, the output power from the tube will be lower because of this fact. When the diode is then switched to full forward bias condition, the operating point will move forward to the end point on these curves. The tube frequency will shift downward for the remaining incremental change and the power output will increase significantly because of the increased value of Q_o. If no rectification occurred in the reverse biased state, the tube operating conditions would be at the two extremes of the curve. The operating tube frequency change would be the same as the cold test measured value and the change in power level with tuning would be much less dictated by the smaller change in Q_o.

The conclusion from this interpretation is that tuning with low voltage diode switching is possible only at the expense of decreasing the coupling between the two systems which then leads to reduced incremental frequency change. Improved diodes or other circuit approaches may change this.

-146

6.3.3   The Second Coupled-Circuit-Tuned, Coaxial Magnetron

The second operating tube was intended to be the same electrical design as the first except that twelve coupled circuits were used instead of six. At cold test this tube was found to be better than the first in that the Q_o for the unperturbed cavity was higher. Again, the properties of the coupled circuits were monitored after each phase of the assembly procedure to determine if and when difficulties were encountered. The heater was turned on during bench test after the tube was removed from exhaust. The heater power was raised more slowly this time in order to allow the vac-ion pump to keep the pressure as low as possible. After this procedure, Q measurements were made with the following results:

	fo	Q_E	Q_o	Q_L
All reverse bias	16385	1063	2264	723
All forward bias	16347.5	923	2501	674

Note that the Q's for this tube are higher than for the first tube even though there are twice the number of coupled circuits employed. The twelve circuits give a total frequency shift of about 38 MHz which is, again, greater than had been anticipated.

The tube was next used to test the self-biasing hypothesis. To do this, the tube was placed on hot test and the peak power available was increased gradually. If the interpretation was correct it was expected that the electronically-tunable bandwidth would be a function of the magnetron power output because the secondary circuit

-147-

RF voltage varies with power output. It was expected that the tunable

bandwidth would decrease with increasing power output. The results

are shown in Figure 47. In this figure, the tunable bandwidth

is plotted as a function of the peak power output from the tube

when it has all coupled circuits in the forward biased state. It

is seen that the tunable bandwidth does decrease with increased

power output. The peak power output with all diodes in the reverse

biased state is also plotted in the same fashion. The power output

variation is nearly a constant ratio while the variation in frequency

is not. This implies a self-limiting condition around a broad

minimum in the variation of Q_o as shown in Figure 38.

The hypothesis was tested further by variation of the

d.c. reverse bias at a fixed value of low peak power output. Lowering

the bias decreased the power output and the tunable bandwidth slightly

whereas increasing the bias permitted a slight increase in bandwidth

and power output. The bias voltage was then connected directly to

the diode without a series limiting resistor and greater changes in

tunable bandwidth were obtained with an additional slight increase

in power output in the reverse biased state.

It is expected that still further improvement can be

obtained using diodes with larger breakdown voltage that can be
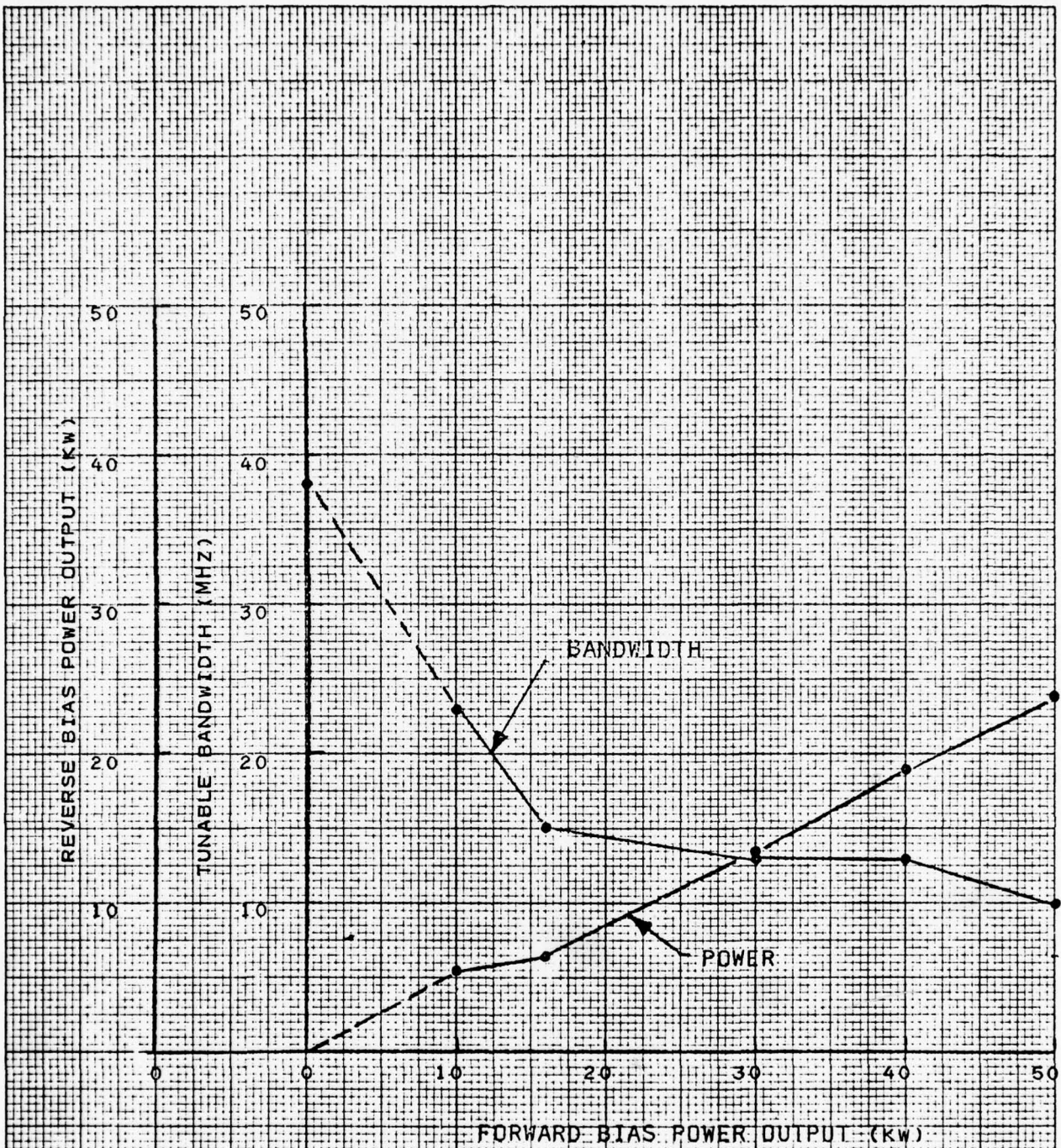
biased more negatively.

FIGURE 47

POWER OUTPUT AND ELECTRONIC TUNING BANDWIDTH

7.0   ELECTRONIC TUNING MODULATOR REQUIREMENTS

The analysis of coupled-circuit tuning presumed that the diodes were never driven into rectification or into reverse breakdown. However, based upon other experience using PIN diodes it was thought that it might be possible to obtain electronic tuning using a d.c. bias voltage whose magnitude was considerablly less than the peak RF voltage. Early tests with the operating tube were made with reverse bias voltage of 200 volts or less. In fact, tuning was demonstrated with d.c. bias voltage as low as 10 volts. However, it was found that this resulted in rectification and self biasing of the diode. It now seems that higher bias voltages will be required.

A design study for an electronic modulator requirement was made during this program. Part of the effort was directed toward appropriate control logic circuitry and part toward the design of solid state driver units for the PIN diodes. This latter portion was done when it was thought that lower bias voltage values could be used. The design of the logic circuitry is still valid, but the design of the driver circuits will have to be changed if, indeed, higher values for reverse bias voltages are necessary.

-150-

7.1   Control Logic Circuits for PIN Diode-Tuned, Coaxial
        Magnetrons

The general control of the diodes accomplishing the
electronic magnetron tuning requires a diode driver for each diode
and an appropriate control logic section to maintain the frequency
tuning control as illustrated in Figure 48. The control logic
provides the control gates $G(1)$, ..., $G(k)$, ... $G(N)$ to control
the state of each tuning diode via the diode drivers. The general
configuration is based on N independently controllable diodes, each
with its own driver. The output gate of the control logic is a TTL
control where a logical 0 produces a non-conducting diode state
or "open circuit" and a logical 1 produces a diode conduction
state or "short circuit".

The tuning control is established from frequency $f(0)$, the
base frequency, which is generated when all diodes are open (non-
conducting). The conduction of each diode produces an incremental
change in frequency of Δf_T, so that with one diode conducting $f_T =$
$f(0) + \Delta f_T$; for two diodes $f_T = f(0) + 2\Delta f_T$, to $f_T = f_0 + N\Delta f_T$ for
all N diodes conducting. Consequently, the differential total
tuning range is $N\Delta f_T$ in steps of Δf_T.

The control logic also generates a number of subsidiary
outputs. A clear gate, $G(C)$, logic output is provided for use in
causing the diode drives to clear the state of all diodes to a non-
conducting or "open" condition. An LO control is provided as a
logical signal for use in establishing the appropriate local oscil-
lator frequency. A magnetron modulator trigger is also provided to
allow the necessary synchronism between the electronic tuning of the

-151-

timing of the magnetron cathode pulse.

Two types of magnetron frequency control will be discussed; interpulse tuning where the magnetron frequency is constant over the RF pulse duration and retuned between pulses, and intrapulse tuning or "chirp" where the RF is tuned during the RF pulse duration.
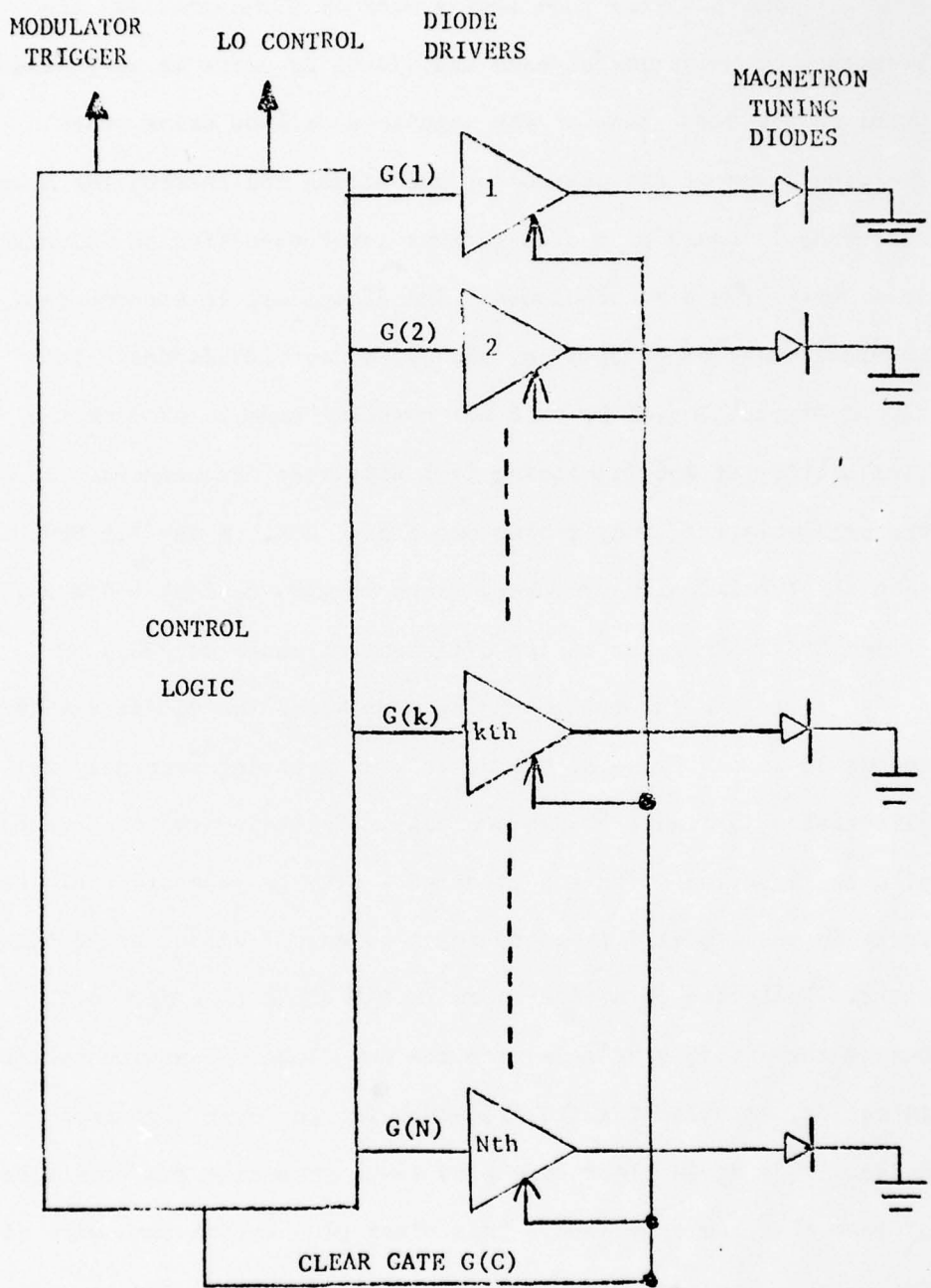
MODULATOR
TRIGGER

LO CONTROL

DIODE
DRIVERS

MAGNETRON
TUNING
DIODES

CONTROL

LOGIC

G(1)   1

G(2)   2

G(k)   kth

G(N)   Nth

CLEAR GATE G(C)

FIGURE 48

GENERAL CONTROL LOGIC CONFIGURATION

7.1.1   Interpulse Tuning

In the interpulse tuning mode of ETM operation, the frequency of operation of each individual RF pulse is established prior to the occurrence of the magnetron cathode drive pulse. The discussion of the control of the diodes and thereby the magnetron frequency is based on a diode/driver interconnection as illustrated in Figure 49 for N = 255 diodes. The diodes are interconnected in binary sets of 1, 2, 4, 8, 16, 32, 64 and 128 diodes. This allows direct control by an 8 bit parallel code to produce the availability of 256 (including f(0) different frequencies. If the available frequency tuning per diode, Δf_T, is say 1.5 MHz, then the total tuning frequency range is f(0) to f(0) + 255 x 1.5 = f(0) + 382.5 MHz for a tuning differential range of 382.5 MHz.

In the interpulse tuning mode where the diodes are interconnected in binary sets, the basic tuning timing sequence, as illustrated in Figure 50, is probable. Following the occurrence of each magnetron pulse the clear gate G(C) is generated for use to cause the diodes/drivers to reset to an all diode, non-conduction state. Following this clear gate is the diode tune gate G(T). During the duration of this gate the new diode conduction pattern is set up, establishing the frequency for the next magnetron pulse. This diode clear time plus re-program time requires times of less than 1 microsecond. This clear plus retune time will allow for pulse repetition rates (PRR) as high as about 1 MHz excluding the interpulse limitations of magnetron duty cycle and radar range
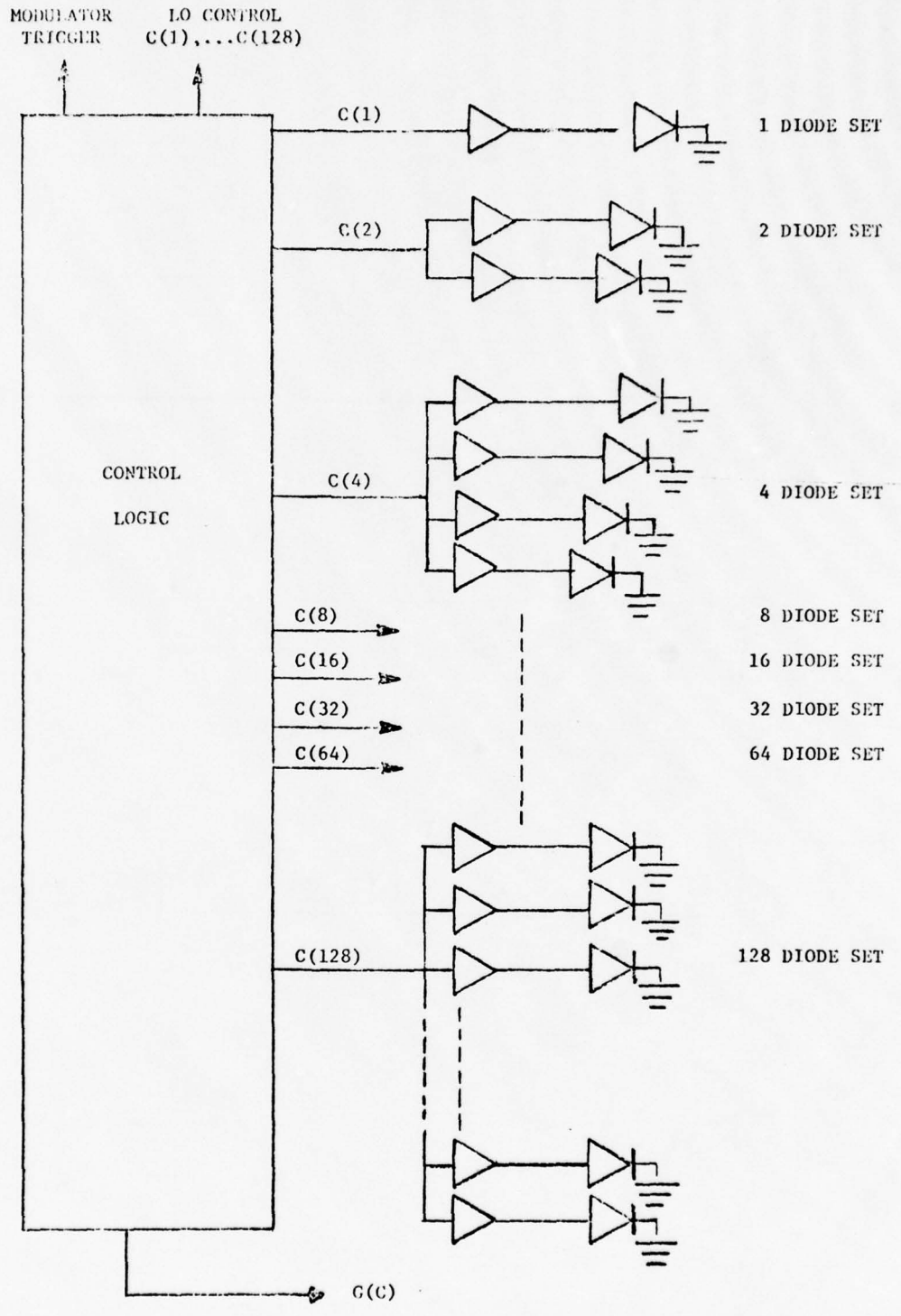
-154-

FIGURE 49

GENERAL INTERPULSE TUNING CONTROL CONFIGURATION

-155-

PRI = $\frac{1}{PRR}$

PULSE WIDTH tp

RF PULSE CYCLE   (a)

G(C)

CLEAR PERIOD

DIODE DRIVER CLEAR GATE   (b)

G(T)

TUNE
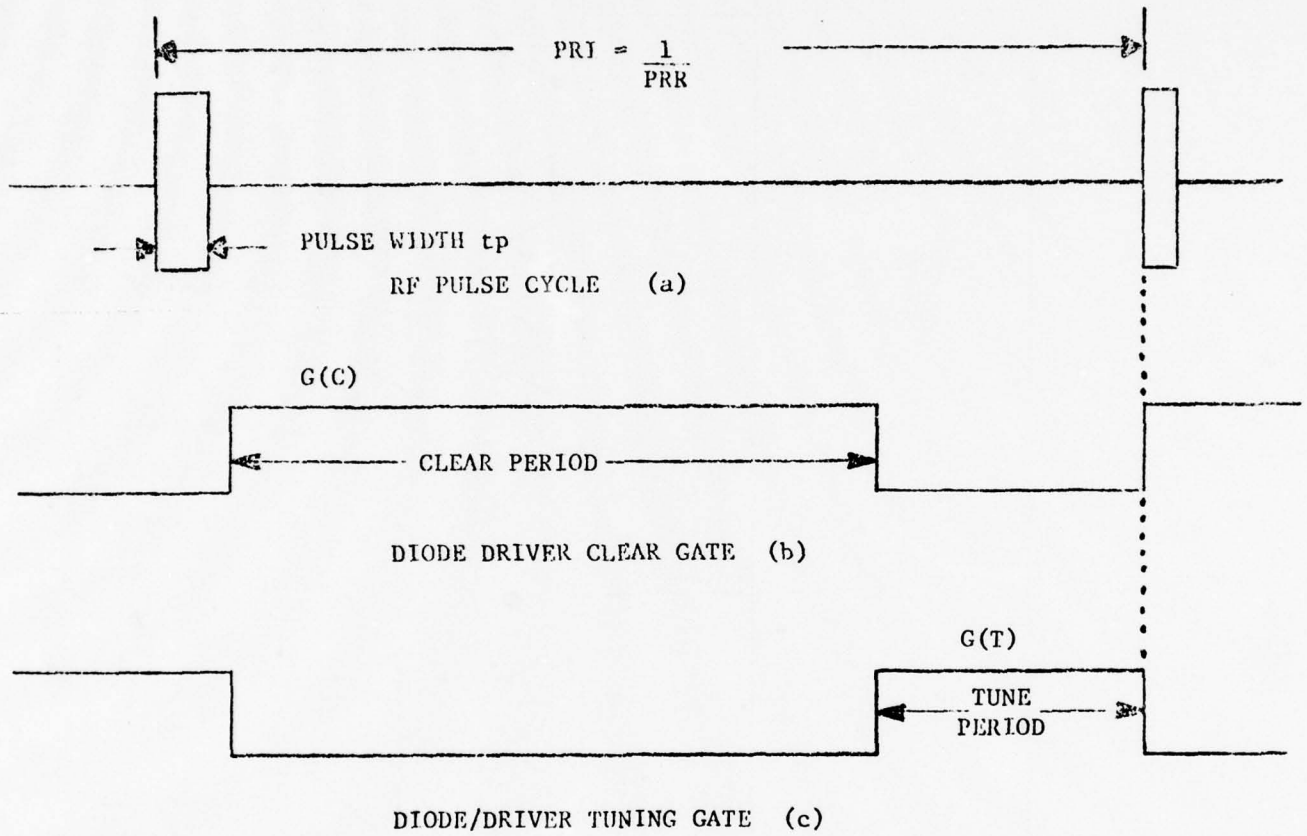PERIOD

DIODE/DRIVER TUNING GATE   (c)

FIGURE 50

INTERPULSE TUNING SEQUENCY

-156-

time of 6.66 microseconds per kilometer of range for radar system application.

The availability of rapid tuning allows for various interpulse mode tuning formats. Figure 51 illustrates three of these formats. The sequential tuning of Figure 51 (a) provides for a Δf_T = 1.5 MHz change in transmitter frequency between steps for a peak-to-peak carrier duration of 382 MHz or so. If this is used as a frequency dither format, the period of the dither cycle will be...

$$Tm = (2 \times 256) \; PRI$$

and the dither frequency will be....

$$fm = \frac{1}{Tm} = \frac{PRR}{(2 \times 256)} = \frac{PRR}{512}$$

for triangular sequential tuning. If the sequential tuning is a sawtooth format tuning from $f(0)$ to $f(0) + 255 \; \Delta f_T$ and then resetting to $f(0)$, the dither frequency will be...

$$fm = \frac{PRR}{256}$$

A random tuning is available as illustrated in Figure 51(b). In this format, instead of a sequential progression of tuning as used in the sequential tuning format, the frequency for each transmitter pulse can be randomly selected within the 382 MHz available tuning range. In this format there is not a set magnetron frequency deviation or rate except as based on the nature (Gaussian, Rayleigh,
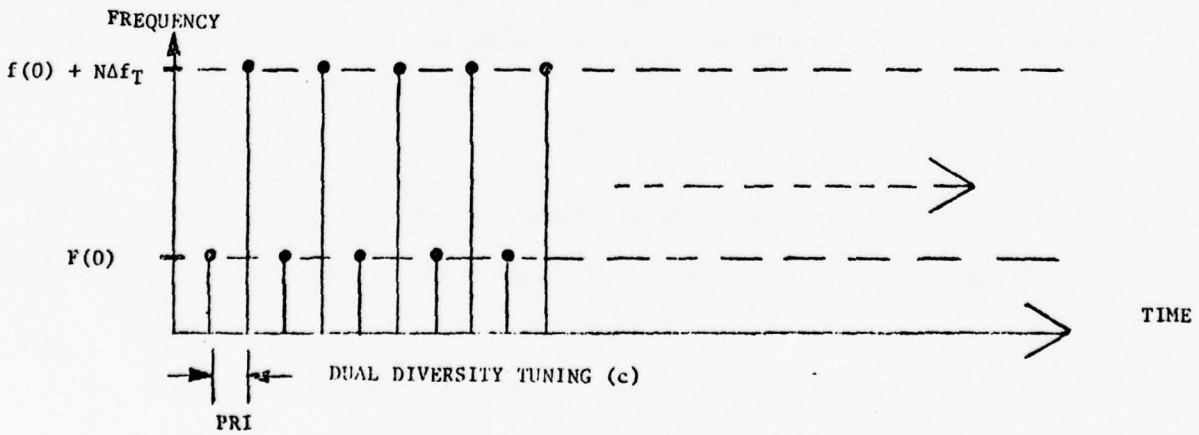
-157-
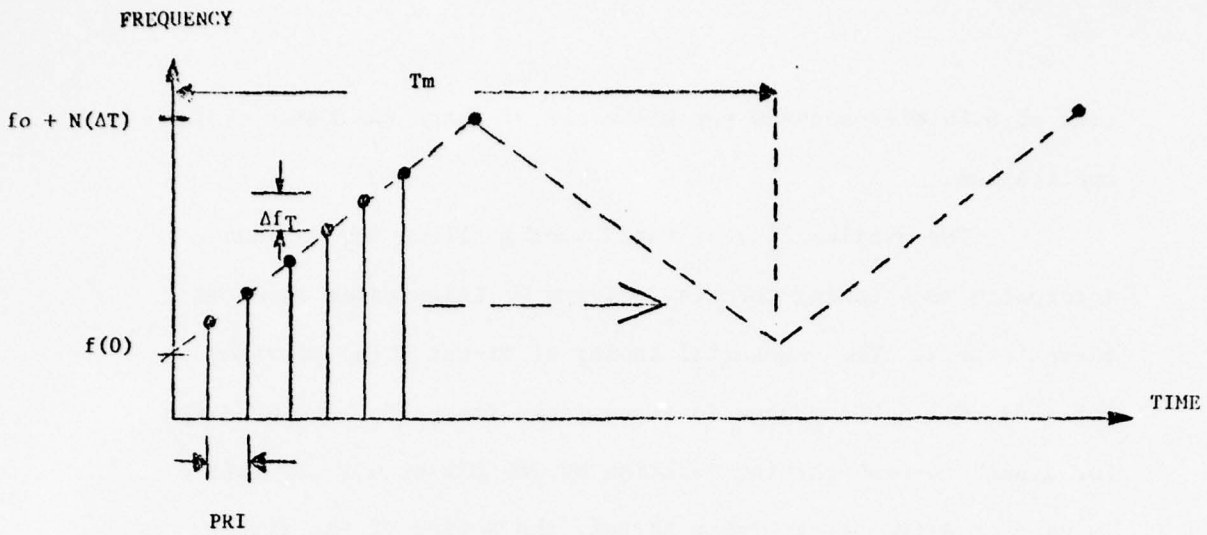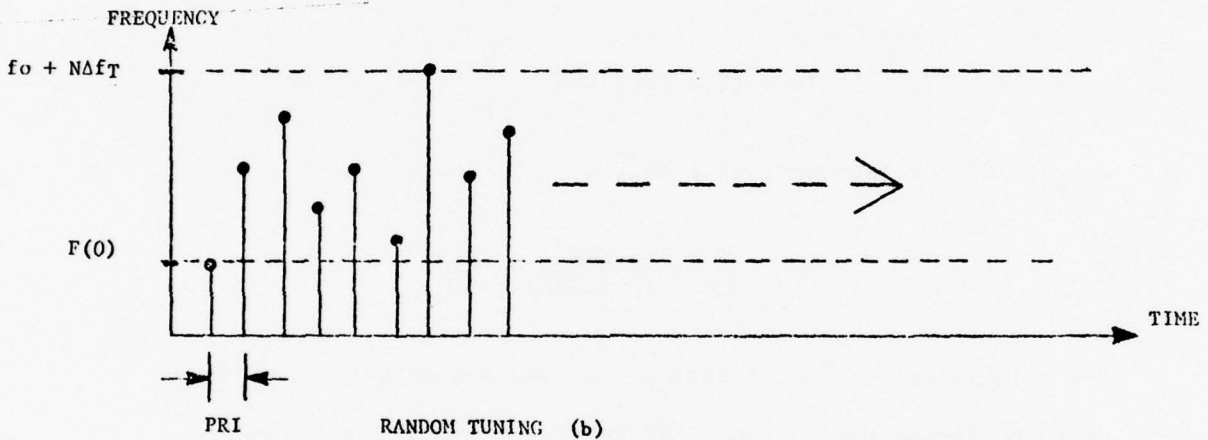
FIGURE 51

INTERPULSE TUNING FORMATS

-158-

etc.) and variance of the random variable used in controlling the frequency.

A dual diversity format is also available as illustrated in Figure 51(c). In this format the magnetron can be operated on alternate pulses at one of two frequencies. This allows a pulse-to-pulse deviation of up to 382 MHz at a dual diversity rate of...

$$fm = \frac{PRR}{2}$$

With a nominal pulse repetition rate (PRR) of 1 KHz the various tuning formats can provide the following characteristics:

Format	RF Excursion	Dither Rate
Triangular Sequential	384 MHz	1.95 Hz
Sawtooth Sequential	384 MHz	3.9 Hz
Random	384 MHz	500 Hz
Dual Diversity	384 MHz	500 Hz

Other control logic programs could be used to provide other effective dither rates as will be discussed in the next section.

7.1.2   <u>Triangular</u> <u>Sequential</u> <u>Tuning</u>

The control logic for the triangular sequential tuning can be accomplished by the generation of an 8 bit code which is advanced by one each interpulse period to count from 00000000 to 11111111 in 256 clock periods. Figure 52 illustrates a typical method of using two cascaded, 4 bit, synchronous up/down counters (54191 TTL MSI). The PRR generator is a 1 KHz clock. The PRR clock also drives a 74123 dual multivibrator to generate a 500 microsecond diode drive clear gate G(C) appropriately delayed from the time of the RF pulse. Since the 191 counters are clocked by a positive-going transition, the positive edge at the end of the complementary clear gate, G(C), can be used as the counter clock. This permits advancing the counter state between magnetron pulses. When clocked, the counter will count up (or down) over their full 8 bit range. The available look ahead MAX/MIN gate can be used to trigger a D flip flop to control the up/down count state.

If initially, the Q output of the D-FF is 0, the counters will count UP. During the 255th count, the MAX/MIN output goes high and at the end of the 255th count it goes low, triggering the D-_F to cause Q to assume the state of the D input $(D = \bar{Q} = 1)$. Once this occurs, $Q = 1$, $\bar{Q} = 0$, the counter counts down to 0. During the 0th count, the MAX/MIN output again goes high, ending in a negative going transition to the D-FF, causing Q to assume the state of $D = \bar{Q} = 0$. Q now becomes 0, $\bar{Q}$ becomes 1 and the process repeats itself with a count up/count down period of (2 x 256) PRI's.
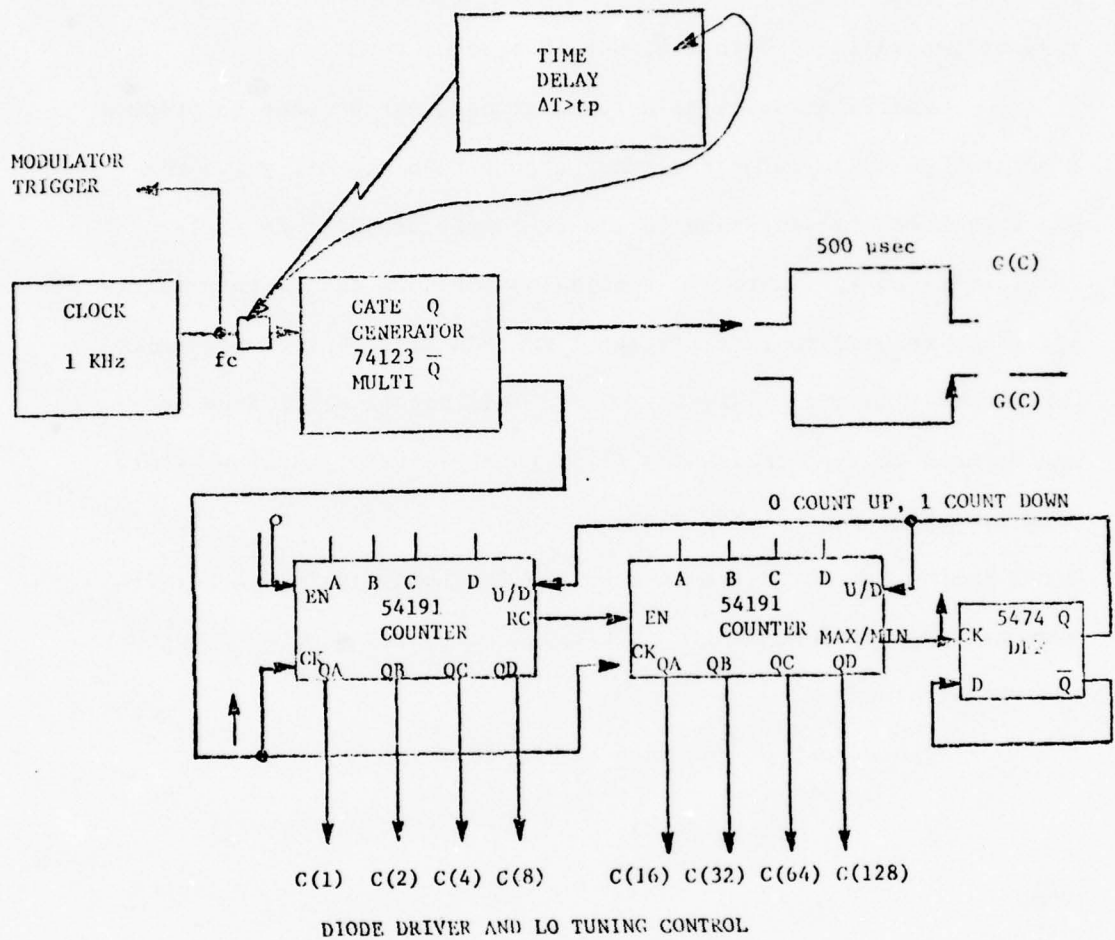
-160-

FIGURE 52

TRIANGULAR SEQUENTIAL CONTROL LOGIC

-161-

The same relative process can be used to generate the
sawtooth sequential tuning function except that the 54191 counters
are preprogrammed to always count up and the MAX/MIN output can be
used to load the counters to 0 at the end of each count cycle
thereby generating a 0 to 256, 0 to 256, etc. count.

Modification of this logic process can be used to produce
a greater pulse-to-pulse frequency change than the Δf_T = 1.5 MHz
and a proportional increase in the frequency dither rate (fm).
As illustrated in Figure 53, a 54167 synchronous decade rate multi-
plier can be used to generate the 1 KHz PRR from a clock frequency
for higher than the original 1 KHz.   This higher clock frequency
can be used to synchronize the clear gate generator and the binary
counters which control the diode drivers. In this manner, the
diode tuning can advance more than one frequency increment between
magnetron pulses depending on the clock frequency and the frequency
scaler rate input M.

The output of the rate scaler is...

$$PRR = \frac{M}{10} \; fc$$

where

$$M = A \cdot 2^\circ + B \cdot 2^1 + C \cdot 2^2 + D \cdot 2^3$$

$$= 1 \text{ to } 15 \text{ integrally depending on the}$$
$$\text{state of the input control A, B, C, D.}$$

If for example M = 1 and fc = 10 KHz to produce...

$$PRR = \frac{1}{10} \text{ X } 10 \text{ KHz} = 1 \text{ KHz}$$

then where the binary counters are driven at a 10 KHz rate compared

-162-

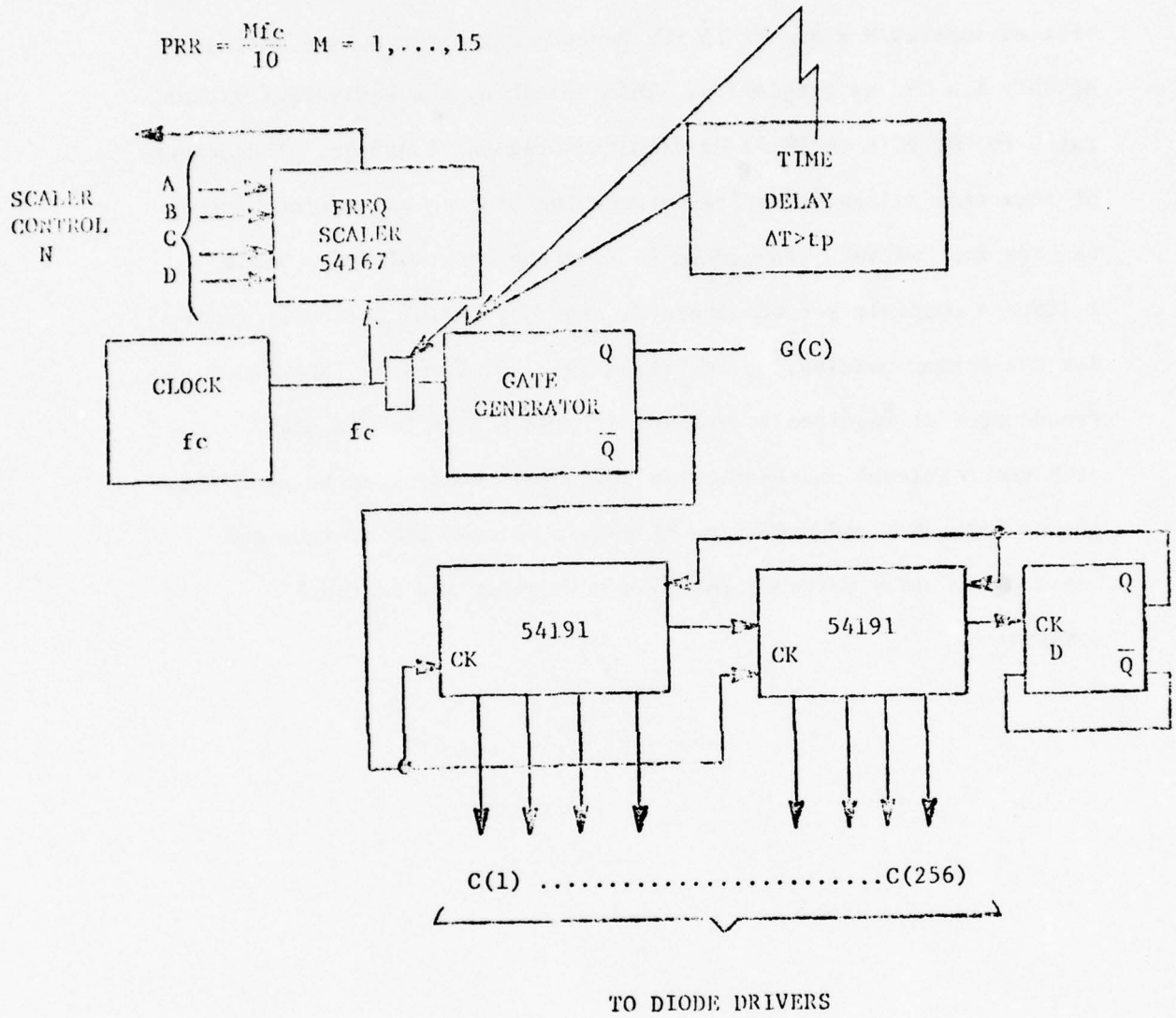$$PRR = \frac{Mfc}{10} \quad M = 1, \ldots, 15$$

FIGURE 53

MODIFIED SEQUENTIAL CONTROL LOGIC

-163-

to the 1 KHz modulator pulse repetition rate, the magnetron frequency
will advance $10/M \times \Delta f_T$ or 15 MHz between magnetron pulses instead
of only 1.5 MHz as originally. This speeds up the equivalent dither
rate, fm, by 10/M to 19.53 Hz from the original 1.953 Hz. The number
of magnetron pulses occurring between the minimum and maximum freq-
uencies is, however, reduced to 25 from the original 256. Table
1 lists a possible set of parameters for sequential frequency tuning
for the scaler modulus, M, of values 1, 2, 3, 4 and 5. The clock
frequency (fc) required to produce a 1 KHz PRR is listed along
with the resultant pulse-to-pulse frequency change and the equivalent
dither rate (fm) and numbering RF pulses between the minimum and
maximum frequency extremes for both triangular and sawtooth
modulation.

TABLE 1

SEQUENTIAL TUNING PARAMETERS VRS SCALER MODULUS M

SCALER MODULUS M	CLOCK fc (KHz)	PRR (KHz)	$\Delta f_T(p\text{-}p)$ M (Hz)	TRIANGULAR		SAWTOOTH	
				f_M (Hz)	# of PULSES	f_M Hz	# of PULSES
1	10	1.0	15	19.53	25	39.06	25
2	5	1.0	7.5	9.76	51	19.53	51
3	3.33	1.0	4.99	6.44	76	12.89	76
4	2.5	1.0	3.75	4.88	102	9.76	102
5	2.0	1.0	3.0	3.90	128	7.81	128

7.1.3   Random Tuning

The generation of the diode driver control random tuning
can conveniently be achieved by utilizing an 8 bit psuedo-random
code generator as illustrated in Figure 54. The magnetron modulator
trigger is provided by the 1 KHz clock which also drives a time
delay function. The time delay function delays the clock edge
generation of the clear gate, G(C), until after the occurrence
of the RF pulse. The clear gate, G(C), clears the tuning diode
states to 0 (non-conducting or "open"). The end of the clear
gate complement, G($\overline{C}$), is a positive-going edge which is used
to trigger the code generator.

The 8 bit psuedo-random code generator consists of two
serial in/parallel out shift registers and the necessary feedback
circuitry. The 8 bit psuedo-random code consists of 256 possible
states, each one selecting a different magnetron frequency.
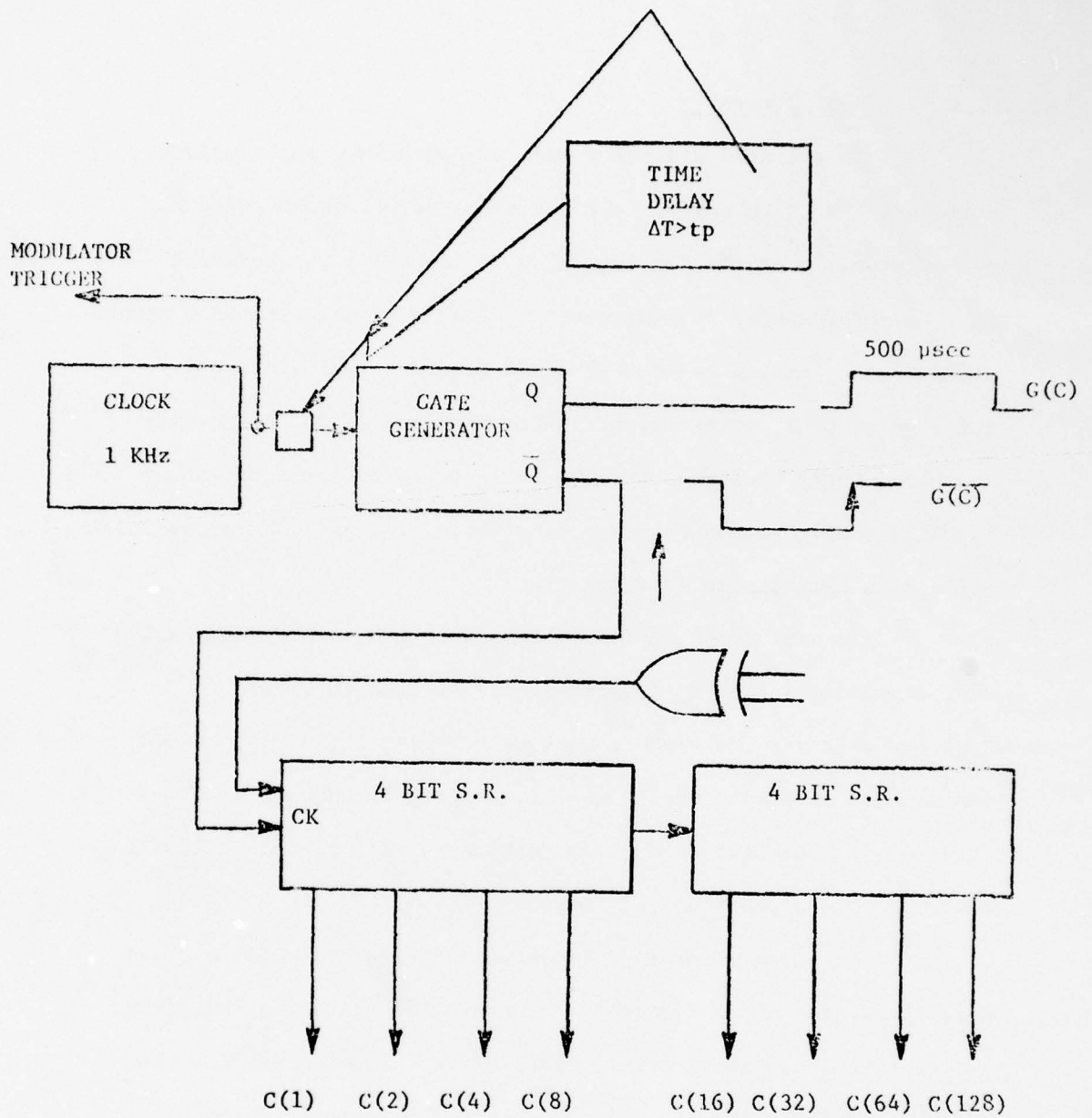
CONTROL TO DIODE DRIVERS AND LOCAL OSCILLATOR

FIGURE 54

RANDOM TUNING FUNCTION GENERATOR

7.1.4   Dual Diversity

In the dual diversity mode of operation, the simplest configuration is to combine all the diode driver inputs together and alternately drive them logical 0 or logical 1 to provide a full band interpulse dual diversity. Figure 55 illustrates a method of achieving this where the PRR clock generates the diode driver clear gate, G(C), after the RF pulse. The end of the clear gate is subsequently used as a trigger for a D-FF used as a divide by 2. This configuration produces alternating 1's and o's to the diode drivers as illustrated in Figure 56.

To expand the dual diversity function, a preprogramable dual diversity can be configured as illustrated in Figure 57. Here two switches are used to each select one of the 256 desired frequencies as preprogram Channel A, preprogram Channel B. The three digit switches, as digital selectors, will produce a 12 BIT BCD code to designate one of 256 channels.

The dual diversity programmer of Figure 57 will be used here to alternately select one of the two BCD codes via inhibiting gates. The resultant inhibit, non-inhibit channel codes can then be combined and converted from decode to 8 BIT binary format to control the 8 BIT input to the diode drivers.
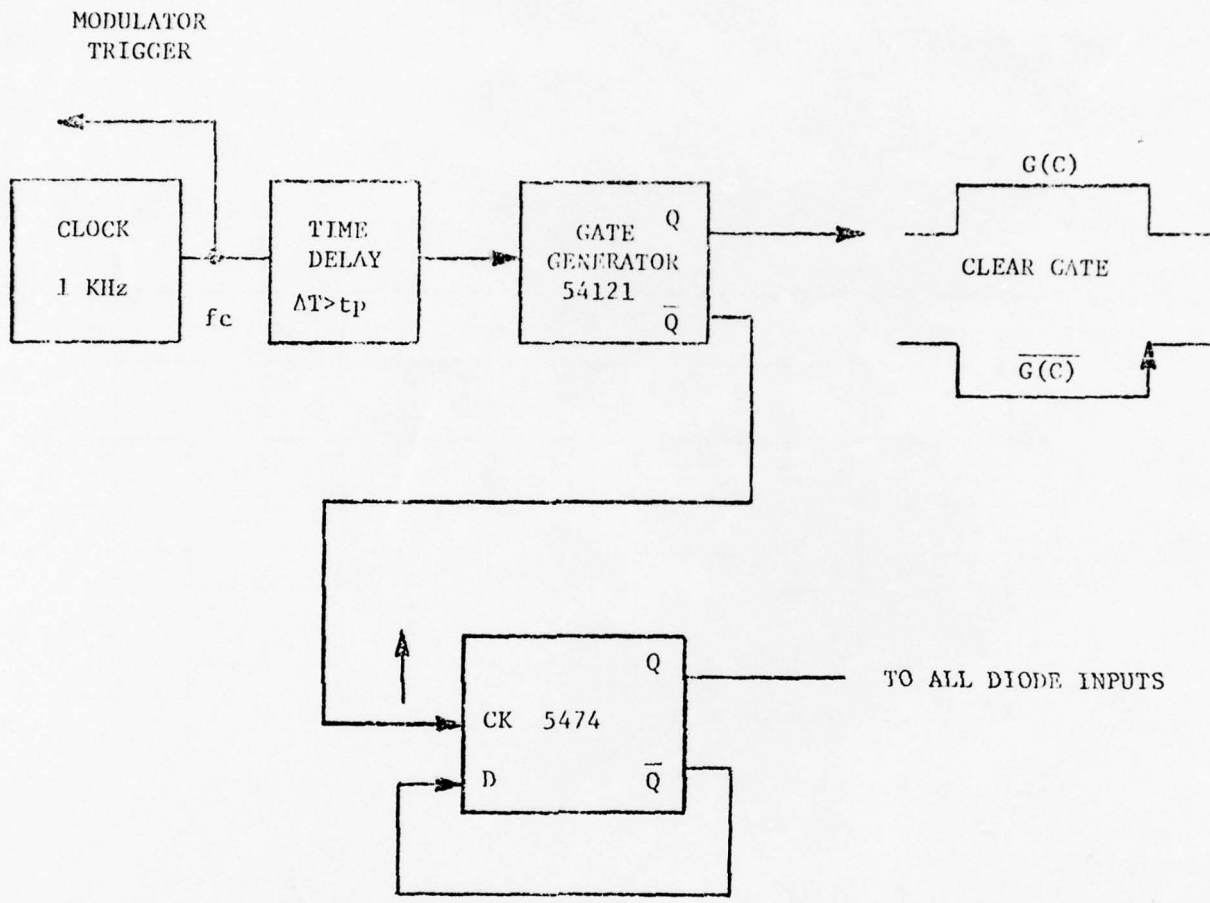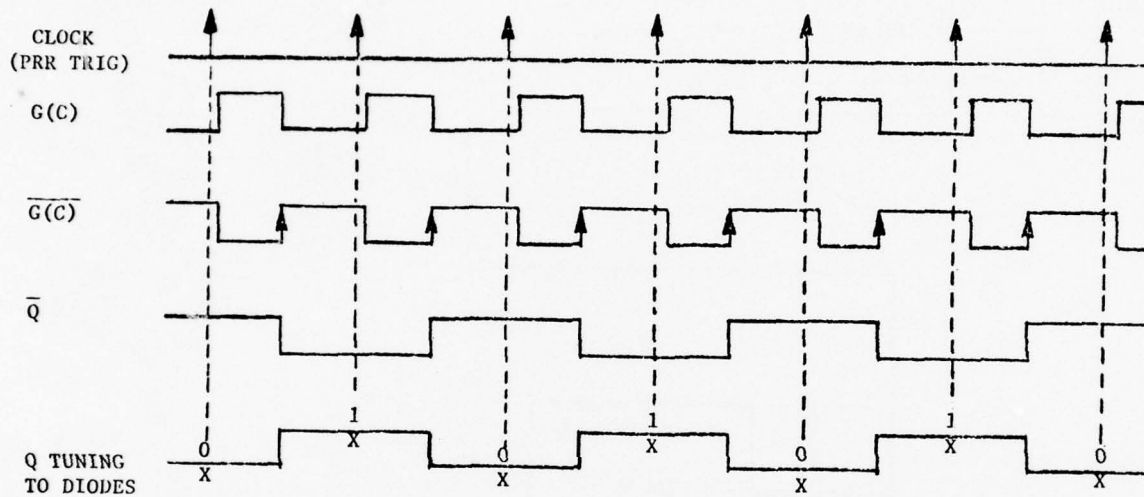
FIGURE 55

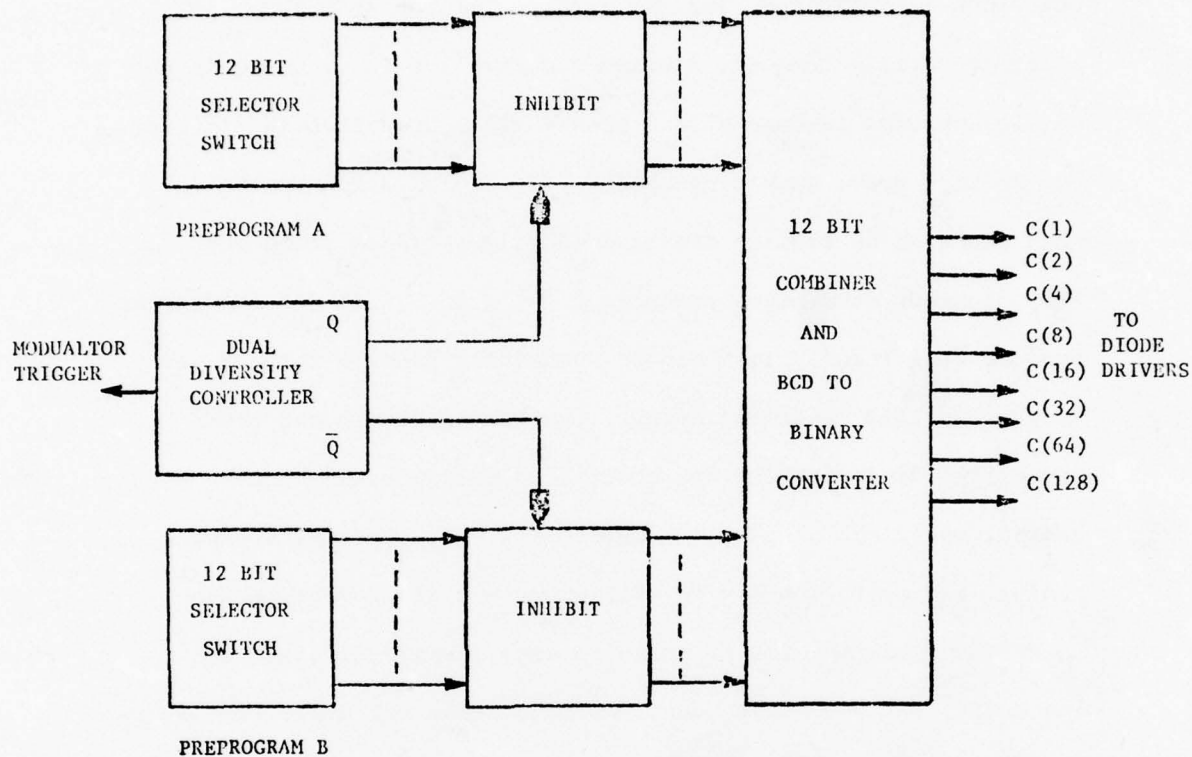DUAL DIVERSITY CONTROLLER

-169-

FIGURE 56

DUAL DIVERSITY TIMING SEQUENCE

-170-

FIGURE 57

DUAL DIVERSITY PREPROGRAMMER

-171-

7.1.5   Intrapulse Tuning

In the intrapulse tuning mode of ETM, the frequency of
operation is changed during the duration of the RF pulse.   In
order to rapidly tune the frequency during the pulse there is not
sufficient time to turn diodes on and off. Operation is limited,
due to high power switching speeds, to sequentially turning
each diode on so that no diodes conducting produce frequency
$F(0)$, 1 diode conducting produces $f(0) + \Delta f_T$, 2 diodes conducting
produce $f(0) + 2\Delta f_T$, to N diodes conducting produce $f(0) + N\Delta f_T$.
To utilize this cascading effect, the tuning diodes and their
associated diode drivers are controlled individually by the
control logic illustrated in Figure 58 . With the intrapulse
tuning, ETM operation $N = 50$ will produce a stepped variation
in frequency during the RF pulse as each individual diode is
sequentially caused to conduct. With a 1 MHz per diode frequency
shift a 50 MHz "chirp" is conceivable for pulse widths on the order
of 0.25 microseconds to 2.0 microseconds.

The logical gate sequence relative to the RF pulse is
illustrated in Figure 59 for a 7 frequency pulse as an example.
The clear gate, $G(C)$, which has cleared the diodes and diode drivers
to a non-conducting condition, ends prior to the pulse tuning cycle.
The series of control gates $G(1)$, $G(2)$, ..., $G(7)$ are generated
beginning a time, $\Delta \tau$, in advance of the RF pulse. This time, $\Delta \tau$, which
can be made adjustable, accounts for possible tuning diode and diode
driver turn on and settling times. Control gate, $G(1)$, becomes
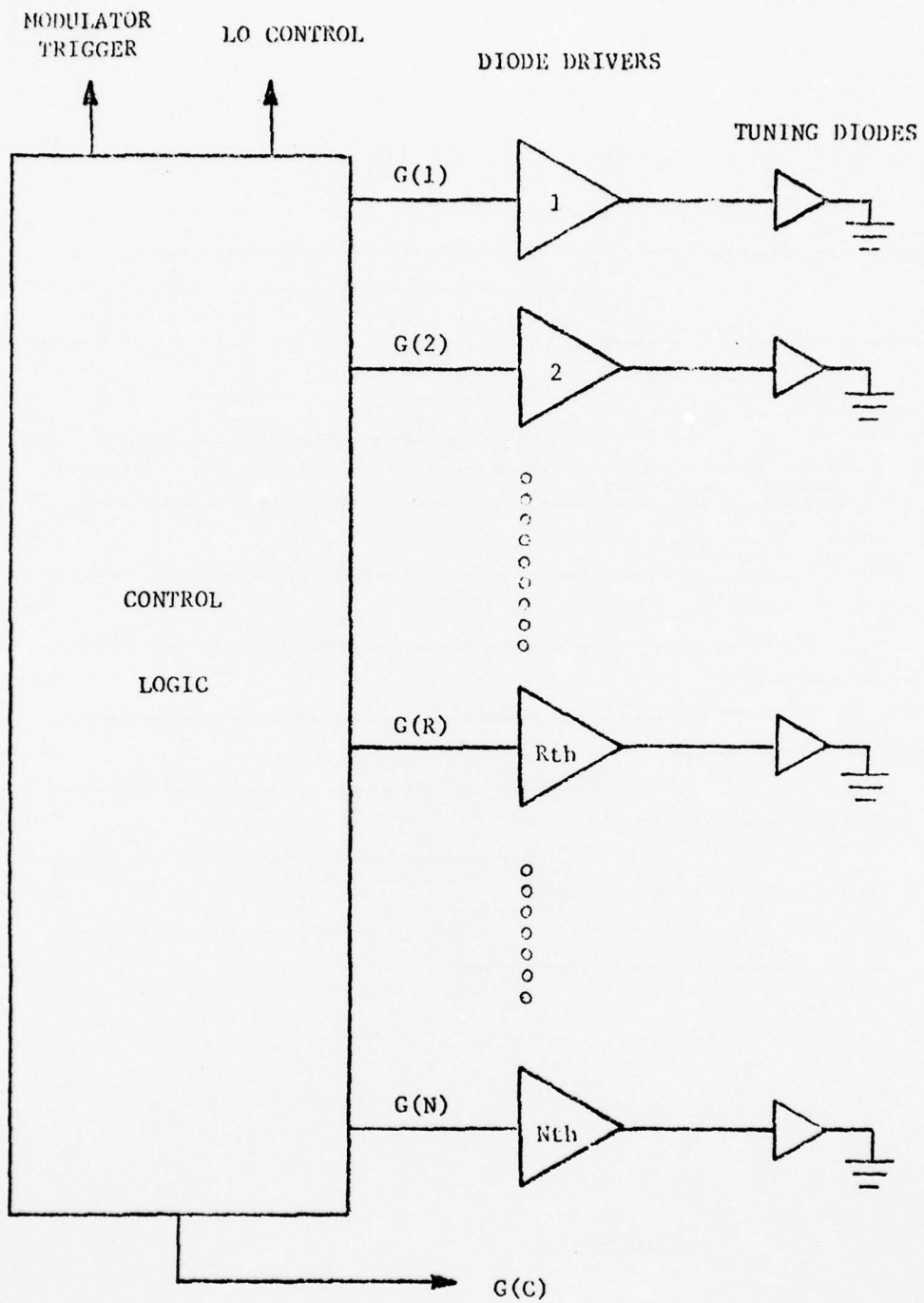logical 1, followed by $G(2)$ a time Tc later when both are logical 1,

-172-

MODULATOR
TRIGGER

LO CONTROL

DIODE DRIVERS

TUNING DIODES

G(1)

1

G(2)

2

CONTROL

LOGIC

G(R)

Rth

G(N)

Nth

G(C)

FIGURE 58

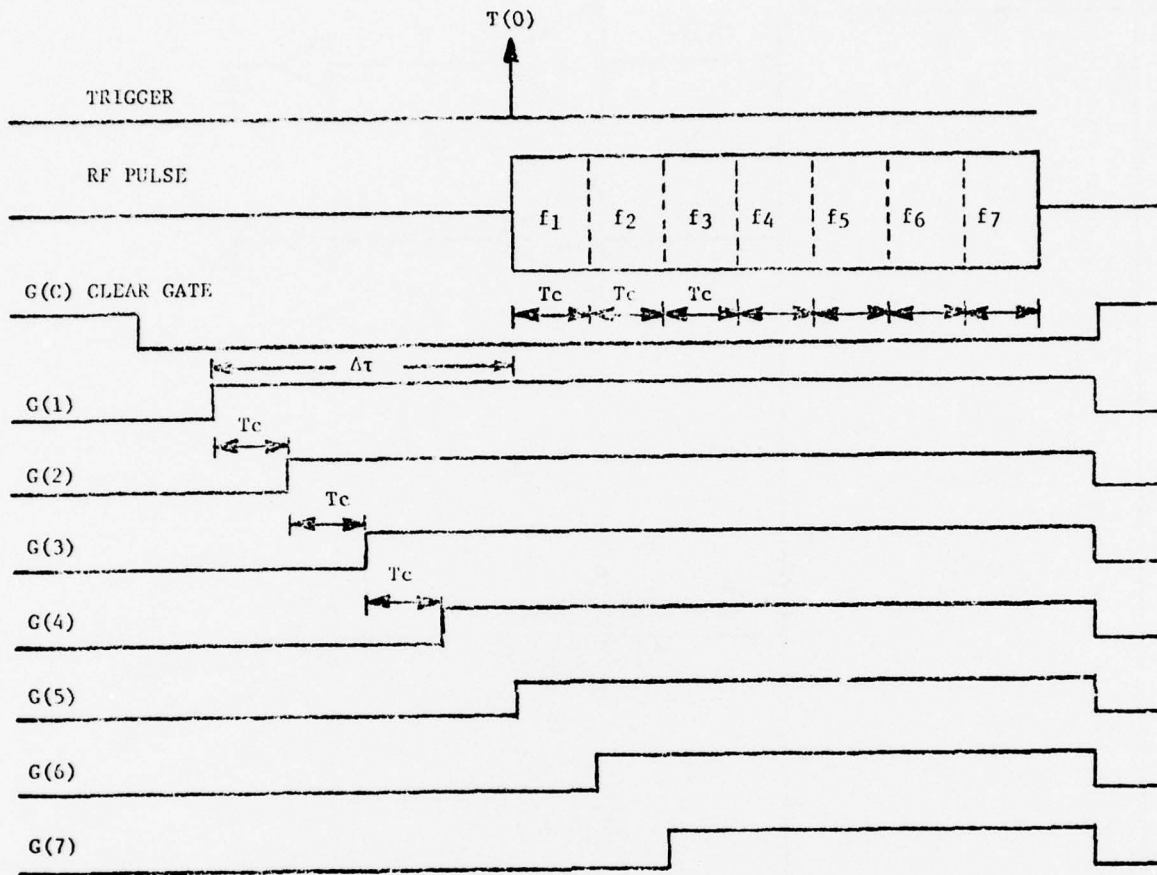GENERAL INTRAPULSE TUNING CONTROL CONFIGURATION

-173-

FIGURE 59

INTRAPULSE TUNING TIMING FORMAT

-174-

followed by G(3) a time Tc later when all three become logical 1, etc. This control gate ripple effect will cause the frequency of the RF pulse to be f1 during the first time increment of Tc of the pulse, f2 during the second time increment Tc, f3 during the third time increment Tc, etc. After the conclusion of the RF pulse, the generation of the diode and diode driver clear gate G(C) occurs, which also clears all control gate outputs to a logical 0 state.

One flexible method of generating the intrapulse tuning control gates is illustrated in Figure 60. A series of D-FF integrated circuits can be cascaded where all are initially cleared to $Q = 0$ state. With the occurrence of the first RF tuning clock pulse (frequency fc), $Q1 \rightarrow D1 = 1$ producing $G(1) = Q1 - 1 = D2$. DDF #1 is then latched to $Q1 = 1$ state. The next clock pulse will cause $Q2 \rightarrow D2 = 1$ producing $G(2) = Q2 = 1 = D3$. This happens sequentially causing the output to progressively become latched to 1, at time intervals of $Tc = 1/fc$, the clock period, until all 50 parallel outputs are 1 and the chirp tuning cycle is completed.

With the occurrence of $Q1 \rightarrow 1$, $\overline{Q1} \rightarrow 0$ and the negative going transition can be used to trigger a time delay generator, the output of which occurs after the end of the RF pulse, generating the diode and diode driver clear gate G(C) and the gate logic clear gate G(CL) as illustrated in Figure 61.

A time delay trimer, ΔT, can be incorporated into the clock input of each D-FF to allow for adjustment of possible variations
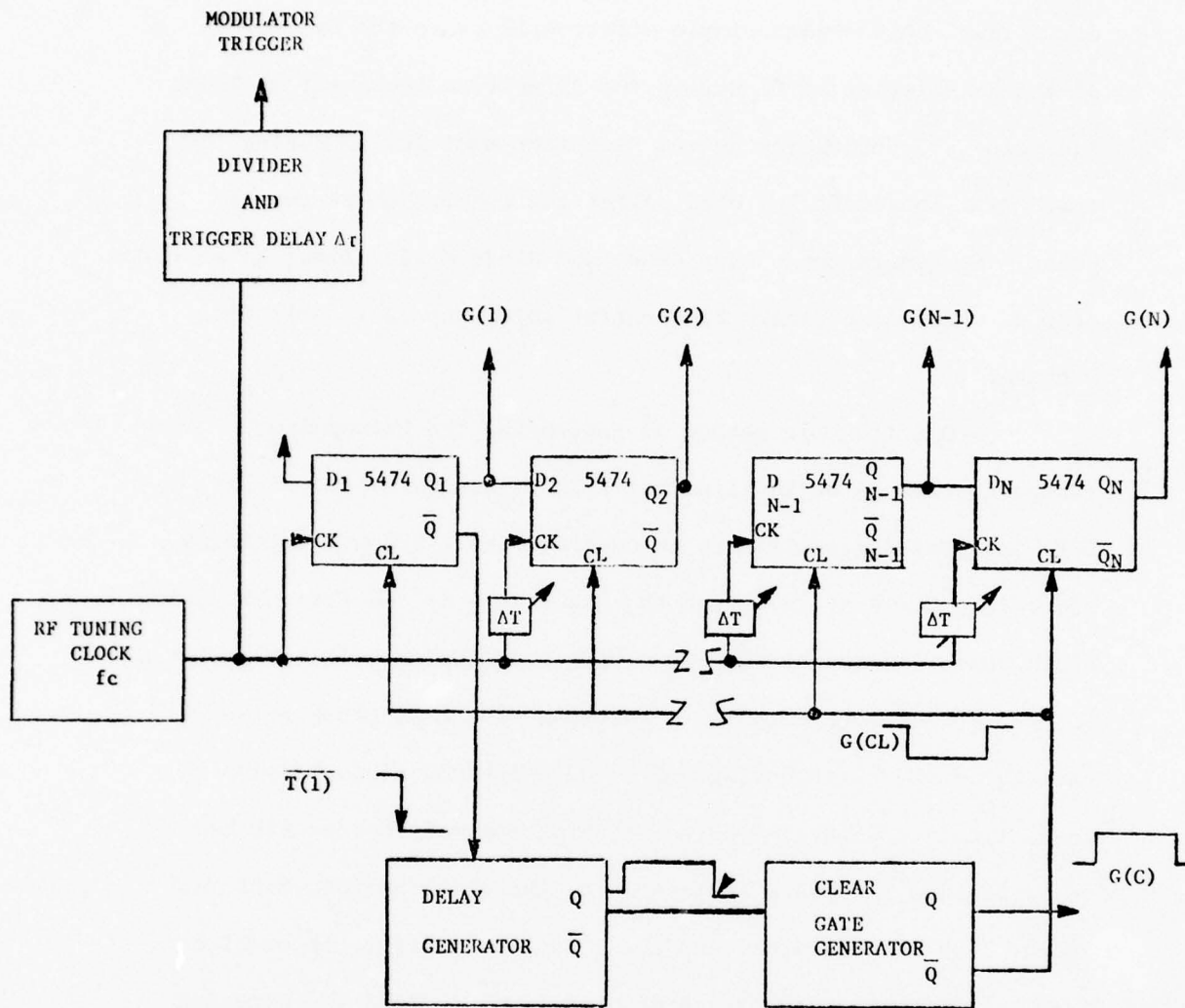
-175-

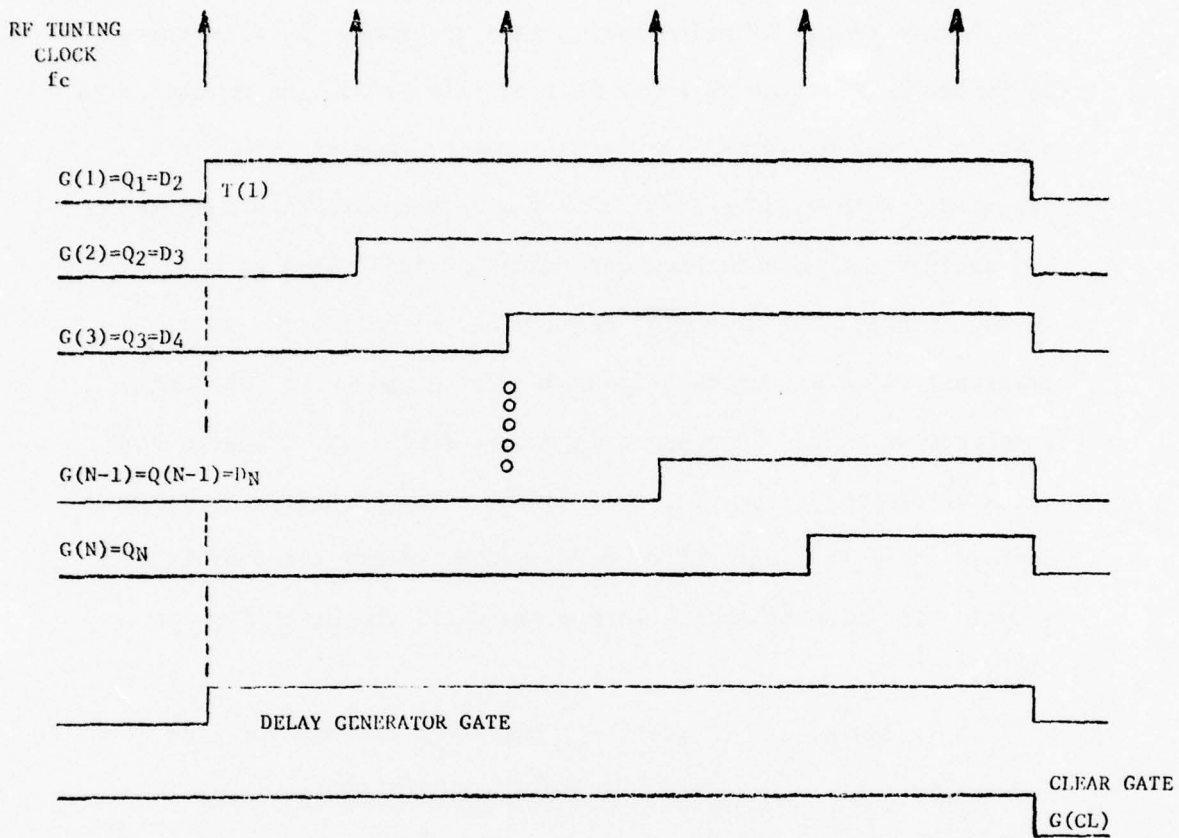**FIGURE 60**

INTRAPULSE TUNING LOGIC

-176-

FIGURE 61

INTRAPULSE TIMING SEQUENCE

-177-

in individual turn on times.

The RF tuning clock, fc, is used to generate the synchronous modulator trigger and to delay the modulator trigger by an amount $\Delta\tau$ relative to the RF pulse tuning gate sequence. As illustrated in Figure 62, for the RF pulse divided into N = 50 increments, with a Δf_T of 1 MHz per diode, a total frequency scan of 50 MHz can be provided. With a pulse width of 0.5 microseconds, this results in 500 nsec/50 = 10 nanoseconds per tuning period. Thus with Tc = 10 nanoseconds, the RF tuning clock needs to be 100 MHz with a resultant 100,000 countdown from 100 MHz to produce a 1 KHz PRR modulator trigger. The base trigger, at $T(0) - \Delta\tau$, triggers a FF which allows the clock, fc, to feed the cascaded D-FF gate generators until the logic clear gate, G(CL), clears the inhibit FF, stopping the flaw of tuning gate clock until the next RF pulse cycle.

Figure 62, in addition, indicates the various clock frequencies and PRR countdown coefficient (100,000 for tp = 0.5 μsec. and fc - 100 MHz).

GIVEN PARAMETERS

$$N = 50$$
$$\Delta f_T = 1 \text{ MHz}$$
$$PRR = 1 \text{ KHz}$$
$$50\Delta f_T = 50 \text{ MHz}$$

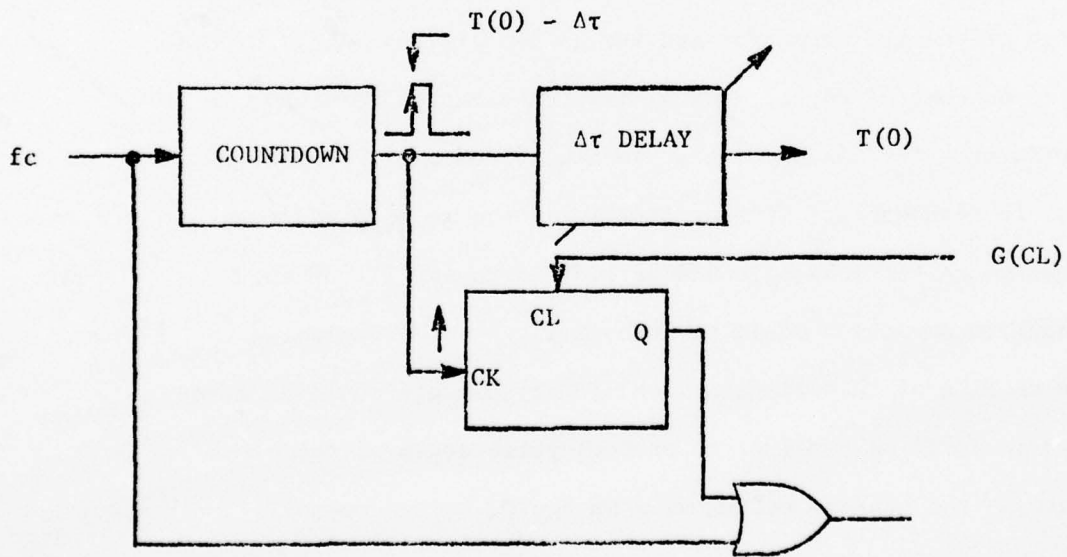| tp (μsec)	Tc = (tp/50) nsec	fc (MHz)	COUNT DOWN FOR 1 KHz PRR
.5	10	100.0	100,000
1.0	20	50.0	50,000
1.5	30	33.33	33,333
2.0	40	25.0	25,000

FIGURE 62

CLOCK/PRR COUNTER, DELAY AND CLOCK ENABLE

7.1.6 '   Configuration

The logic control circuitry for the intrapulse tuning ETM can be relatively small since the output is coded, the basic decoding function being provided by the magnetron diode interconnections themselves. For the triangular (or sawtooth) sequential tuning, random tuning or dual diversity tuning, a functional printed circuit module of 4 x 5 inches is reasonable to expect for each of these three tuning methods for prototype purposes. On any type of production basis, the use of special purpose LSI chips can reduce this size.

The control circuitry for the intrapulse tuning involves a possible sequence of integrated circuits operating at a relatively high clock frequency (100 MHz). Fabrication of a unit using RF techniques can be envisioned in a circular package which can be mounted around the magnetron and its diode drivers. If 50 diodes were to be controlled, if 25 dual in-line packages were used, a circumference (or linear package length if desirable) of say 24 inches is reasonable. If flat pack IC's were to be used, the circumference (or length) could be reduced to say 11 inches, although construction would be more difficult. The relative cross section of this circular (or linear) package would be maintained as small as possible to prevent propagation of the clock frequency; the package acting as a waveguide beyond cut-off.

-180-

7.2 PIN Diode Driver Circuits

In order to achieve a practical, electronically-tuned magnetron, a solid state driver is required to interface between the low level control logic and the PIN diodes used to perform the frequency tuning. The diode driver must be capable of providing a two state, switchable output. One state provides a high voltage to reverse bias the diodes. The other state provides a controlled current to forward bias the diode to a low resistance state. The input section of the driver must provide the required amplification and interface in order to allow the choice of output state to be made by low voltage, low power TTL logic.

The RF studies conducted on this program have determined that each diode set requires the following driver parameters for proper operation:

Reverse Bias Voltage (V_R) = 100 volts (State 1)

Forward Bias Current (I_B) = 200 ma   (State 2)

This represents the minimum output requirements for the two diode driver states.

Two types of magnetron frequency control must also be considered: interpulse tuning where the magnetron frequency is constant over the RF pulse and retuned between pulses and intrapulse tuning where the frequency is changed during the RF pulse duration. In the case of interpulse tuning, there is no requirement on switching speed and the diode driver design is concerned mainly with load handling capability and simplicity of design. For intrapulse

-181-

tuning, switching speed of the diode from the reverse voltage

state to the forward conduction state is of prime importance.

7.2.1   Interpulse Tuning

As discussed in the previous section on the control logic, in the interpulse tuning mode the frequency of operation is established between pulses. Times as long as 500 microseconds have been allocated for this purpose and, therefore, the switching time of the diode and driver from one state to another does not have to be considered.

In order to facilitate frequency control, the diode pairs will be switched in binary sets of 1, 2, 4, 8, 16, 32, 64 and 128 pairs. Ideally, one lead per combination would feed through the vacuum envelope. This would require the following driver currents:

No. Diode Pairs	1	2	4	8	16	32	64	128
Drive Current	0.2A	0.4A	0.8A	1.6A	3.2A	6.4A	12.8A	25.6A

The output of the diode driver for this type of tuning must, therefore, be capable of supplying the following two output stages:

> STATE 1: 100 volts
>
> STATE 2: 26 A (pulsed) if the highest set of combinations is to be switched

The simplest form of driver that can be used is shown in Figure 63. When the TTL input is at a Logic "0" (0 volts), the output transistor Q1 is bias "OFF" and the PIN diodes are connected to the reverse bias supply (V_R). When the TTL input is set at Logic "1" (~3 V), Q1 is turned full "ON". This connects the PIN diode to the supply V_f which establishes the forward bias current. The

-183-
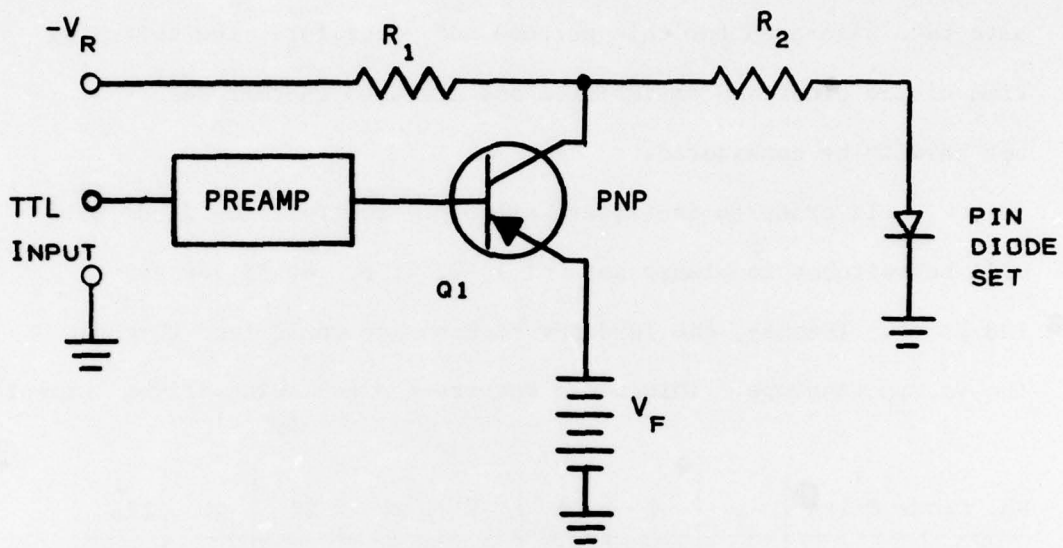
$R_1 \approx 100 \text{ K}\Omega$

$R_2 \approx 10 \ \Omega$

$V_R \approx 100 \text{ V}$

$V_F \approx 5 \text{ V}$

FIGURE 63

BASIC DRIVER DESIGN

supply V_R is effectively isolated because of the high resistance of R_1. The PREAMP shown is a simple one or two stage transistor circuit which provides the proper drive to Q1.

The critical item in this circuit is the output ransistor Q1; one state must be capable of supporting collector to emitter voltage of $V_R + V_f$ and in the other state of passing the required bias current. This requires both a high voltage and high current (handling the higher order combinations) devices. One of the best devices in this class is the 2N6211 with the following characteristics:

$$V_{CER \ (SUS)} \quad = -250 \ V$$

$$I_C \quad = 2 \ A \ (cw), \ 6 \ A \ (pulsed \ to \ 100 \ \mu sec.)$$

$$P_T \quad = 20 \ W$$

$$t_r, \ t_f \quad = 0.6 \ \mu sec.$$

This device has a high degree of safety margin for handling the required reverse bias voltage (100 - 150 V) and is capable of up to 6 A peak current. From the previous chart showing required drive current, it can be seen that one driver of this type can easily handle up to 16 diode pairs. Combinations above this number would require using multiple drivers with several leads per combination. (Seven drivers would be required to handle the highest number of 128 diode pairs.)

This is not a serious drawback since considerations of current sharing by large combinations of parellel diodes will probably limit the practical limit to below 16 pairs. This would necessitate

-185-

using a smaller number of parallel sets being fed through separate series current limiting resistors.

If is becomes practical to incorporate some of the current limiting resistors within the tube so that a minimum of bias lead feed throughs can be used, it would then be advantageous to have a driver with more current capability. This can be accomplished by either parallel several output transistors or using the driver circuit shown in Figure 64. In this circuit a NPN transistor is used as the output stage. This type of transistor is available with higher current capability for a given V_{CER} than the PNP type used previously. An appropriate type is the 2N6249 with the following characteristics:

$$V_{CER\ (SUS)} = 225\ V$$
$$I_C = \begin{array}{l} 10\ A\ (cw) \\ 30\ A\ (peak) \end{array}$$
$$P_T = 175\ W$$
$$t_r = 0.8\ \mu sec.$$
$$t_f = 0.8\ \mu sec.$$

With this circuit, the total combination of 128 diode sets could be handled with one driver. The trade off is a more complicated PREAMP because of the requirement of using a floating collector on Q1.

The polarities used have been those required by the present PIN diodes used in the experimental tube. It is entirely feasible to fabricate diodes with identical parameters, but with reversed polarity; i.e., NIP diodes. If diodes of this polarity are used further on in

-186-

V_R R_1 TTL   FLOATING PREAMP   NPN   Q1 V_F PIN DIODE SET
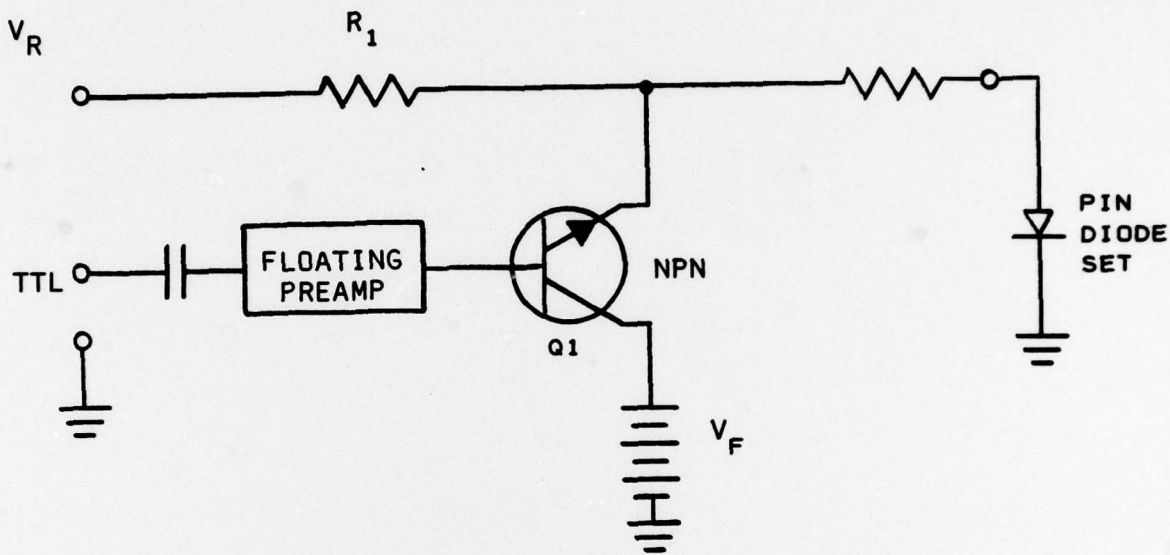
FIGURE 64

HIGH CURRENT DRIVER DESIGN

this program, a simple driver such as shown in Figure 63 with a

NPN output transistor can be used. This would allow handling the

128 diode sets with one simple driver design.

7.2.2   <u>Intrapulse</u> <u>Tuning</u>

In the intrapulse tuning mode, the frequency of operation
is changed during the RF pulse. As discussed earlier, it is esti-
mated that a total of 50 diode sets, each individually switched
with their own driver, will be used in the mode of operation. For
a nominal 0.5 microsecond pulse width, this allows 10 nanoseconds
per frequency bit. Due to the large charge storage in the
high power PIN diodes used, it will be impossible to consider
switching them from the "ON" (forward biased) to the "OFF" (reverse
biased) condition. We, therefore, only need to consider the turn
"ON" condition where a large amount of charge must be injected into
the diode within the time required.

In order to determine the output requirements of the
driver, we must first consider the diode set parameters. The
following are the pertinent diode set parameters to be considered:

$$V_R \;\; = \;\; -100 \; V \; \text{(reverse bias requirement)}$$

$$I_B \;\; = \;\; 200 \; \text{ma/set (100 ma/diode)}$$
$$\text{(forward bias requirement)}$$

$$C_{j-50} \;\; = \;\; 0.1 \; \text{pf (each side)}$$

$$\tau_L \;\; = \;\; 1 \; \mu\text{sec. (carrier life time)}$$

The charge stored in a diode in the forward conduction
state is given by....

$$Q_B = I_B \cdot \tau_L \cdot$$

For the diode parameters listed above...

$$Q_{STORED/DIODE} = 100 \times 10^{-3} \times 10^{-6} = 100 \times 10^{-9} \text{ coulombs}$$

and

$$Q_{STORED/SET} = 200 \times 10^{-9} \text{ coulombs}$$

or

$$Q_B = 200 \times 10^{-9} \text{ coulombs}$$

Another parameter of interest is the bias current (I_{Bf}) that is just sufficient to produce the full frequency shift associated with each diode set. This has been found experimentally to 0.5 ma/set. The bias current of 200 ma/set used previously is the current required to achieve the best Q and prevent diode burn out. The total stored charge associated with the bias current I_{Bf} is:

$$Q_f = I_{Bf} \cdot \tau_L = 0.5 \times 10^{-3} \times 10^{-6} = 0.5 \times 10^{-9}$$

$$Q_f = 0.5 \times 10^{-9}$$

The actual switching speed of the PIN diodes is determined by how long it takes to inject the required stored charge to sustain the final bias current. This is determined by the magnitude of the initial current that can be applied to the device.

In order to generate 10 nanosecond wide frequency pulses, we will require that the frequency change occur in 2 nanoseconds. The diode pair must, therefore, have a stored charge of Q_f after 2 nanoseconds. The peak current required to inject this charge

-190-

is given by....

$$I_{pf} = \frac{Q_f}{t}$$

$$I_{pf} = \frac{0.5 \times 10^{-9}}{2 \times 10^{-9}}$$

$$I_{pf} = 0.25 \text{ A/set}$$

We will also assume that two pulse periods are allowed for the diode pairs to reach the full bias condition. This is still sufficiently short to prevent diode heating while in the lossy transition state. It also allows only two diode pairs to be in a lossy state at any instant of time so that the Q of the tube will not be severely degraded. The required peak current (I_{PB}) to achieve this is....

$$I_{PB} = \frac{Q_B}{t}$$

$$I_{PB} = \frac{200 \times 10^{-9}}{20 \times 10^{-9}}$$

$$I_{PB} = 10 \text{ A}$$

The drive pulse supplied to each diode set must, therefore, supply a current pulse that reaches a minimum of 0.25 A in 2 nanoseconds, and a peak of 10 A in 20 nanoseconds. It then settles to the steady state bias condition of 200 ma for the remainder of the pulse. This type of current spiking is a well established technique used to fast switch PIN diodes. The difficulties in this design is that the driver must not only switch large current extremely fast, but withstand

-191-

high voltage in the OFF stage. This puts state-of-the-art requirements on the switching device.

A driver design suitable for this type of operation is shown in Figure 65. This is very similar to the circuit shown in Figure 63. For this high speed of operation, it is assumed that NIP diodes will be used in the tube in order that NPN transistors in the simplest possible configuration can be used. NPN types have been chosen because they offer the best switching speed performance. In addition to these changes, a capacitor has been added across the resistor R_2. Its purpose is to act as a low impedance path during the start of the pulse so that the required charge can be quickly injected into the diode.

The critical item for proper operation will be the output power transistor. A possible candidate is the Unitrode UPT-430 (Industry Type D75430). This has the following ratings:

$$V_{CEO\ (SUS)} = 300$$

$$I_C = 5\ A\ (cw)$$

$$f_T = 30\ MHz\ (typical)$$

$$t_{ON} = 40\ nsec.\ (I_C = 2.5\ A)$$

Other possibilities are:

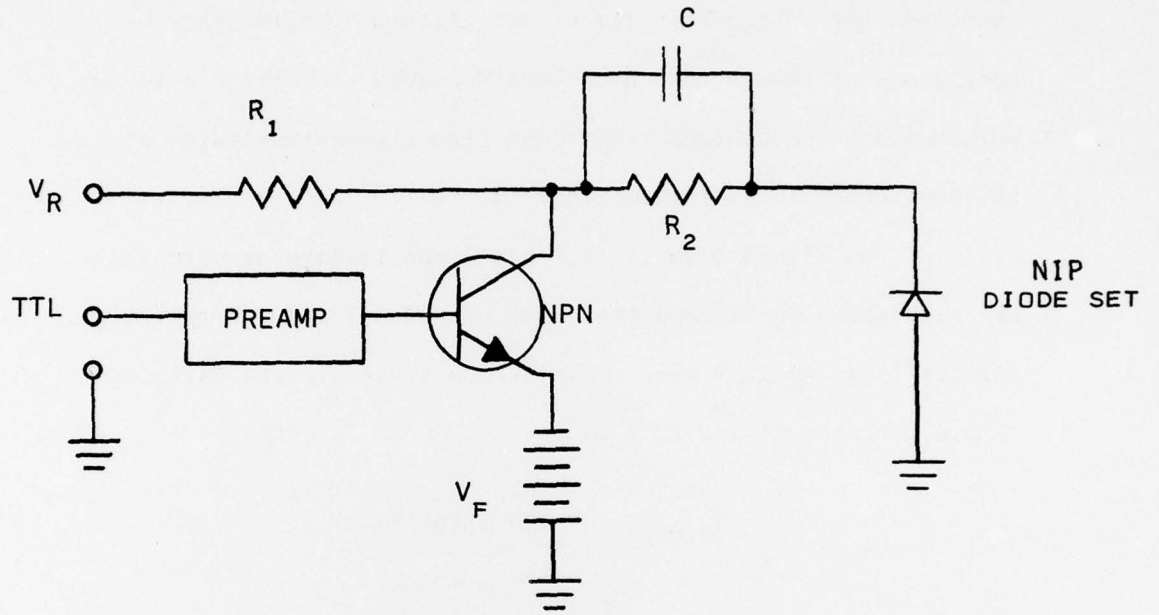|	2N5664	VPT835	2N5487
V_{CER}	250	150	120 V
I_C	10 A	10 A	5 V
f_T	40 MHz	50 MHz	80 MHz
t_{ON}	150 nsec.	250 nsec.	60 nsec.

-192-

FIGURE 65

HIGH SPEED TRANSISTOR DRIVER

Although the typical switching speeds quoted above appear higher than our requirements, they are conservative ratings based on a square wave base current drive. As with the PIN diodes, it is possible to substantially decrease the switching time by over driving the base with a high current input. This would be the function of the PREAMP in the driver circuit. Solid State modulators of this nature have been designed to deliver a 10 amp pulse with 50 nanosecond rise times from transistors rated at 500 nanosecond typical rise time.

An alternative is to replace the transistor with the new high speed thyristors that have been developed. A typical circuit is given in Figure 66. Such a device is the Unitrode GA301A with the following ratings:

$$V_{BLOCKING} = 100 \text{ V (minimum)}$$
$$I_F = 100 \text{ A (peak)}$$
$$t_r = 20 \text{ nsec. (to 30 amps)}$$

The modulators constructed have been developed to deliver current pulses with a 10 nanosecond rise time to 10 amperes and 20 nanoseconds to 30 amperes. Higher voltages can be obtained by series connecting several devices.

From the above analysis, the desired high speed diode switching required for intrapulse tuning appears to be within the state-of-the-art of currently available devices. The exact circuit and device type used would have to be assessed at the time of the final design after several experimental circuits were fabricated.
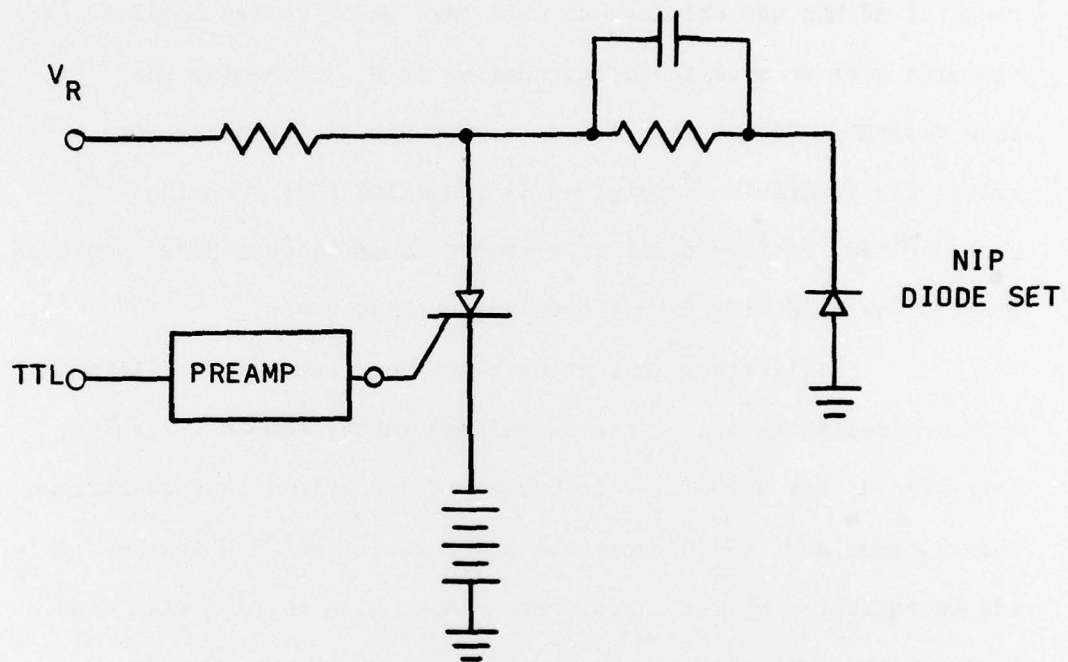
-194-

FIGURE 66

HIGH SPEED THYRISTOR DRIVER

8.0   CONCLUSION

The feasibility of using PIN diode-controlled, coupled
circuits for electronically tuning a pulsed, coaxial magnetron at
Ku-band has been demonstrated. The first experiments were made
using a coupled-circuit geometry best suited for intrapulse
tuning rather than for interpulse tuning. An electronic tuning
range of 38 MHz was obtained at cold test using twelve coupled
circuits with an acceptable degradation in Q_o. Assuming the
same tolerable degradation for a coupled circuit geometry more
suited for interpulse tuning, it is projected that a tuning
range of four to five times this amount could be obtained. Improved
diode properties will permit even more tuning range.

The first hot test experiments were found to be limited
by diode rectification of the RF voltage in the coupled circuits.
Self bias of the diodes led to operating conditions that restricted
tuning range and caused excessive power variation with tuning. This
can be inhibited by using appropriate d.c. bias voltage with diodes
having larger reverse voltage breakdown values.

The theoretical analysis of this tuning concept has been
substantiated and it is expected that further development effort will
lead to a device suitable for system use.

Some of the experimental results suggested that it may
be possible to arrive at a tuning configuration capable of both
interpulse tuning and intrapulse tuning. This needs further
investigation.